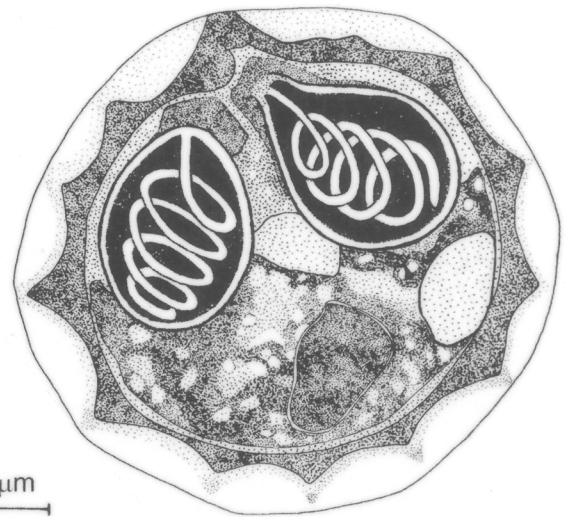# Final report

Myxosporidia disease and Biodiversity of Parasites in Economic Marine Fish of Thailand

2 µm

Myxobolus supamattayai n. sp.

(U-taynapun *et. al.*, 2011)

Asst. Prof. Chutima Tantikitti : Head of Project

บทคัดย่อ

Myxosporean เป็นปรสิตที่พบโดยทั่วไป บางชนิดส่งผลร้ายแรงต่อสุขภาพของปลาเจ้าบ้าน เช่น *Myxobolus cerebralis* ที่ก่อให้เกิดโรค whirling diseases ในปลากลุ่มแซลมอน ซึ่งการศึกษาส่วนใหญ่ของปรสิตกลุ่มนี้มีรายงานอย่างกว้างขวางในหลายภูมิภาคทั่วโลก เช่น ยุโรป อเมริกา ญี่ปุ่น ตะวันออกกลาง และ ทวีปออสเตรเลีย แต่การศึกษาในแถบเอเชียตะวันออกเฉียงใต้เพิ่งเริ่มสำรวจอย่างจริงจังเมื่อไม่กี่ปีที่ผ่านมา นอกจากนี้ปรสิตกลุ่มนี้ยังพบก่อโรคในปลาสวยงามของไทยที่ส่งออกไปยังยุโรป แสดงให้เห็นว่าการศึกษา ปรสิต myxosporean ในประเทศไทยจำเป็นต้องได้รับการพัฒนา

การศึกษาครั้งนี้ได้สำรวจปรสิต myxosporean ในปลาทะเลเศรษฐกิจของไทย 4 กลุ่ม ได้แก่ ปลากระบอก ปลากะรัง ปลาดุกทะเล และปลากะพง รวม 9 ชนิด จากการศึกษาพบปรสิต myxosporean จำนวน 6 สกุล 7 ชนิด โดยพบในปลาทุกกลุ่ม ซึ่งในจำนวนนี้พบว่าเป็นปรสิตที่มีรายงานการค้นพบก่อนหน้านี้เพียง ชนิดเดียว คือ *Sphaerospora epinepheli* อย่างไรก็ตามการศึกษาก่อนหน้าได้รายงานการพบในปลากะรังดอกดำ ขณะที่การศึกษาครั้งนี้พบทั้งในปลากะรังดอกดำและปลากะรังดอกแดงและไม่พบการติดเชื้อปรสิตในปลากะรัง อีก 3 ชนิดที่ทำการศึกษา ซึ่งเป็นข้อมูลที่น่าสนใจอย่างยิ่งทางปรสิตวิทยา เนื่องจากส่วนใหญ่ปรสิตกลุ่มนี้มี ความจำเพาะต่อเจ้าบ้านสูง โดยลักษณะการเกิดโรคและพยาธิสภาพของปรสิต *S. epinepheli* ในปลากะรังดอก แดง พบว่าปรสิตมีการทำลายท่อไตอย่างรุนแรง นอกจากนี้การศึกษาสายวิวัฒนาการพบว่าปรสิตชนิดนี้อยู่ใน กลุ่ม sphaerosporid ซึ่งเป็นกลุ่มที่มีการวิวัฒนาการที่แตกต่างจากปรสิต myxosporean ทั่วไป อีกทั้งปัจจุบันทั่ว โลกมีรายงานปรสิตกลุ่มนี้เพียง 6 ชนิดเท่านั้น และจากการศึกษาการแพร่ระบาด พบว่าปรสิต *S. epinepheli* มี การแพร่ระบาดอย่างกว้างขวางทั้งในเขตอ่าวไทย ทะเลสาบสงขลา และทะเลอันดามัน ซึ่งการจัดจำแนกปรสิต ชนิดนี้ทำได้ยาก ดังนั้นจึงศึกษาและพัฒนากระบวนการตรวจวินิจฉัยอย่างรวดเร็วโดยประยุกต์ใช้เทคนิคด้าน พันธุกรรม ซึ่งศึกษาเปรียบเทียบประสิทธิภาพการตรวจวินิจฉัย 2 เทคนิค ได้แก่ real time loop-mediated isothermal amplification (real time LAMP) และ SYBR qPCR ซึ่งพบว่าทั้ง 2 เทคนิคมีประสิทธิภาพใกล้เคียง กัน อย่างไรก็ตาม real time LAMP มีการใช้งานที่ง่ายและประหยัดกว่า qPCR

จากข้อมูลปรสิตที่ไม่สามารถจัดจำแนกชนิดได้จำนวน 6 ชนิด ผู้วิจัยได้เลือกปรสิต *Myxobolus* sp. ที่พบในเนื้อเยื่อผิวหนังใต้เกล็ดของปลากระบอก (*Valamugil seheli*) มาทำการศึกษายืนยันการค้นพบ สิ่งมีชีวิตชนิดใหม่ของโลก โดยตั้งชื่อ *M. supamattayai* n. sp. และศึกษาอย่างละเอียดทั้งในส่วนของลักษณะทาง สัณฐานวิทยา ultra-structure และสายวิวัฒนาการ รวมถึงวิธีการตรวจวินิจฉัยอย่างง่าย (semi-nested PCR) และ ได้รายงานการพบปรสิต myxosporean ในปลาทะเลเศรษฐกิจของไทยทั้งในแง่ของชนิด การแพร่กระจาย และ

ให้รายละเอียดเกี่ยวกับสายวิวัฒนาการ ลักษณะพยาธิสภาพ ultra-structure รวมถึงเทคนิคในการตรวจวินิจฉัย
ปรสิตที่สนใจ 2 ชนิด ได้แก่ *S. epinepheli* และ *M. supamattayai* n. sp.

ABSTRACT

Myxosporean are common eukaryotic parasites in culture and wild fish. Some of them are important pathogens of host fish such as *Myxobolus cerebralis*, causative agent of the whirling diseases in salmonids. There has been studies of this pathogen worldwide including Europe, America, Japan, Middle East and Australia. However, the studies on this parasite group in Southeast Asia have been started recently. The important incidence with high impact is the detection of just myxosporean species in ornamental fish exported from Thailand to Europe. Thereafter, myxosporean studies in Thailand started to be remarkable in order to gain up-to-date knowledge to solve the problem.

In this study, we surveyed myxosporean in 9 fish species from 4 groups of marine economic fish of Thailand, mullet, grouper, marine catfish and Asian sea bass. Seven species in 6 genera of myxosporean were found to infect the fish observed. However, most of the found parasites are unidentified species. *Spherospora epinepheli* is the only known species previously described in malabar grouper. In our report, *S. epinepheli* were detected in malabar and orange spotted grouper, but could not be found in other studied grouper species. This observation, a capability to infect narrow host range, is important for parasitology because it is contradictory with the previous principle that myxosporean normally show high degree of host specific. Histopathological changes caused by *S. epinepheli* expressed violent destruction in renal tubes. In addition, the phylogenetic position classified *S. epinepheli* in sphaerosporid clade, an ancestor taxa of Myxosporea class of which only 6 species have been recently reported in the world record. Moreover, geographic distribution revealed the broad occurrence of this species that could be detected in the Gulf of Thailand, Songkhla Lake and Andaman coast. Since it is very complicated to identify *S. epinepheli*, rapid molecular assays, real time loop mediated isothermal

amplification (real time LAMP) and SYBR qPCR, were developed and compared for their advantages. Even though the sensitivity and specificity of these two techniques was similar, real time LAMP was recommended for field diagnosis because of it is simple, fast and cheaper technique than qPCR.

From our observation of 6 un-classified species, *Myxobolus* sp., on epithelial in scale pocket of mullet, was selected for further studies. We can describe a new recorded species of myxosporean, named *M. supamattayai* n. sp. Biological data, molecular phylogeny, ultra-structure and simple diagnosis (Semi-nested PCR) of this species were thoroughly investigated. Other myxosporeans infected in economic fish were also described for their distribution, histopathology, ultrastructure and phylogeny. Rapid diagnosis techniques were also developed for *S. epinepheli* and *M. supamattayai* n. sp.

ACKNOWLEDGEMENTS

CONTENTS

CONTENTS (Continued)

LIST OF TABLES

LIST OF FIGURES

1. INTRODUCTION

1.1 Research background

Myxosporean are aquatic, eukaryotic parasites that have a complex life cycle requiring two hosts. Some myxosporean have caused serious problems not only in aquaculture but also wild economic fish, such as whirling disease in salmonids. The invertebrate host identified so far is an annelid or bryozoan (Kent *et al.*, 2001). Wide ranges of vertebrate hosts have been reported, eg. fish, amphibians, ducks and even some mammals such as the shrew and mole including immunodeficiency human (Bartholomew *et al.*, 2008; Garner *et al.*, 2005; Kent *et al.*, 2001; Lom and Dyková, 2006; Moncada *et al.*, 2001; Prunescu *et al.*, 2007). *Myxobolus cerebralis*, a classical model of myxosporean life cycle development within the hosts has been described. The model suggested that the invertebrate host is the site of sexual reproduction while asexual reproduction occurs in the vertebrate host (Wolf and Markiw, 1984). Transmission of the parasite typically occurs indirectly via the spore stage released from the invertebrate host while direct transmission from fish to fish has been shaded in *Myxidium leei* (Diamant, 1997) and *Kudoa ovivora* (Swearer and Robertson, 1999).

Myxosporean parasite causes devastating diseases in freshwater, brackish water and marine fish for example, trout, common carp and channel catfish. Moreover, there have been reports for its worldwide biodiversity and its effects in wild fish (Baska *et al.*, 2009; Lom and Dyková, 2006; Supamattaya *et al.*, 1991) including North America, South America, Europe, Africa and Asia. In Thailand, myxosporean have also been found in several groups of economic fish both brackish water and marine fish such as mullet, grouper, spotted scat and Asian sea bass and also in freshwater fish, giant gourami. However, studies on myxosporean for its

ability to cause diseases in fish remain scarce. In Southeast Asia there has been rare reported on molecular study, evolution, phylogenetic taxonomy and biodiversity in nature and life cycle of this pathogen. Moreover, the host responses against this pathogen and its diagnosis have not been determined. This report studies therefore aim to investigate and characterize myxosporean species and distribution in four Thai economic fish, mullet, grouper, gray eel-catfish and sea bass, collected from small scale fisheries and cage culture in southern Thailand including the Gulf of Thailand, the Andaman Sea and Songkhla Lake.

1.2 Objectives

1. To study the occurrence and distribution of parasitic myxosporean in marine economic fish of Thailand.

2. To study the species description and phylogeny of interesting parasite species, new species classification.

3. To study pathology and develop the rapid molecular diagnosis for high impact myxosporean economic fish.

References

Bartholomew, J. L., Atkinson, S. D., Hallett, S. L., Lowenstine, L. J., Garner, M. M., Gardiner, C. H., Rideout, B. A., Keel M. K. and Brown, J. D. 2008. Myxozoan parasitism in waterfowl. Int. J. Parasitol. 38 : 1199–1207.

Baska, F., Voronin, V., Eszterbauer, E., Müller, L., Marton, S. and Molnár M. 2009. Occurrence of two myxosporean species, *Myxobolus hakyi* sp. n. and *Hoferellus pulvinatus* sp. n., in *Pangasianodon hypophthalmus* fry imported from Thailand to Europe as ornamental fish. Parasitol. Res. 105 : 1391–1398.

Diamant, A. 1997. Fish-to-fish transmission of a marine myxosporean. Dis. Aquat. Org. 30 : 99–105.

Garner, M. M., Bartholomew, J. L., Whipps, C. M., Nordhausen, R. W. and Raiti, P. 2005. Renal myxozoanosis in crowned river tutles *Hardella thurjii*: Description of the putative agent *Myxidium hardella* n. sp. by histopathology, electron microscopy, and DNA sequencing. Vet. Pathol. 42 : 589–595.

Kent, M. L., Andree, K. B., Bartholomew, J. B., El-Matbouli, M., Desser, S. S., Devlin, R. H., Feist, S. W., Hedrick, R. P., Hoffmann, R. W., Khattra, J., Hallett, S. L., Lester, J. G., Longshaw, M., Palenzuela, O., Siddall, M. E. and Xiao, C. 2001. Recent advances in our knowledge of the Myxozoa. J. Eukaryot. Microbiol. 48 : 395–413.

Lom J. and Dyková, I. 2006. Myxozoan genera: definition and notes on taxonomy, life-cycle terminology and pathogenic species. Folia Parasitol. 53 : 1–36.

Moncada, L. I., López, M. C., Murcia, M. I., Nicholls, S., León, F., Guío, O. L. and Corredor, A. 2001. *Myxobolus* sp., Another opportunistic parasite in immunosuppressed patients? J. Clin. Microbiol. 39 : 1938–1940.

Prunescu, C. C., Prunescu, P., Pucek, Z. and Lom, J. 2007. The first finding of myxosporean development from plasmodia to spores in terrestrial mammals: *Soricimyxum fegati* gen. et sp n. (Myxozoa) from *Sorex araneus* (Soricomorpha). Folia Parasitol. 54 : 159–164.

Supamattaya, K., Fischer-Scherl, T., Hoffmann, R. W. and Boonyaratpalin, S. 1991. *Sphpaerospora epinepheli* n. sp. (Myxosporea: Sphaerosporidae) observed in grouper (*Epinephelus malabaricus*). J. Eukaryot. Microbiol. 38 : 448–454.

Swearer, S. E. and Robertson, D. R. 1999. Life history, pathology, and description of *Kudoa ovivora* n. sp. (Myxozoa, Myxosporea): an ovarian parasite of Caribbean labroid fishes. J. Parasitol. 85 : 337–353.

Wolf, K. and Markiw, M. E. 1984. Biology contravenes taxonomy in the Myxozoa: new discoveries show alternation of invertebrate and vertebrate hosts. Science 225 : 1449–1452.

2. REVIEW OF LITERATURE

2.1 Current knowledge of parasitic myxosporean

Myxozoa is one of important group of parasites in economic fish. They are best known as pathogenic parasites in commercially important fish hosts. Globally, there are more than 2,180 species have been assigned to only 62 genera of *Myxozoa* (Lom and Dyková, 2006) and fish myxosporean have been reported mostly from Europe and North America while only a few reports especially in marine economic fish have been reported in South East Asia. Recently a myxozoan-like parasite has been found in the brain of a mole, *Talpa europrea* (Kent *et al.*, 2001).

The life cycle of myxosporean has been shown by Wolf and Markiw (1984). The landmark discovery of the life cycle of *Myxobolus cerebralis* involves alternation with an actinosporean form in *Tubifex tubifex*. Furthermore, the establishment of laboratory infection has led a more precise understanding of the early development of myxozoans (El-Matbouli *et al.*, 1999). In the first stage of life cycle, myxospores are ingested by tubificid worms. In the gut lumen of the worm, the spores extrude their polar capsules and attach to the gut epithelium by polar filaments. The shell valves then open along the suture line and the binucleate germ cell penetrates between the intestinal epithelial cells of the worm. This cell multiplies and produces many amoeboid cells by an asexual cell fission process called merogony. As a result of the multiplication process, the intercellular space of the epithelial cells in more than 10 neighboring worm segments may become infected. Around 60–90 days post-infection, sexual cell stages of the parasite undergo sporogenesis, and develop into pansporocysts, each of which contains eight triactinomyxon-stage spores. These spores are released from the oligochaete anus into the water. Alternatively, a fish can

become infected by eating an infected oligochaete. Infected tubificids can release triactinomyxons for at least 1 year. The triactinomyxon spores swim through the water to infect a salmonid through the skin. Penetration of the fish by these spores takes only a few seconds. Within five minutes, a sac of germ cells called a sporoplasm has entered the fish epidermis, and within a few hours, the sporoplasm splits into individual cells and will consequently spread through the fish. Within the fish, there are both intracellular and extracellular stages that reproduce in its cartilage by asexual endogeny, meaning that new cells grow within old cells. The final stage within fish is the myxospore, which is formed by sporogony. They are released into the environment when the fish decomposes or is eaten. Some recent research indicates that some fish may expel viable myxospores while still alive (Fig. 2.1).
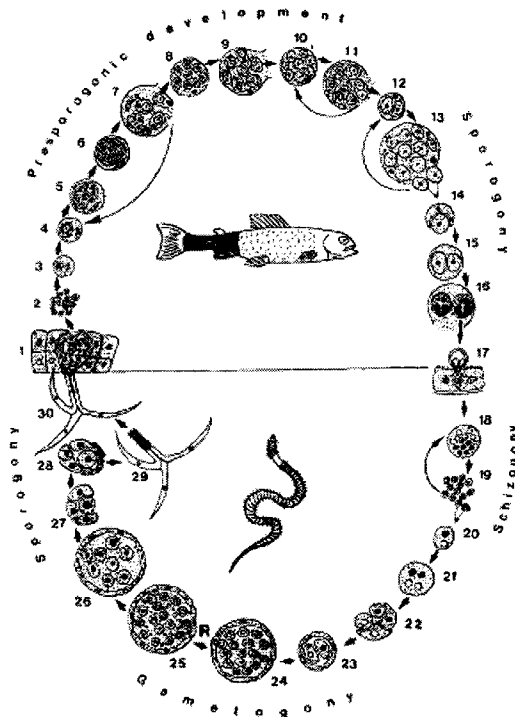
Fig. 2.1 The life cycle and development of the Myxozoa, based largely on the life cycle of *Myxobolus cerebralis*. Myxosporean development in the fish host (1-16). Actinosporean development in the annelid host (17-30). 1)

6

Actinospore attaches to surface of the fish and releases sporoplasm into the fish. 2) Sporoplasm internal cells divided by endogeny, 3) – 13) Presporogonic or extrasporogonic vegetative, 14) – 16) Sporulation with formation of multicelluar spores within plasmodia. 17) Fully-developed myxospores released from fish host replication and ingested by annelids. 18) –20) Schizogony was developed in gut epithelium of the worm. The resulting binucleate cells have an α and β nucleus, which develop into complementary gametes by the end of gamogony. 21) – 26) Gamogony, internal cells in pansporocysts undergo 3 mitotic and 1 meiotic divisions. 24)-25) Resulting gametes fuse to form a pansporocyst with 8 zygotes. 27) – 29) Sporogony, multicellular spores are formed with 3 valves, 3 polar capsules, and a sporoplasm. Inflated spores (29) are released with the worm's feces, float in the water, and contact the fish host to complete the life cycle (Kent *et al.*, 2001).

2.1.1 Definition of Myxosporea Butschli, 1881

Myxosporea exceeds the unicellular level typical of protozoa characterized by spore. These parasites are composed of several cells transfigured into 2 to 7 spore shell valves, valvogenic cell, 1–2 amoeboid infective germs, sporoplasms, and 2-7 nematocyst-like polar capsules. The latter contains an extrudible filament with an anchoring function. Morphological and functional specializations of cells are also found in trophozoite stages. Being pluricellular, Myxosporea as parasites of cavities and tissues of fish, a few representatives are found in amphibians, reptiles, mammals and invertebrates. The class Myxosporea constitutes together with the class Antinosporea the phylum Myxozoa (Lom and Dyková, 1992). The important structure

of Myxosporea mature spore consists of polar filament, polar capsule, valvogenic cell

and sporoplasmic cell (Fig. 2.2)
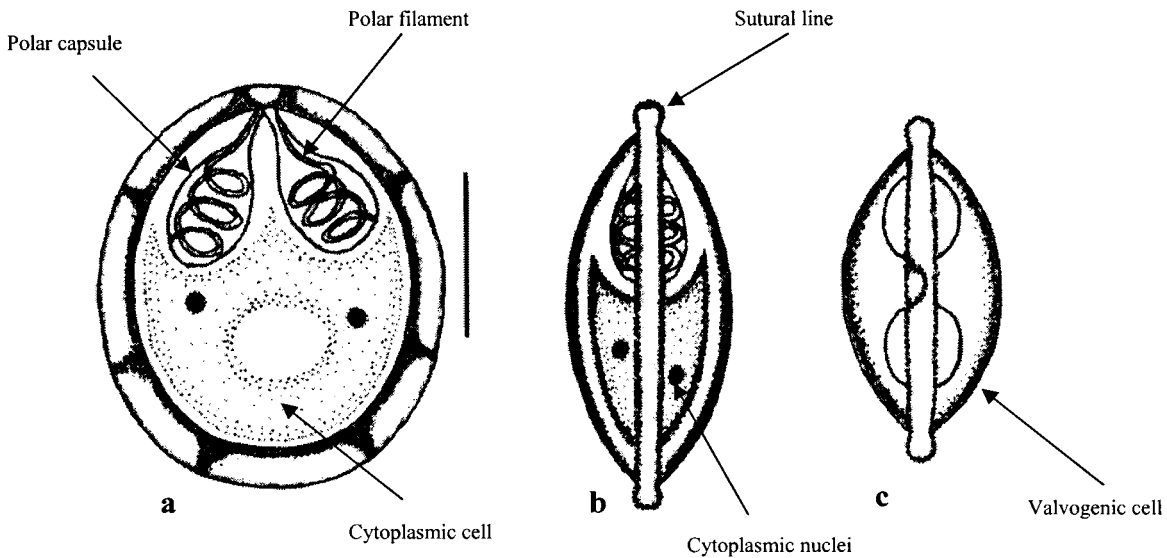
Fig. 2.2 Schematic representation of organs in mature spore of *Myxobolus* spp.: **a**-

frontal view, **b**- lateral view, **c**- apical view of anterior end. Scale bar = 3

μM. (modified from Adriano *et al.*, 2002).

2.1.2 Overview of class Myxosporea Butschli, 1881

Myxosporea Butschli, 1881, a class of phylum Myxozoa Grassé, 1970

have been recorded since the early nineteenth century. They are microscopic

multicellular organisms (Supamattaya, et al., 1991). Coelozoic species are found in

cavities such as gall bladder and urinary tract, while histozoic species occur in

variation of tissue organs, mostly in gills, kidney, muscle and nerve system.

Myxosporidia are important parasites of fresh water fish as well as marine fish,

however, they are uncommon in amphibians, reptiles, and mammals. According to

Lom and Dyková (2006), 60 genera with 2,180 species have been recorded and many

of them have a disease potential, however, the studies regarding morphological or

molecular data have not been completed. A large number of myxosporidia from fresh water fish have been studied, while relatively few from the marine environments have been described. Previously, Myxozoa were classified as protozoa. They have now been transferred to the metazoa because of their complex structure with multicellular spores consisting of specialized cells. The debate still continues as to what assemblage of metazoans they belong, either to the Radialia or to Bilateria. Thus, they are an interesting group from both practical and theoretical standpoints (Lom, 1990; Lom and Dyková, 1992; 1995; Kent *et al.*, 2000; 2001 and Canning and Okamura, 2004). Following the landmark model of *Myxobolus*-triactinomyxon transformation presented by Wolf and Markiw (1984), it has been accepted that the life cycle takes place in two hosts. The term myxosporean covers two distinct life-cycle phases, the myxospore and actinospore. The generally better known myxospore phase, resulting in production of myxospores, takes place in lower vertebrates, typically in fish. Hosts of the actinospore phase, involving a sexual process and production of actinospores, are annelids and rarely sipunculids. The myxospores are hard shelled with two to seven shell valves which produced in small or large sporogonial plasmodium. A typical feature in developmental stages is the cell-in cell condition, when the endogenously produced cell persists inside the primary cell. Myxosporea lacks centrioles and displays a closed mitosis. The microtubules of the spindle are often karyokinesis. Mitochondrial cristae are of variable shape, plate-like, tubular or discoid.

Myxosporean plasmodium and spore morphology

After sporoplasms of triactinomyxon have been injected to host tissues and developed to the sporogenic phase, a series of presporogonic stages which may be

intra- or intercellular subsequently occurs. They migrate to the site where the sporogonic stage, plasmodium or pseudoplasmodium develops. Both may develop temporary cytoplasmic projections, pseudopodia, and may divide by plasmotomy, i.e., cleavage into two or more daughter parts. Plasmodia can be taken for an extremely reduced sac- or worm-like stage of malacosporea; their cytoplasm may include a variety of cytoplasmic inclusions. Plasmodial stages may be histozoic, situated in the tissue and often appearing as cysts, or coelozoic, in cavities of body organs, mainly urinary tract or gall bladder. The plasmodium may be a large body with many vegetative nuclei of its own and with endogenously produced generative cell. These may be of one type, sporogonic cell, each of which produces a spore by division and differentiation of two types, sporogonic cell and pericyte. These two latter cells engage in spore formation, sporogony. The pericyte envelops the sporogonic cell which divides into differentiation capsulogenic, valvogenic and sporoplasmogenic cells. Corresponding numbers of these cells develop into two sporoblasts and consequently mature into myxospores inside the pericyte. Myxospores generally have a hard shell. The pericyte with the progeny of the sporogonic cell represents the pansporoblast. Plasmodia may also enclose lobocytes, large cell of presumable produced many spores, are polysporic. Pseudoplasmodia are rather small containing one nucleus and generative cell necessary to compose one or two spores, and are monosporic or disporic plasmodium. The myxospore consists mostly of one to four polar capsules, one or two sporoplasms and the actual infective grems. All these are encased with two to seven shell valves. Capsulogenesis involves regularly production of an external tube associated with the capsular primordium. Shell valves adhere together along the line of dehiscence, the suture line, and also cover the apex of polar capsule. Sporoplasm contains sporoplasmosomes, without the central lucent

invagination known in malacosporeans. Under certain conditions, the development in the fish may be arrested before the onset of sporogenesis (Lom and Dyková, 2006).

2.1.3 Taxonomy of phylum Myxozoa Grasse, 1970

The taxonomy of the parasites in this phylum persists until now are mainly according to Lom and Noble (1984) and Lom and Dyková (2006). The drawback is classification of spore morphology, namely the number and configuration of shell valves and polar capsules. This spore-based taxonomy is generally artificial but clearly at the family level and with quite vague boundaries between many genera such as *Leptotheca* and *Ceratomyxa* and *Myxidium* or between some species of *Myxobolus* and *Thelohanellus*. It does not reflect the life cycle with alternative hosts, morphology of actinospores within the definitive invertebrate hosts, host and tissue preferences and phylogenetic relationships as revealed by SSU rDNA analyses. All morphological features important in describing the Myxozoa species are listed in Lom and Dyková (2006). However categories indicated in the clades may suggest the future outlines of the classification. It would be desirable to find some other features, particularly the molecular analysis, to support them. Histozoic parasites must have evolved several times both in marine and freshwater fish and it is only some extent indicating of evolution of pertinent taxa. The molecular data which are very incomplete and based on a single gene are far from being sufficient to launch a well substantiated new classification, a situation similar to that occurs in microsporidia (Vossbrinck and Debrunner-Vossbrinck, 2005). Future classification of myxosporea should represent a synthesis of molecular phylogeny and the combined evidence of both life cycle stages of known (Xiao and Desser, 2000). Taxonomic relationship of a myxosporean should also take into account tissue tropism, which may reflect rRNA

grouping of the species in question. Also geographic origin may be decisive, as Hervio *et al.* (1997) have shown in *Kudoa* spp., which cluster according to origin rather than by spore morphology (Lom and Dyková, 2006).

Myxosporean genera

Most previous described myxosporean species established without complete morphological or molecular data. Therefore, species inventory cannot be properly revised until sufficient resolution is provided both by detailed morphological study and molecular analysis, so that numbers given for each genus may eventually be lower or perhaps even higher. Certainly, a large number of species is still unresolved.

Phylum: Myxozoa

Class: Malacosporea

Order: Malacovalvulida

Family: Saccosporidae

Genus: *Buddenbrockia*

Genus: *Tetracapsuloides*

Class: Myxosporea

Order: Bivalvulida

Suborder: Sphaeromyxina

Family: Sphaeromyxidae

Genus: *Sphaeromyxa*

Suborder: Variisporina

Family: Myxidiidae

Genus: *Myxidiium*

Genus: *Enteromyxum*

   Genus: *Zschokkella*

   Genus: *Coccomyxa*

  Family: Ortholineidae

   Genus: *Ortholinea*

   Genus: *Neomyxobolus*

   Genus: *Cardimyxobolus*

   Genus: *Triangula*

   Genus: *Kentmoseria*

  Family: Sinuolineidae

   Genus: *Sinuolinea*

   Genus: *Davisia*

   Genus: *Myxoproteus*

   Genus: *Bipteria*

   Genus: *Paramyxoproteus*

   Genus: *Neobipteria*

   Genus: *Schulmania*

   Genus: *Noblea*

  Family: Fabesporiae

   Genus: *Fabespora*

  Family: Ceratomyxidae

   Genus: *Caratomyxa*

   Genus: *Leptotheca*

   Genus: *Meglitschia*

   Genus: *Ellipsomyxa*

  Family: Sphaerosporidae

Genus: *Sphaerospora*

Genus: *Polysporoplama*

Genus: *Hoferellus*

Genus: *Wardia*

Genus: *Palliatus*

Genus: *Myxobilatus*

Family: Chloromyxidar

Genus: *Chloromyxum*

Genus: *Caudomyxum*

Genus: *Agarella*

Family: Auerbachiidae

Genus: *Auerbachia*

Genus: *globospora*

Family: Alatosporidae

Genus: *Alaatospora*

Genus: *Pseudoalatospora*

Genus: *Renispora*

Family: Paricapsulidae

Genus: *Parvicapsula*

Genus: *Neoparvicapsula*

Suborder: Platysporina

Family: Myxobolidae

Genus: *Myxobolus*

Genus: *Spirosuturia*

Genus: *Unicauda*

14

Genus: *Dicauda*

Genus: *Phlogospora*

Genus: *Laterocaudata*

Genus: *Henneguya*

Genus: *Hennegoides*

Genus: *Tetrauronema*

Genus: *Thelohanellus*

Genus: *Neothelohanellus*

Genus: *Neohenneguya*

Genus: *Trigonosporus*

Order: Multivalvulida

Family: Trilosporidae

Genus: *Trilospora*

Genus: *Unicapsula*

Family: Kudoidae

Genus: *Kudoa*

Genus: *Pentacupsula*

Genus: *Hexacupsula*

Genus: *Septemcapsula*

Genus: *Trilosporides*

Family: Spinavaculidae

Genus: *Octospina*

2.1.4 Pathology

Most of the coelozoic myxosporidia infecting fish are harmless. Histozoic or cytozoic species, however, are more harmful as they can destroy cells

and tissues. In *M. cerebralis,* the well known myxosporidia species which causes whirling disease, the trophozoites can invade cartilaginous tissues and cause movement disorder and black tails. Presporogonic stages of the coelozoic species, *Hoferellus cyprini,* infect the tubular epithelium of renal tubules of carp, and can cause large extension of tubular cell (Supamattaya, et al., 1991). However, a lot of species in phylum Myxozoa are non-violent parasite and some species have not been observed for histopathology effect in host tissue. *Sphaerospora epinepheli* is a parasite in kidney of back spotted grouper exhibiting non-distinct of histopathology change. At present, it is possible to discuss only the myxosporidia affecting fish and some important cases were mentioned.

Scales, fins and gills

Fish skin is a delicate tissue directly exposed to environment and many pathogens that can cause skin lesions including myxosporidia. This parasite can infect both fresh water and marine fish. Pathological changes of gill associated with parasite include the thickening of cutaneous epithelium filled with spores and developmental stages of parasite. A high numbers of *Myxozoa* reported as a parasite in gill tissue relate with respiratory system of host, for example *M. dykovae* reported from Malaysia (Székely *et al.,* 2009). The parasite was found intralamellary in the gill of tinfoil barb. The histological section show plasmodium located inside a gill lamella. Around the plasmodium, serum filled the space inside the lamella while the lip of lamella was not damaged. The scales of mullet were infected by *M. episquamalis* (Bahri *et al.,* 2003). Pathology effect was deformation and eventual detachment of the scales with the fibrillary layer being liquefied. Molnár *et al.* (2006) have reported the effect of three species of *Henneguya* spp. in Asian redtail catfish *Hemibagrus nemurus,* no general alterations have been found in the gills. In some fish with

Henneguya mystusia infection, whole filaments are occupied by growing and mature plasmodia which deform the lamellae. The multi-layered epithelium between the lamellae is replaced by plasmodia, and in these sections the apical parts of the lamellae are overgrown by plasmodia. In less heavily infected areas, the non-infected lamellae are also deformed by the compression exerted by plasmodia developing among the neighboring lamellae. At the tip of the filaments large, plasmodia supposedly formed by the fusion of small inter lamellar ones, completely deformed the structure of the filaments. At the base of the hemibranchia the large plasmodia of *H. basifilamentalis* compresses the neighboring filaments and no lamellae are found in this section. Above the plasmodia the basal epithelial layer is lifted up in an apical direction. At the time of examination only minor signs of recovery were observed. As a sign of past infection, granulomatous inflammatory reaction was observed in some filaments.
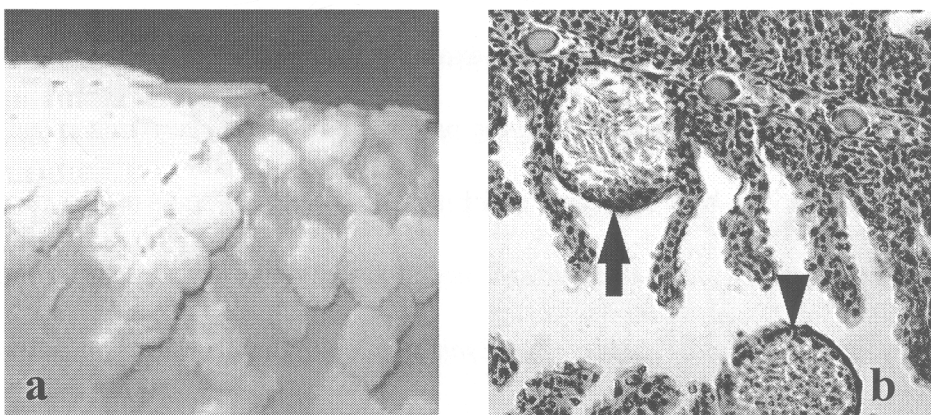
Fig. 2.3 (a, b) Pathological change of fish tissue infected with parasitic myxosporean, a; *M. episquamalis* on scales of mullet, *Mugil cephalus* (Bahri *et al.*, 2003). b; An interlamellar (*H. mystusia*) plasmodium (arrow) between gill lamellae and an intralamellar (supposedly *H. hemibagri*) plasmodium (arrowhead) inside a gill lamella (Molnár *et al.*, 2006).

Eye

There have been few reports on myxosporidia infecting the eye of fish. *M. scleroperca* infected the eye of yellow perch. Cysts of parasites are found in the scleral cartilage and adjacent periocular tissue that cause degenerative change in the lens and detachment of the ratina. *H. lagodon* is isolated from the eye of *Lagodon rhomboides* and *H. episclera* infected the episclera of the eye of pumpkinseed sunfish (*Lepomis gibbosus*). While three species of *Myxobolus* spp. and two species of *Thelohanellus* spp. are reported in the eye of many species of fish in genus *Notropis*, however, no tissue reactions and pathological changes are reported (Supamattaya, et al., 1991).

Liver and gall bladder

Most of the coelozoic myxosporidia have been found in the gall bladder of fish but some have exhibited histozoic characteristics by infecting both gall bladder and liver parenchyma, for example *Chloromyxum reticulatum*. Early developmental stages are found in liver parenchyma and polysporus plasmodia are observed later in the bile duct and gall bladder of burbot, *Lota lota*. Moreover, no pathological changes or host responses are observed. Most of myxosporidia species which are found in gall bladder are *Zschokkella* spp. and *Ceratimyxa* spp. Five-bearded rockling, *Ciliata mustela* are infected with *Z. russelli*. This parasite caused proliferation, enlargement and thickening of hepatic ducts and pericholangitis. However, many other harmless species of *Zschokkela* have been recorded in the gall bladders of fish (Lom and Dyková, 1992).

2.2 Rapid identification of pathogens

2.2.1 Loop-mediated isothermal amplification (LAMP)

Loop mediated isothermal amplification (LAMP) is a single tube technique for the amplification of DNA. It may be combined with a reverse transcription step to allow the detection of RNA. LAMP is a novel approach to nucleic acid amplification which uses a single temperature incubation thereby obviating the need for expensive thermal cyclers. Amplification product can be detected by photometry for turbidity caused by increasing quantity of magnesium pyrophosphate in solution or with addition of SYBR green, a color change can easily be observed. LAMP has the potential to be used as a simple screening assay in the field or at the point of care by clinicians. It is characterized by the use of 4 different primers specifically designed to recognize 6 distinct regions on the target gene and the reaction process proceeds at a constant temperature using strand displacement reaction. Amplification and detection of gene can be completed in a single step, by incubating the mixture of samples, primers, DNA polymerase with strand displacement activity and substrates at a constant temperature (about 65°C). It provides high amplification efficiency, with DNA being amplified 109-1010 times in 15-60 minutes. Because of its high specificity, the presence of amplified product can indicate the presence of a target gene (Notomi *et al.*, 2000).

Characteristics of LAMP technique

- There is no need for a step to denature double stranded into a single stranded form.

- The whole amplification reaction takes place continuously under isothermal conditions.

- The amplification efficiency is extremely high.

- By designing 4 primers to recognize 6 distinct regions, the LAMP method is able to specifically amplify the target gene.

- The total cost can be reduced, as LAMP dose not require special reagents or sophisticated equipments.

- The amplified products have a structure consisting of alternately inverted repeats of the target sequence on the same strand.

- Amplification can be done with RNA templates following the same procedure as with DNA templates, simply through the addition of reverse transcriptase.

Principle of LAMP technique

LAMP which can amplify nucleic acid with high specificity and rapidity under isothermal conditions is a new technique developed in recent years. The method employs a set of four specific primers and a DNA polymerase that recognizes a total of six distinct sequences on the target DNA making the amplification of the target sequence highly selective. In principle, it is an autocycling strand displacement method where the outer forward primer hybridizes and displaces the synthesized first strand with the inner primer linked complementary strand resulting in a stem loop DNA structure at one end. This strand initiates a process in which a backward inner primer hybridizes to the other end of the target DNA and

results in strand displacement by the backward outer primer to form a dumbbell shape. This process continues in subsequent lamp cycles resulting in final products of multiple stem loop DNAs as described by Notomi *et al.* (2000). When these stem loop DNAs are visualized by agarose gel electrophoresis, several bands of different sizes are seen in a single well.

When the target gene (DNA template as an example) and the reagents are incubated at a constant temperature between 60-65°C, the following reaction steps proceed. The continuing steps are shown in the Fig. 2.4–2.12 (modified from http://loopamp.eiken.co.jp/e/lamp/index.html).
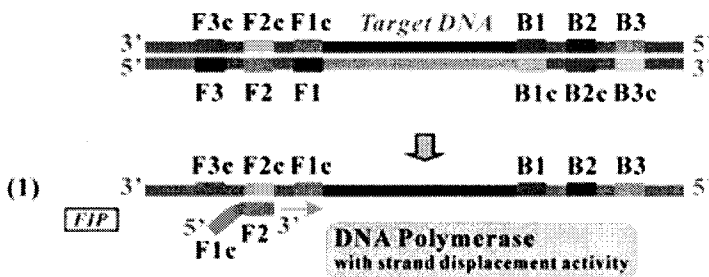
Fig. 2.4 Reaction step of Loop-mediated isothermal amplification (LAMP); Step (1): As double stranded DNA is in the condition of dynamic equilibrium at the temperature around 65°C, one of the LAMP primers can anneal to the complimentary sequence of double stranded target DNA, then initiates DNA synthesis using the DNA polymerase with strand displacement activity, displacing and releasing a single stranded DNA. With the LAMP method, unlike with PCR, there is no need for heat denaturation of the double stranded DNA into a single strand. The following amplification mechanism explains from when the FIP anneals to such released single stranded template DNA.

(2)

F3c F2c F1c   B1 B2 B3

3'   5'
5'   F2 F1   B1c B2c B3c   3'
F1c
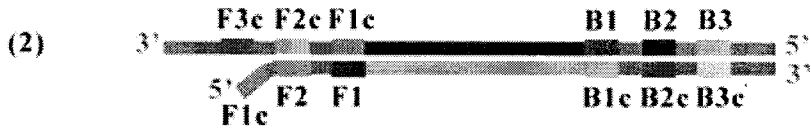
Fig. 2.5 Reaction step of LAMP; Step (2): Through the activity of DNA polymerase with strand displacement activity, a DNA strand complementary to the template DNA is synthesized, starting from the 3' end of the F2 region of the FIP.

(3)

F3c F2c F1c   B1 B2 B3

3'   5'
F3 Primer   3'
F3   F2 F1   B1c B2c B3c
F1c
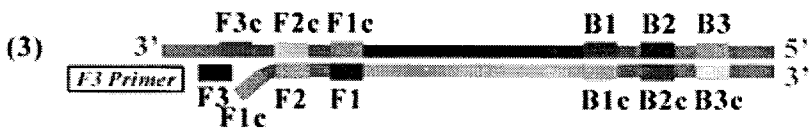
Fig. 2.6 Reaction step of LAMP; Step (3): The F3 Primer anneals to the F3c region, outside of FIP, on the target DNA and initiates strand displacement DNA synthesis, releasing the FIP-linked complementary strand.

(4)

F3c F2c F1c   B1 B2 B3

3'   5'
5'   3'
F3 F2 F1   B1c B2c B3c
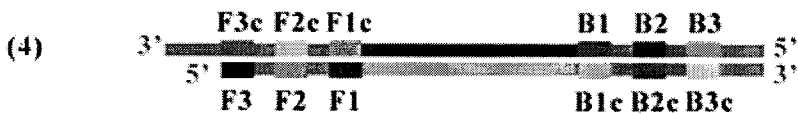
Fig. 2.7 Reaction step of LAMP; Step (4): A double strand is formed from the DNA strand synthesized from the F3 Primer and the template DNA strand.

(5)

5'   3'
F1c F2 F1   B1c B2c B3c

Fig. 2.8 Reaction step of LAMP; Step (5): The FIP-linked complementary strand is released as a single strand because of the displacement by the DNA strand

22

synthesized from the F3 Primer. Then, this released single strand forms a stem-loop structure at the 5' end because of the complementary F1c and F1 regions.

(6)

Fig. 2.9 Reaction step of LAMP; Step (6): This single strand DNA in Step (5) serves as a template for BIP-initiated DNA synthesis and subsequent B3-primed strand displacement DNA synthesis. The BIP anneals to the DNA strand produced in Step (5). Starting from the 3' end of the BIP, synthesis of complementary DNA takes place. Through this process, the DNA reverts from a loop structure into a linear structure. The B3 Primer anneals to the outside of the BIP and then, through the activity of the DNA polymerase and starting at the 3' end, the DNA synthesized from the BIP is displaced and released as a single strand before DNA synthesis from the B3 Primer.

(7)
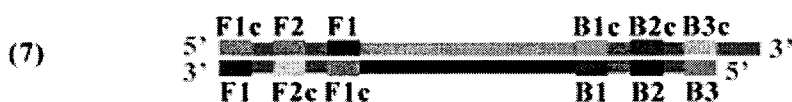
Fig. 2.10 Reaction step of LAMP; Step (7): Double stranded DNA is produced through the processes described in Step (6).

(8)

Fig. 2.11 Reaction step of LAMP; Step (8): The BIP-linked complementary strand displaced in Step (6) forms a structure with stem-loops at each end, which looks like a dumbbell structure. This structure serves as the starting structure for the amplification cycle in the LAMP method (LAMP cycling).

The above process can be understood as producing the starting structure for LAMP cycling.
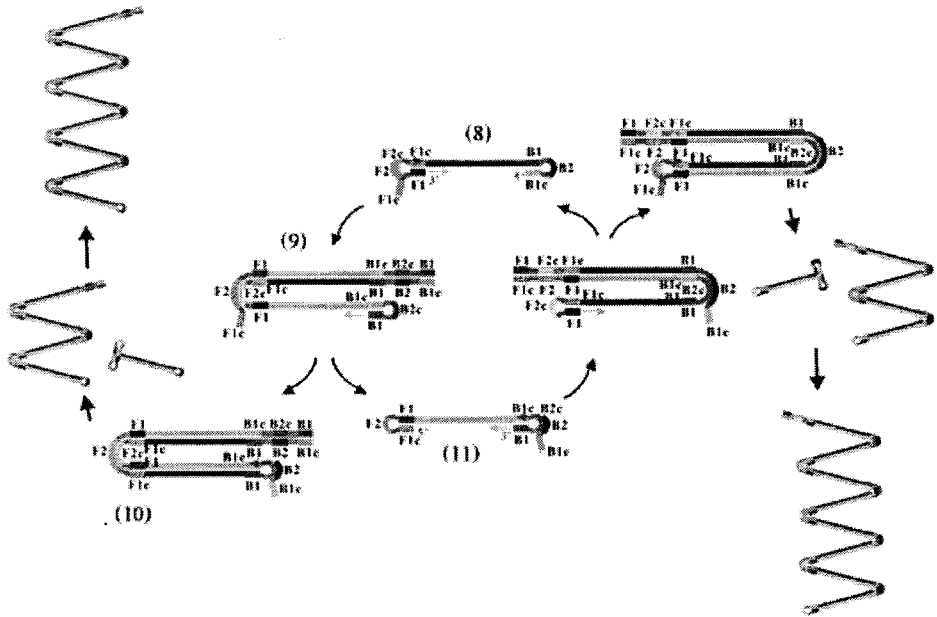
Fig. 2.12 Cycling amplification step of LAMP: A dumbbell-like DNA structure is quickly converted into a stem-loop DNA by self-primed DNA synthesis. FIP anneals to the single stranded region in the stem-loop DNA and primes strand displacement DNA synthesis, releasing the previously synthesized strand. This released single strand forms a stem-loop structure at the 3' end because of complementary B1c and B1 regions. Then, starting from the 3' end of the B1 region, DNA synthesis starts using self-structure as a template, and releases FIP-linked complementary strand (Step (9)). The released single strand then forms a dumbbell-like structure as both ends have complementary F1 - F1c and B1c - B1 regions, respectively (Step (11)). This structure is the 'turn over' structure of the structure formed in Step (8). Similar to the Steps from (8) to (11), structure in Step (11) leads to self-primed DNA synthesis starting from the 3' end of the B1 region. Furthermore, BIP anneals to the B2c region

and primes strand displacement DNA synthesis, releasing the B1-primed

DNA strand. Accordingly, similar structures to Steps (9) and (10) as well

as the same structure as Step (8) are produced. With the structure

produced in Step (10), the BIP anneals to the single strand B2c region,

and DNA synthesis continues by displacing double stranded DNA

sequence. As a result of this process, various sized structures consisting of

alternately inverted repeats of the target sequence on the same strand are

formed.

Primer design

Four types of primers (described in Fig. 2.13) are designed based on

the following 6 distinct regions of the target gene: the F3c, F2c and F1c regions at the

3' side and the B1, B2 and B3 regions at the 5' side.
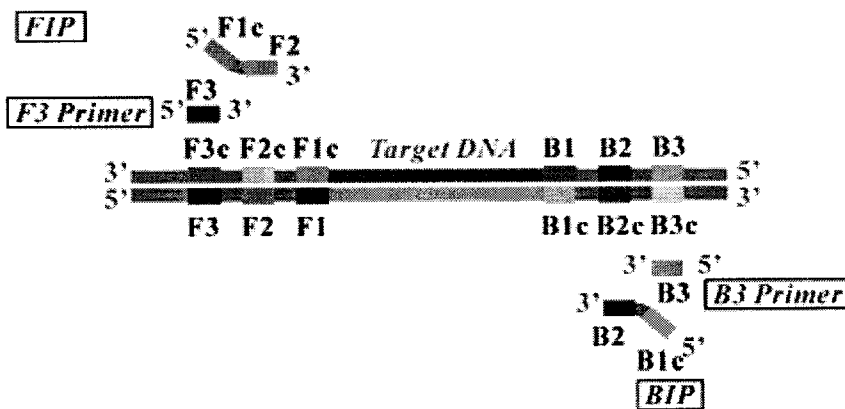
Fig. 2.13 Diagram of primer design for LAMP technique: FIP, Forward Inner Primer

(FIP) consists of the F2 region (at the 3' end) that is complementary to the

F2c region, and the same sequence as the F1c region at the 5' end., F3

Primer, Forward Outer Primer consists of the F3 region that is

complementary to the F3c region., BIP, Backward Inner Primer (BIP)

consists of the B2 region (at the 3' end) that is complementary to the B2c region, and the same sequence as the B1c region at the 5' end and B3 Primer, Backward Outer Primer consists of the B3 region that is complementary to the B3c region (modified from http://loopamp.eiken.co.jp/e/lamp /index.html).

2.2.2 Real time polymerase chain reaction (Real time PCR)

The advent of real-time PCR and real-time reverse transcription PCR (real time RT-PCR) has dramatically changed the field of gene expression measurement. Real-time PCR is the technique of collecting data throughout the PCR process as it occurs, thus combining amplification and detection into a single step. This is achieved using a variety of different fluorescent chemistries that correlate PCR product concentration to fluorescence intensity (Higuchi *et al.*, 1993). Reactions are characterized by the point in time (or PCR cycle) where the target amplification is first detected. This value is usually referred to as cycle threshold (C_t), the time at which fluorescence intensity is greater than background fluorescence. Consequently, the greater the quantity of target DNA in the starting material, the faster a significant increase in fluorescent signal will appear, yielding a lower C_t (Heid *et al.*, 1996).

There are many benefits of using real-time PCR over other methods to quantify gene expression. It can produce quantitative data with an accurate dynamic range of 7 to 8 log orders of magnitude (Morrison *et al.*, 1998) and does not require post-amplification manipulation. Real-time PCR assays are 10,000- to 100,000-fold more sensitive than RNase protection assays (Wang and Brown, 1999), 1000-fold more sensitive than dot blot hybridization (Malinen *et al.*, 2003), and can even detect a single copy of a specific transcript (Palmer *et al.*, 2003). In addition, real-time PCR

assays can reliably detect gene expression differences as small as 23% between samples (Gentle *et al.*, 2001) and have lower coefficients of variation (cv; SYBR® Green at 14.2%; TaqMan® at 24%) than end point assays such as band densitometry (44.9%) and probe hybridization (45.1%) (Schmittgen *et al.*, 2000). The major disadvantage to real-time PCR is that it requires expensive equipment and reagents. In addition, due to its extremely high sensitivity, sound experimental design and an in-depth understanding of normalization techniques are imperative for accurate conclusions.

Theory of real-time PCR

PCR can be divided into four major phases: (1) the linear ground phase (2) early exponential phase (3) log-linear (also known as exponential) phase and (4) plateau phase (Tichopad *et al.*, 2003). During the linear ground phase (usually the first 10–15 cycles), PCR is just beginning, and fluorescence emission at each cycle has not yet risen above background. Baseline fluorescence is calculated at this time. At the early exponential phase, the amount of fluorescence has reached a threshold where it is significantly higher (usually 10 times the standard deviation of the baseline) than background levels. This value is representative of the starting copy number in the original template and is used to calculate experimental results (Heid *et al.*, 1996). During the log-linear phase, PCR reaches its optimal amplification period with the PCR product doubling after every cycle in ideal reaction conditions. Finally, the plateau stage is reached when reaction components become limited and the fluorescence intensity is no longer useful for data calculation (Bustin, 2000).

References

Adriano, E. A., Arana, S., Ceccarelli, P. S. and Coederio, N. S. 2002. Light and scanning electron microscopy of *Myxobolus porofilus* sp. n. (Myxosporea: Myxobolidae) infecting the visceral cavity of *Prochilodus lineatus* (Pisces: Characiformes: Prochilodontidae) cultivated in Brazil. Folia Parasitol. 49 : 259–262.

Bahri, S., Andree, K. B. and Hedrick, R. P. 2003. Morphological and phylogenetic studies of marine *Myxobolus* spp. from mullet in Ichkeul Lake, Tunisia. J. Eukaryot. Microbiol. 50 : 463–470.

Bustin, S. A. 2000. Absolute quantification of mRNA using real-time reverse transcription polymerase chain reaction assays. J. Mol. Endocrinol. 25 : 169–193.

Canning, E. U. and Okamura, B. 2004. Biodiversity and evolution of the Myxozoa. Adv. Parasitol. 56 : 43–131.

Eiken GENOME SITE. The Principle of LAMP method. Available: http://loopamp.eiken.co.jp/e/lamp/principle.html [accessed February, 24, 2009].

El-Matbouli, M., McDowell, T. S., Antonio, D. B., Andree, K. B. and Hedrick, R. P. 1999. Effect of water temperature on the development, release and survival of the triactinomyxon stage of *Myxobolus cerebralis* in its oligochaete host. Int. J. Parasitol. 29 : 627–641.

Gentle, A., Anastasopoulos, F. and McBrien, N. A. 2001. High-resolution semi-quantitative real-time PCR without the use of a standard curve. BioTechniques 31 : 502–508.

Heid, C. A., Stevens, J., Livak, K. J. and Williams, P. M. 1996. Real time quantitative PCR. Genome Res. 6 : 986–994.

Hervio, D. M. L., Khattra, J., Devlin, R. H., Kent, M. L., Sakanari, J. and Yokoyama, H. 1997. Taxonomy of *Kudoa* species (Myxosporea), using a small-subunit ribosomal DNA sequence. Can. J. Zool. 75 : 2112–2119.

Higuchi, R., Fockler, C., Dollinger, G. and Watson, R. 1993. Kinetic PCR analysis: real-time monitoring of DNA amplification reactions. Biotechnology (NY) 11 : 1026–1030.

Hornung, V., Rothenfusser, S., Britsch, S., Krug, A., Jahrsdörfer, B., Giese, T., Endres, S. and Hartmann, G. 2002. Quantitative expression of Toll-like receptor 1–10 mRNA in cellular subsets of human peripheral blood mononuclear cells and sensitivity to CpG oligodeoxynucleotides. J. Immunol. 168 : 4531– 4537.

Kent, M. L., Andree, K. B., Bartholomew, J. B., El-Matbouli, M., Desser, S.S., Devlin, R. H., Feist, S. W., Hedrick, R. P., Hoffmann, R. W., Khattra, J., Hallett, S. L., Lester, J. G., Longshaw, M., Palenzuela, O., Siddall, M. E. and Xiao, C. 2001. Recent advances in our knowledge of the Myxozoa. J. Eukaryot. Microbiol. 48 : 395–413.

Kent, M. L., Khattra, J., Hedrick, R. P. and Devlin, R. H. 2000. *Tetracapsula renicola* n. sp. (Myxozoa : Saccosporidae); the PKX myxozoan--the cause of proliferative kidney disease of salmonid fishes. J. Parasitol. 86 : 103–111.

Krieg, A. M. 2002. CpG motifs in bacterial DNA and their immune effects. Annu. Rev. Immunol. 20 : 709–760.

Lipford, G. B., Sparwasser, T., Zimmermann, S., Heeg, K. and Wagner, H. 2000. CpG-DNA-mediated transient lymphadenopathy is associated with a state of Th1 predisposition to antigen-driven responses. J. Immunol. 165 : 1228–1235.

Lom, J. 1990. Phylum Myxozoa. *In* Handbook of Protoctista. (eds. L. Margulis, J. O. Corliss, M. Kelkonian and D. J. Chapman), pp. 36–52. Boston : Jones and Bartlett.

Lom, J. and Dyková, I. 1992. Protozoan parasites of fish. Amsterdam : Elsevier.

Lom, J. and Dyková, L. 1995. Myxosporea (Phylum Myxozoa). *In* Fish Diseases and Disorders. (ed P. T. K. Woo) Vol. 1, pp. 97–148. Waling Ford : CAB International.

Lom, J. and Dyková, I. 2006. Myxozoan genera: definition and notes on taxonomy, life-cycle terminology and pathogenic species. Folia Parasitol. 53 : 1–36.

Lom, J. and Noble, E. R. 1984. Revised classification of the class Myxosporea Bütschli, 1881. Folia Parasitol. 31 : 193–205.

Malinen, E., Kassinen, A., Rinttila, T. and Palva, A. 2003. Comparison of real-time PCR with SYBR Green I or 5′-nuclease assays and dot-blot hybridization with rDNA-targeted oligonucleotide probes in quantification of selected faecal bacteria. Microbiology 149 : 269–277.

Mena, A., Nichani, A. K., Popowych, Y., Ioannou, X. P., Godson, D. L., Mutwiri, G. K., Hecker, R., Babiuk, L. A. and Griebel, P. 2003. Bovine and ovine blood mononuclear leukocytes differ markedly in innate immune responses induced by Class A and Class B CpG-oligodeoxynucleotide. Oligonucleotides 13 : 245–259.

Molnár, K., Székely, C., Mohamed, K. and Shaharom-Harrison, F. 2006. Myxozoan pathogens in cultured Malaysian fishes. I. Myxozoan infections of the sutchi catfish Pangasius hypophthalmus in freshwater cage cultures. Dis. Aquat. Org. 68 : 209–218.

Morrison, T. B., Weis, J. J. and Wittwer, C.T. 1998. Quantification of low-copy transcripts by continuous SYBR Green I monitoring during amplification. Bio.Techniques. 24 : 954–962.

Mutwiri, G. K., Nichani, A. K., Babiuk, S. and Babiuk, L. A. 2004. Strategies for enhancing the immunostimulatory effects of CpG oligodeoxynucleotides. J. Control Release 97 : 1–17.

Nichani, A. K., Mena, A., Popowych, Y., Dent, D., Townsend, H. G. G., Mutwiri, G. K., Hecker, R., Babiuk, L. A. and Griebel, P. J. 2004. In vivo immunostimulatory effects of CpG oligodeoxynucleotide in cattle and sheep. Vet. Immunol. Immunopathol. 98 :17–29.

Notomi, T., Okayama, H., Masubuchi, H., Yonekawa, T., Watanabe, K., Amino, N. and Hase, T. 2000. Loop-mediated isothermal amplification of DNA. Nucleic Acids Res. 28 : e63.

Palmer, S., Wiegand, A. P., Maldarelli, F., Bazmi, H., Mican, J. M., Polis, M., Dewar, R. L. and Planta, A. 2003. New real-time reverse transcriptase-initiated PCR assay with single-copy sensitivity for human immunodeficiency virus type 1 RNA in plasma. J. Clin. Microbiol. 41 : 4531–4536.

Schmittgen, T. D., Zakrajsek, B. A., Mills, A. G., Gorn, V., Singer, M. J. and Reed, M. W. 2000. Quantitative reverse transcription-polymerase chain reaction to study mRNA decay: comparison of endpoint and real-time methods. Anal. Biochem. 285 : 194–204.

Supamattaya, K., Fischer-Scherl, T., Hoffmann, R. W. and Boonyaratpalin, S. 1991. *Sphpaerospora epinepheli* n. sp. (Myxosporea: Sphaerosporidae) observed in grouper (*Epinephelus malabaricus*). J. Eukaryot. Microbiol. 38 : 448–454.

Székely, C., Shaharom-Harrison, F., Cech, G., Mohamed, K. and Molnár, K. 2009. Myxozoan pathogens of Malaysian fishes cultured in ponds and net-cages. Dis. Aquat. Org. 83 : 49–57.

Tassakka, A. C. M. A. R. and Sakai, M. 2002. CpG oligodeoxynucleotides enhance the non-specific immune responses on carp, *Cyprinus carpio*. Aquaculture 209 : 1–10.

Tassakka, A. C. M. A. R. and Sakai, M. 2004. Expression of immune-related genes in the common carp (*Cyprinus carpio* L.) after stimulation by CpG oligodeoxynucleotides. Aquaculture 242 : 1–12.

Tassakka, A. C. M. A. R. and Sakai, M. 2005.Current research on the immunostimulatory effects of CpG oligodeoxynucleotides in fish. Aquaculture 246 : 25–36.

Tichopad, A., Dilger, M., Schwarz, G. and Pfaffl, M.W. 2003. Standardized determination of real-time PCR efficiency from a single reaction set-up. Nucleic Acids Res. 31 : e122.

Vossbrinck, C. R. and Debrunner-Vossbrinck, B. A.2005. Molecular phylogeny of the Microsporidia: ecological, ultrastructural and taxonomic considerations. Folia Parasitol. 52 : 131–142.

Wang, T. and Brown, M. J. 1999. mRNA quantification by real time TaqMan polymerase chain reaction: validation and comparison with RNase protection. Anal. Biochem. 269 : 198–201.

Wolf, K. and Markiw, M. E. 1984. Biology contravenes taxonomy in the myxozoa: new discoveries show alternation of invertebrate and vertebrate hosts. Science 225 : 1449–1452.

Xiao, C. and Desser, S. S. 2000. Cladistic analysis of myxozoan species with known alternating life-cycles. Syst. Parasitol. 46 : 81–91.

Yamamoto, T., Yamamoto, S., Kataoka, T. and Tokunaga, T. 1994. Lipofection of synthetic oligodeoxyribonucleotide having a palindromic sequence of AACGTT to murine splenocytes enhances interferon production and natural killer activity. Microbiol. Immunol. 38 : 831–836.

3. THE SURVEY OF MYXOSPOREAN PARASITES ON WILD AND CULTURED ECONOMIC FISH OF THAILAND

Abstract

The phylum Myxozoa Grasse, 1970 is composed of two classes Malacosporea and Myxosporea. Myxosporidia are important parasites of cavities and tissues of freshwater and marine fish. Although there are numerous detailed descriptions of myxosporean species from important fishery areas, in Southeast Asia the studies in Thai marine economic fish species have been scarce. During a survey of these parasites in 4 high value marine fish groups, 5 species of grouper, Asian sea bass (*Lates calcarifer*), marine catfish, *Plotosus canius* and 2 species of mullet from southern Thailand including the Gulf of Thailand, Songkhla Lake and Andaman sea, six unidentified species from five genera and one known species, *Spherospora epinepheli* were found. Morphometry and light microscopy (DIC) of mature spores of each species are presented.

Introduction

Since 1995, Myxosporean have been classified as metazoan. They are primitive metazoan organisms secondarily degraded by parasitism with morphological and functional cell specialization. Because of long tradition of assignment to protozoa and, their microsopic size and considerable classified in early stage parasitology, they are always treated together with protists. One belonging to the two classes of Myxozoa is Malacosporea which lives in bryozoans while another one could infect fish. Members of the latter class, Myxosporea, infect in course of their complicated life cycle in vertebrates, mainly fish, and invertebrates, annelids and some sipunculids

34

(Lom and Dyková, 2006). Myxosporean are characterized by spore morphology composed of several cells, which gradually transform into shell valves, polar capsules and amoeboid infections cell or sporoplasms. Polar capsules are conspicuous by being refractile when viewed in fresh stage. Their polar filament serves for attachment of an ingested spore to the host tissue such as gill, skin and intestine. Then, myxosporean are transformed into trophozoites and generated in the target host tissue (Dyková and Lom, 2007).

Fish culture and fishery is an important developing branch of agriculture industrial in Southeast Asia (SE-Asia). Although the semi-intensive marine culture of fish species such as orange spotted grouper and Asian sea bass and their economic utilization are expanding in tropical countries, little is known about myxosporean infection and invasive agents causing damages to stocks of these species which is important for sustainable food development in SE-Asia. It is a group of important microscopic multi-cellular parasite of ectothermic aquatic vertebrates, particularly fish. Among numerous myxosporean, high pathological potential or unserious species are known in freshwater and marine fish. In SE-Asia, only eighteen *Myxozoa* species, less than 0.9% of worldwide reports, have been described and only one species are reported in marine fish species.

The aim of this study is therefore to explore the biodiversity of myxosporean parasites in 5 species of grouper, Asian sea bass (*Lates calcarifer*), marine catfish, *Plotosus canius* and 2 species of mullet of Thailand. Morphology, based on classical criterion and distribution of myxosporean parasites are discussed.

Materials and Methods

1. Sample collections

Nine species in four groups of fish samples both from wild and cultured fish were collected between September, 2006 and August, 2009 from four sampling sites in the southern Thailand;

1) Five species of grouper group: *E. coioides*, *E. malabaricus*, *E. fuscoguttatus, E. bleekeri*, and *E. sexfasciatus*

2) Two species of mullet group: *Liza* sp. and *Valamugil seheli*

3) Asian sea bass: *Lates calcarifer*

4) Gray eel-catfish: *Plotosus canius*

The sampling sites include; (1) Songkhla province, (2) Songkhla Lake as a representative of the area containing salt sea water (≥ 10 ppt), and two sampling sites in Andaman Sea, (3) Satun and Trang provinces including some area of Krabi (Southern Andaman Coast), (4) Phang-Nga and Phuket provinces (Northern Andaman Coast) (Fig. 3.1). After collection, fish were transported live to the laboratory or killed on sites using high concentrations of Quinadine and then myxosporidia were identified immediately. Fish organs, gill, skin, brain, gall bladder, nerve system, liver, spleen, and kidney, were examined. Founded myxosporidia plasmodia from one fish were separated into 3 groups and fixed in 3 different solutions; 0.85% (w/v) NaCl (-20°C), 10% (v/v) formalin (room temp.), 2.5–6.25% (v/v) glutaraldehyde buffered in 0.2 M sodium cacodylate (room temp.) These treated plasmodiums were used for further studies.

36

2. Myxosporean morphology analysis

Morphological measurement of species description was obtained among 30 spores according to Lom and Arthur (1989), Lom and Dyková (1992) and Lom and Dyková (2006). Semi permanent slides of fresh spores prepared by glycine-gelatin (Lom and Authur, 1989) and stained with Giemsa or Diff-Q were used for morphometric analysis (Fig. 3.2) and photographed. Species descriptions were based on several *Myxobolus* populations from more than one host specimens. Spores were observed under Olympus AX 70 microscope and photographed by using Olympus DP 71 cool CCD camera with differential interference contrast (DIC) optics. The line drawings of spores were made directly from fresh specimens.
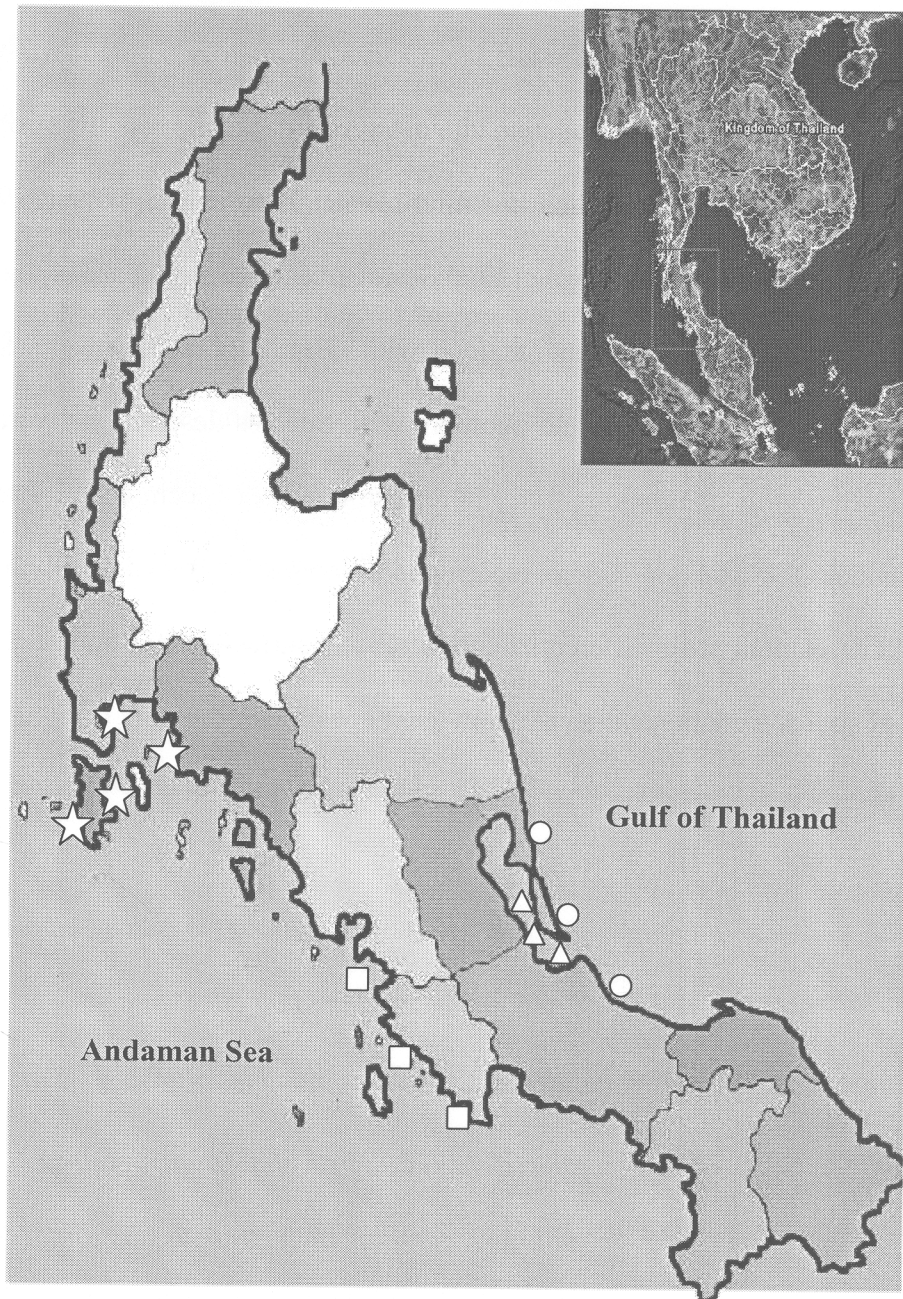
Fig. 3.1 The sampling sites for sample collection in this study. ◯ , △ ,□ , and ☆ represent 1; Gulf of Thailand, 2; Songkhla Lake, 3; South (S) of Andaman Sea and 4; North (N) of Andaman Sea.
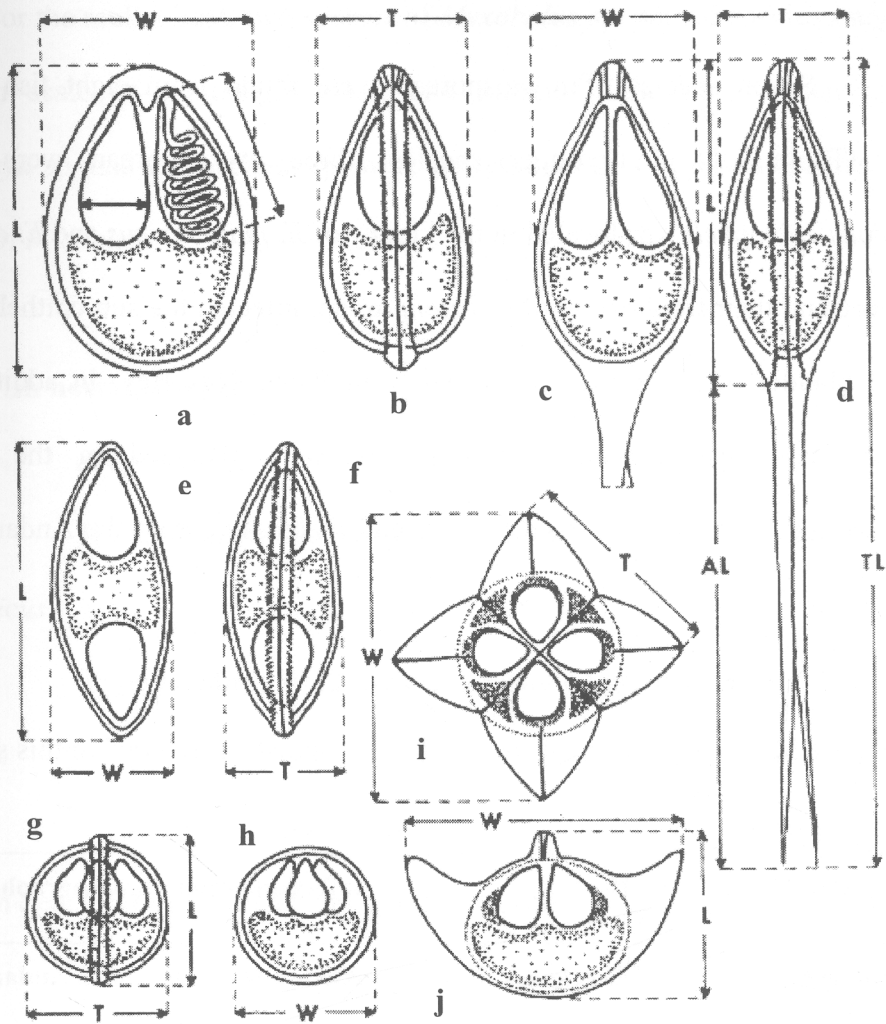
Fig. 3.2 Measurement of myxosporean spores of various genera: **a** and **b** – *Myxobolus* in frontal and side sutural view; **c** and **d** - *Henneguya* in frontal and side view; **e** and **f** - *Myxidium* in frontal and side view; **g** and **h** - *Chloromyxum* in side or sutural (**g**) and frontal (**h**) view; **i** - *Kudoa* in apical view; **j** - *Kudoa* in one of the possible side views which is the diagonal one. Measurement of the polar capsule is indicated in a: L - length of the spore, W - width of the spore, T - thickness of the spore; in spores with caudal appendages such as *Henneguya*, Al - length of the caudal appendage, Tl - total length of the spore (Lom and Dyková, 1992).

Results

Seven species of myxosporean were found from eight fish species examined (Table 3.1). In grouper species, three myxosporean were found. *Sphaerospora epinepheli* was located in the kidney of *E. malabaricus* and *E. coioides*. Mature spore and their trophozoite of *Ceratomyxa* sp. infected the sub-epithelial layer of the gall bladder of *E. coioides* collected from Phang-Nga Bay. In addition, the spores of small myxosporean, *Myxidium* sp. were detected in the gill of *E. fuscoguttatus*, *E. coioides*, *E. malabaricus* and *E. bleekeli* from the Andaman Sea sampling sites.

Table 3.1 Myxosporean found from eight fish species examined in this study

No.	Myxosporean species	Host	Infection organ	Geographic occurrence
1	*S. epinepheli*	*E. coioides*	Kidney	N/S Andaman Sea, Gulf of Thailand
		E. malabaricus		
2	*Ceratomyxa* sp.	*E. coioides*	Gall bladder	N Andaman Sea
3	*Myxidium* sp.	*E. fuscoguttatus,*	All organs	N/S Andaman Sea
		E. coioides,		
		E. malabaricus		
		E. bleekeri		
4	*Myxobolus* sp. I (*M. supammattayai* n. sp.)	*V. seheli*	Scale	N/S Andaman Sea
5	*Myxobolus* sp. II	*Lisa* sp.	Gill lamella	Gulf of Thailand
6	*Henneguya* sp.	*L. calcarifer*	Gill lamella	N/S Andaman Sea, Gulf of Thailand
7	*Zschokkella* sp.	*P. canius*	Gall bladder	N/S Andaman Sea, Gulf of Thailand

40

For the mullet host, two species of *Myxobolus* sp. named species I and II were found in scale of *Valamugil seheli* and gills of *Lisa* sp., respectively, while *Henneguya* sp. and *Zschokkella* sp. were detected in gills of Asian sea bass and gall bladder of *P. canius*.

Fish host: Grouper

S. epinepheli

Host: Orange spotted grouper, *E. coioides* and malabar grouper, *E. malabaricus*

Type locality: Wild life orange spotted grouper from Phang-Nga Bay, Thailand.

Geographic occurrence: Net cage cultured and wild fish in the Andaman Sea, Gulf of Thailand and Songkhla Lake.

Site of tissue development: Developmental stages could be differentiated from presporogonic stage to sporogonic stage. Presporogonic stage (blood stage) was round to oval (6.48±0.8 μm) and was found in the blood stream. Both pensporoblast formation (sporogonic stage) and mature character were found in kidney tissue. Mature plasmodia located in target organs were elongated up to 1.75±0.3 μm and 1.2±0.2 μm in disporus and monosporus plasmodia, respectively.

Spore description: Subspherical to spherical spore were measured 8.81±0.5 μm in length and 8.35±0.5 μm in width. The sutural ridge was prominent and formed a notch at apex and posterior end of the spore. Two subspherical polar capsules were measured 3.61±0.3 μm in length, 3.48±0.4 μm in width and contained a polar filament with 6–7 turns (57.23±5.2 μm in length) opening at the anterior end of the spore. The fresh spore of *S. epinepheli* is shown in Fig. 3.3.

Prevalence of infection: 42/131 (32.06%) of the orange spotted grouper and 7/77 (9.09%) of malabar grouper.
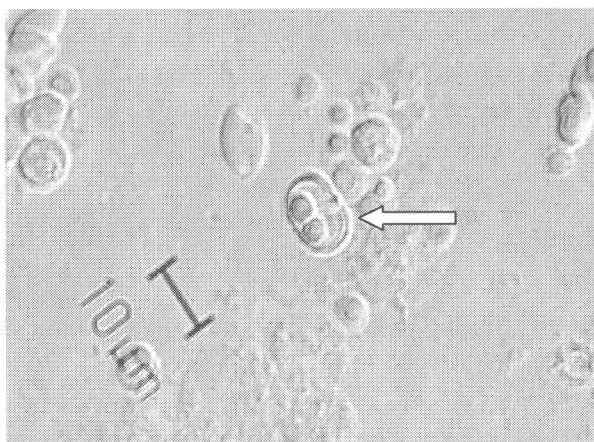
Fig. 3.3 Fresh mature spore of *S. epinepheli* observed under light microscopy with DIC filter.

Species note: The morphometric parasitic spore in orange spotted grouper is similar to the spore of *S. epinepheli*, a parasite infecting the kidney of malabar grouper. However, we could not find this parasite in other grouper species in this survey. Beside the host range theory of myxosporean which has been reported to be the host specific or narrow host range (Lom and Dyková, 2006), our present study demonstrated the possibility of a new host record of *S. epinepheli*. This emerging point needs more in-depth details of parasite in new host record because orange spotted grouper is important economic fish.

***Ceratomyxa* sp.**

Host: Orange spotted grouper, *E. coioides*

Type locality: Cage cultured orange spotted grouper, Phang-Nga Bay, Thailand

Geographic occurrence: Found only in Phang-Nga Bay

Site of tissue development: Gall bladder, the bile was turbid due to the presence of large number of free floating plasmodia or spores with cell debris.

Spore description: Vegetative stages were not observed. The infection was detected as a huge number of mature spore free floating in the bile. Spores were slightly arcuate to crescent shaped in the sutural view. Sutural line is prominent. Anterior and posterior margins of shell valves tapered gradually and terminated as thin rounded valvular tips. Spores measured 16.07±4.2 μm in length and 0.72±0.3 μm in width. The nearly equal polar capsules were spherical and measured 1.31±0.1 μm. The polar filament could not be observed. The fresh spore of *Ceratomyxa* sp. is shown in Fig. 3.4.

Prevalence of infection: The prevalence was 5/34 (14.71%) in grouper, *E. coioides*, samples collected only from Phang-Nga Bay.

Species note: In our survey, the geographical distribution of *Ceratomyxa* sp. seemed to be specific at only Phang-Nga Bay. In addition, the data showed high degree of host specificity in orange spotted grouper. However, the distinction among *Ceratomyxa* genera is more or less a matter of convention. The shape of *Ceratomyxa* sp. in *E. coioides* found in this study was similar to those of other *Ceratomyxa* spp. found in bile of marine fish, mullet and sea cat-fish from Red Sea (Abdel-Ghaffar *et al.*, 2008). This problem could hardly be solved except investigating life cycle and molecular phylogeny (Ali *et al.*, 2007).
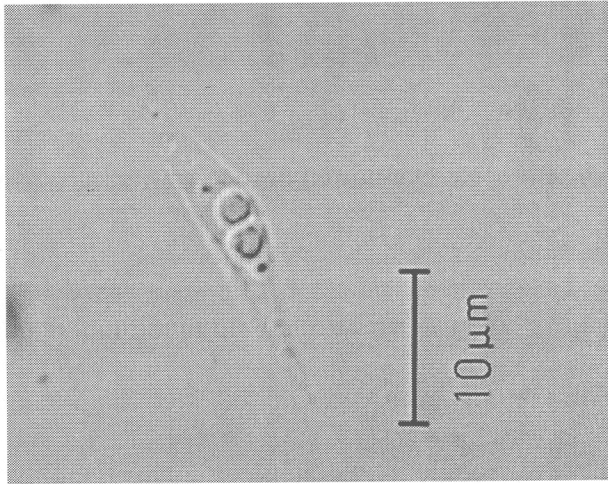
Fig. 3.4 Fresh mature spore of *Ceratomyxa* sp. observed under light microscopy with DIC filter.

Myxidium sp.

Host: *E. fuscoguttatus*, *E. coioides*, *E. malabaricus* and *E. bleekeri*

Type locality: Phang-Nga province (8°2159.56″ N, 98°38′06.40″ E)

Geographic occurrence: Andaman Sea, Thailand

Site of tissue development: Systemic infection including gill, kidney and blood

Spore: Spores were typical of the genus *Myxidium*. Mature spores were elongate with blunt pointed ends in the frontal view. Sutural line was indistinctive. The spore measurements were 5.11 ± 0.2 µm in length and 3.72 ± 0.3 µm in width. The two equal polar capsules were spherical and located at center of the spore along the spore longitudinal axis. The polar capsule measurements were 3.18 ± 0.1 µm in length and 3.29 ± 0.1 µm in width. The polar filament turns could not be observed.

Prevalence of infection: From 5 grouper species with total of 295 samples, 89 (30.17%) fish in 4 grouper species were found to be infected with the

44

parasite. Moreover, high degree of occurrence of 90.91% and 88.24% was found in orange spotted grouper and *E. bleekeri* in Phang-Nga Bay, respectively.

Species note: Species of the genus *Myxidium* are fusiform, ellipsoidal and sigmoid or S-shapes with pointed or rounded end. Valves are smooth or with ridge, with sinuous sutural line. Polar capsules are pyriform in most cases with opening situated in the sutural plane. Sporoplasm is single binucleated and opposite directions (Lom and Dyková, 2006). The characters of this genus are considerably overlapped with those of genus *Zschokkella* (Ali *et al.*, 2006 and Abdel-Baki, 2009). Although the distinction between both genera is more or less controversial (Viozzi and Flores, 2003), our *Myxidium* sp. exhibits morphological features typical to the genus *Myxidium* characteristics described by Lom and Dyková (2006). The spore characteristic micrograph of *Myxidium* sp. was shown in Fig. 3.5.
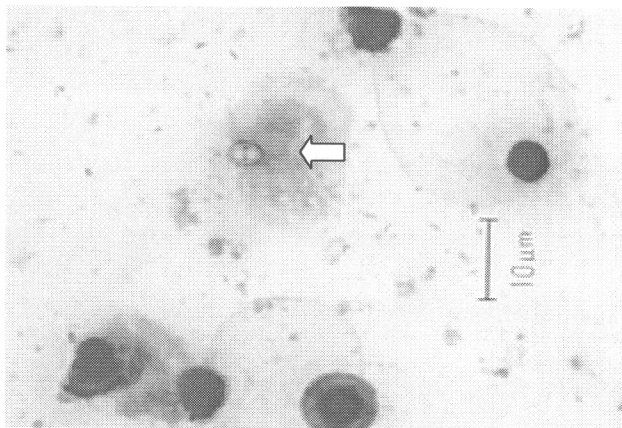
Fig. 3.5 Gimsa stained spore of *Myxidium* sp. from fresh spores preparation.

Fish host: Mullet

Myxobolus **sp. I (*M. supammattayai* n. sp.)**

Host: Bluespot mullet, *Valamugil seheli*

Type locality: The coast of the Andaman Sea, Satun province, Thailand (6°47'03.68" N, 99°49'44.60" E)

Geographic occurrence: Andaman Sea, Thailand

Site of tissue development: Sporogonic stages and mature spores were observed in the epithelium tissue above the scale.

Spore: The mature spores were round to ellipsoidal in frontal view. Most of them are round with several edge markings (normally 5–7), whereas a few are variable in shape. Spore size was 6.6±0.3 μm in length and 6.5±0.21 μm in width. The two spherical polar capsules were equal in size and close together in the plane of sutural line at the apical end which measured 3.5±0.13 μm in length and 2.0±0.09 μm in width. Polar filaments formed four to five coils opening at the spore anterior near the sutural line.

Prevalence of infection: Up to 17.48% (25/143)

Species note: This species shows unique clinical sign and black plasmodium. Its important basic characteristics are different from those of other reported *Myxobolus* sp. in the same host record. Moreover, morphology of its mature spore differed from all myxobolus species that have been reported among mullet host. The detail characteristics of this species including molecular phylogeny and ultra-structure have to be further investigated to classify new species of myxosporea. Some photographs of *Myxobolus* sp.I in mullet are displayed in Fig. 3.6.

Fig. 3.6 a–c *Myxobolus* sp. I in mullet; **a** Clinical sign, **b** Fresh mature spore, **c** Pathology of parasite in scales (arrow).

Myxobolus sp. II

Host: Mullet, *Lisa* sp.

Type locality: Songkhla province

Geographic occurrence: Gulf of Thailand and Songkhla Lake

Site of tissue development: Gill lamella

Spore: The polysporus plasmodia were found in subepitherial layer in secondary gill lamella. Round to roundish spore shape in frontal view, thin valves and symmetrical spore shape were presented as species characteristics of *Myxobolus* sp. II. Sutural rim around spore presented distinct marginal markings over surface of spore. Spore size was 6.4±0.31 μm in length and 6.3±0.63 μm in width. The two spherical polar capsules were equal in size and close together in the plane of sutural line at the apical end which measured 2.7±0.25 μm in length and 2.2±0.2 μm in width within 6–7 polar filament turns.

Prevalence of infection: 57/192 (29.69%) of juvenile and mature (7–150 g) wild mullet, *Lisa* sp.

Species note: The simple, roundish spores of *Myxobolus* sp. resemble several known and undescribed myxosporean that infect different mullet and other fish species in various geographical locations. Similar to the above session, we found two species of myxobolus in the same host group, mullet. The correct identification is possible only after considering host-specific, morphological study and directed SSU rDNA sequence from the type host. Current report suggests that the consistent and characteristic polymorphic loci are important data for classification. For example, the taxonomic report of *M. rotundus*, a parasite of goldfish (Wu and Wang, 2000; Lu *et al.*, 2002; Zhang *et al.*, 2006) erroneously identified the species that infected goldfish,

Carassius auratus as *M. rotindua* (Molnár *et al.*, 2009). The spore characteristic micrograph of *Myxobolus* sp. II and sporic plasmodium are shown in Fig. 3.7.
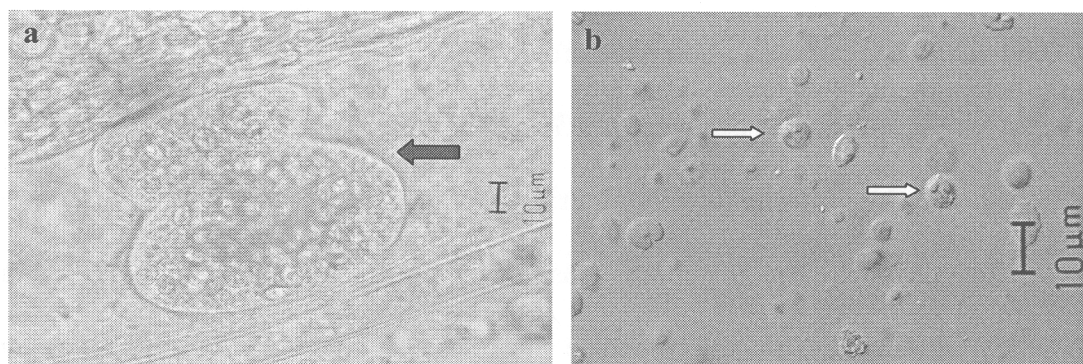
Fig. 3.7 a–b *Myxobolus* sp. II in mullet, *Lisa* sp. **a** location of *Myxobolus* sp. II in interfilament-epithelial tissue of host, **b** Fresh mature spore of *Myxobolus* sp. II (DIC photography).

Fish host: Asian sea bass, *L. calcarifer*

Henneguya **sp.**

Host: Asian sea bass, *L. calcarifer*

Type locality: Songkhla Lake, Songkhla, Thailand

Geographic occurrence: Cage cultured and wild fish in Andaman Sea, Gulf of Thailand and Songkhla Lake.

Site of tissue development: epithelium layer in second lamella of gill

Spore: Mature spores were elongate (total length 17.6–20 µm; spore length 9.5±0.4 µm; spore width 6.0±0.4 µm; caudal appendix length 13.2±1.7 µm) and sporoplasma was binucleate. Two polar capsules were elongate and of equal size (length 4.0±0.2 µm, width 2.1±0.2 µm). Polar filament with 21.57±2.7 µm in length (ejected), arranged perpendicular to the axis of the capsule. Spore wall was smooth

and consisted of two symmetrical valves with a visible line of suture. Mucous envelope or iodinophilous vacuole was not seen.

Prevalence of infection: 17/212 (8.01%) of net cage cultured and wild fish

Species note: *Henneguya* spp. belongs to the most common parasites of fish. In a synopsis on this genus, Eiras (2002) has reported the existence of 146 *Henneguya* spp., described mostly from fish of the temperate climate zones. *Henneguya* spp. and *Hennegoides* spp. seem to be the most common parasites in non-cyprinid fishes in other parts of SE-Asia. Moreover, *Hennegoides longitudinalis* n. gen. n. sp., a myxosporean parasite of *Osphronemus gourami*, freshwater fish was first described from Thailand (Székely *et al.*, 2009 and Lom *et al.*, 1991). Therefore, the occurrence of *Henneguya* sp. on the gills of Asian sea bass is not surprising. The spore characteristic micrograph of *Henneguya* sp. is shown in Fig. 3.8.
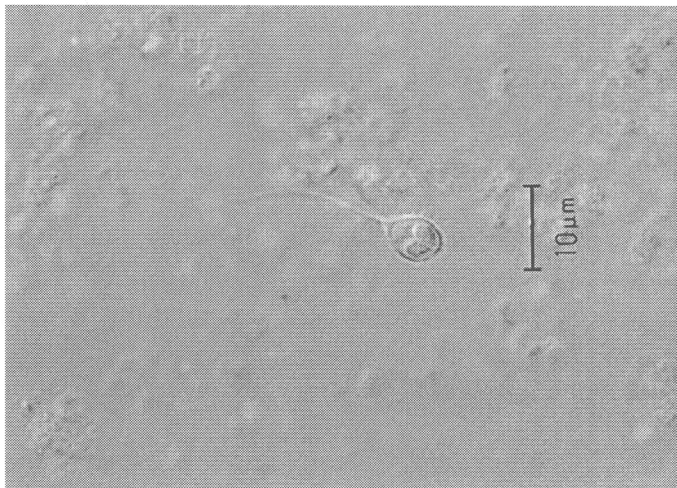
Fig. 3.8 Fresh preparation of mature spore of *Henneguya* sp. from parasitic infected the gill of Asian sea bass, *L. calcarifer* (DIC photograph).

Fish host: Marine cat-fish, *P. canius*

Zschokkella **sp.**

Host: Marine cat-fish, *P. canius*

Type locality: Wild fish from Songkhla Lake, Thailand

Geographic occurrence: Andaman Sea, Gulf of Thailand and Songkhla Lake.

Site of tissue development: Gall bladder, the bile was little turbid due to the present of large number of free floating plasmodia or spore with cell debris.

Spore: Mature spores were ellipsoid with rounded poles in the frontal view. The sutural line was irregularly curved. Shallow and curved striations were visible on each spore valve. The striations were not clearly observed. The mean spore length was 11.5 ± 0.6 µm, while the mean width was 6.71 ± 0.4 µm. Polar capsules were round, equal in size, and measured 3.30 ± 0.2 µm in diameter. The polar filament showed four to five turns, coiled tightly along the inner wall of the capsule and arranged perpendicular to the longitudinal axis of the capsule.

Prevalence of infection: 36/50 (72%) of wild fish from Andaman Sea, Gulf of Thailand and Songkhla Lake.

Species note: Regarding the fish hosts *P. canius* belongs to family Plotosidae which is one of thirty families of catfish. Among them, only two families are truly marine species, Ariidae and Plotosidae; each is represented in the Thailand Sea by two species, *P. canius* and *P. anguillaris*, respectively. Reviewing the literature revealed that only one species, *Z. egyptica* (Ali *et al.*, 2007) was reported from Red Sea, Egypt eel catfish (*P. lineatus*). Moreover, according to the available literature, no myxosporean infection was reported from the two species of genus *Plotosidae* in Thailand. It is noted worthy to mention that these two presently infected

hosts show the same mode of living and feeding (bottom feeder), which probably potentiate the risk of infection with this parasite in the future. The spore characteristic micrograph of *Zschokkella* sp. is shown in Fig. 3.9.
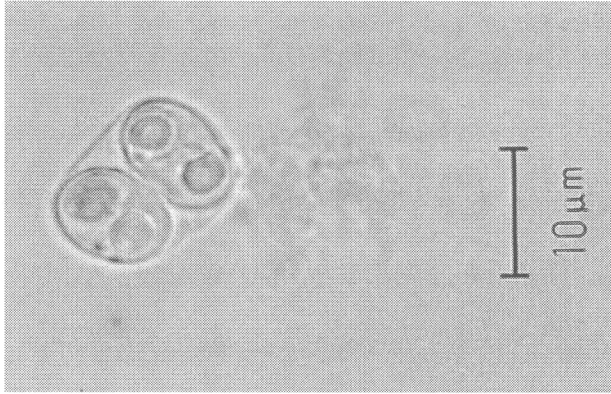
Fig. 3.9 Fresh preparation of mature spore of *Zschokkella* sp. in bile of *P. canius* (DIC photograph).

Discussion

Aquaculture in Thailand has expanded rapidly in the last decade, mainly with the involvement of the intensive farming of freshwater and marine fish species, as well as decreasing commercial fisheries of economic fish. This rapid development and degenerated environment have been inevitably accompanied by an increased occurrence of different pathogens, including myxosporea, creating a considerable constraint on the further development of the aquaculture industry. Recently, significant problems due to myxosporean infections in SE-Asian fish culture have emerged (Székely *et al.*, 2009). The present study primarily described the occurrence of myxosporean pathogens in cage culture and wild fish along coastal line of southern Thailand.

The epidemiology and pathology of myxosporean parasites in economic marine fish of Thailand have not been well studied, making the

identification of new species is thus very difficult. An unidentified myxosporean have been reported from the various organs of 8 economic fish species including 4 species of grouper, 2 species of mullet, Asian sea bass and marine catfish. Moreover, some parasites show high degree of occurrence. According to our findings, it seems that the actual and potential pathogenic situation and impact of myxosporean infection for Thailand marine culture is a subject requiring more consideration. Seven myxosporeans are presented in studied locations which are the important sites of fish culture production in Thailand. There has been reported that this parasite sometimes causes significant loss of fish, or most commonly, reduces growth rate, so the myxosporean infection could become an economic problem. Among the fishes examined in the present survey, not only moderately infected but also severely infected specimens could be found. Since the examination period was short, no disease symptoms were recorded. Therefore, we cannot provide the data on the pathogenicity of the myxozoan infections of Thai economic fish. The large number of myxozoan species, the intensive infection of some fish specimens and the local changes around the parasites, however, suggest the possibility that more severe symptoms and losses might also appear in intensive culture systems.

References

Abdel-Baki, A. S. 2009. Two new *Myxidium* species (Myxosporea: Myxidiidae) infecting the gallbladder of African flying fish, *Cheilopogon nigricans* and Suez fusilier, *Caesio suevicus* from the Red Sea, Egypt: a morphological and morphometric study. Parasitol. Res. 105 : 513–518.

Abdel-Ghaffar, F., Ali, M. A., Al Quraishy, S., Al Rasheid, K., Al Farraj, S., Abdel-Baki, A. S. and Bashtar, A. R. 2008. Four new species of *Ceratomyxa* Thelohan 1892 (Myxozoa: Myxosporea: Ceratomyxidae) infecting the gallbladder of some Red Sea fishes. Parasitol. Res. 103 : 559–565.

Ali, M., Abdel-Baki, A. S. and Sakran, T. 2006. *Myxidium elmatboulii* n. sp. and *Ceratomyxa ghaffari* n. sp. (Myxozoa: Myxosporea) parasitic in the gallbladder of the Red Sea Houndfish *Tylosurus choram* (Rüppell, 1837) (Teleostei: Belonidae) from the Red Sea, Egypt. Acta Protozool. 45 : 97–103.

Ali, M., Abdel-Baki, A. Z. and Abdel-Ghaffar, F. 2007. *Zschokkella egyptica* n. sp. (Myxosporea: Bivalvulaida) infecting the gallbladder of the eel catfish *Plotosus lineatus* Thunberg, 1787 and the freckled goatfish *Upeneus tragula* Richardson, 1846 in the Red Sea, Egypt. Parasitol. Res. 100 : 625–628.

Dyková, I. and Lom, L. 2007. Histopathology of Protistan and Myxozoan Infections in Fishes. Praha : Academia.

Eiras, J. C. 2002. Synopsis of the species of the genus *Henneguya* Thélohan, 1892 (Myxozoa: Myxosporea: Myxobolidae). Syst. Parasitol. 52 : 43–54.

Lom, J. and Arthur, J. R. 1989. A guideline for preparation of species description in Myxosporea. J. Fish Dis. 12 : 151–156.

Lom, J. and Dyková, I. 1992. Protozoan parasites of fish. Amsterdam : Elsevier.

Lom, J. and Dyková, I. 2006. Myxozoan genera: definition and notes on taxonomy, life-cycle terminology and pathogenic species. Folia Parasitol. 53 : 1–36.

Lom, J., Tonguthai, K. and Dyková, I. 1991. *Hennegoides longitudinalis* n. gen. n. sp., a myxosporean parasite of *Osphronemus gourami* from Thailand. Dis. Aquat. Org. 11 : 143–145.

Lu, Y. S., Li, M., Wu, Y. S. and Wang, J. G. 2002. Antigenic study of *Myxobolus rotundus* (Myxozoa: Myxosporea) using monoclonal antibodies. J. Fish Dis. 25 : 307–310.

Molnár, K., Székely, C., Hallett, S. L. and Atkinson, S. D. 2009. Some remarks on the occurrence, host-specificity and validity of *Myxobolus rotundus* Nemeczek, 1911 (Myxozoa: Myxosporea). Syst. Parasitol. 72 : 71–79.

Székely, C., Shaharom-Harrison, F., Cech, G., Ostoros, G. and Molnár, K. 2009. Myxozoan infections in fishes of the Tasik Kenyir Water Reservoir, Terengganu, Malaysia. Dis. Aquat. Org. 83 : 37–48.

Viozzi, G. P. and Flores, V. R. 2003. *Myxidium biliare* sp. n. (Myxozoa) from gall bladder of *Galaxias maculatus* (Osmeriformes: Galaxiidae) in Patagonia (Argentina). Folia Parasitol. 50 : 190–194.

Wu, Y. S. and Wang, J. G. 2000. The immunogenicity of *Myxobolus rotundus* Nemeczek, 1911. Acta Hydrobiologica Sinica, 24 : 246–251 (In Chinese with English abstract).

Zhang, J. Y., Wang, J. G., Wu, Y. S., Li, M., Li, A. H. and Gong, X. L. 2006. A combined phage display ScFv library against *Myxobolus rotundus* infecting crucian carp, *Carassius auratus auratus* (L.), in China. J. Fish Dis. 29 : 1–7.

4. A NEW HOST RECORD *Sphaerospora epinepheli* (MYXOSPOREA: BIVALVULIDA) OCCURING ON ORANGE-SPOTTED GROUPER *Epinephelus coioides* FROM THAILAND: EPIDEMOLOGY, HISTOPATHOLOGY AND PHYLOGENETIC POSITION

Abstract

In 1991, the first record of *Sphaerospora epinepheli* was described as a kidney parasite of wild and cultured malabar grouper, *Epinephelus malabaricus* along coastlines of Thailand, the Gulf of Thailand and Andaman Sea. However, the high infection of this parasite was recently detected in kidney renal tubes of orange spotted grouper, *E. coioides*, collected from Andaman Sea. The highest infection rate of 36.82% was observed during a rainy season in 2009 in the north of Andaman Sea (Phang-Nga Bay) which is an important grouper production site in Thailand. The biological and histopathological data of the parasite in a new host record were presented. Species classification was described based on morphological data of mature spore and molecular analysis of myxosporean 18S rDNA including that of *S. epinepheli* which infect *E. malabaricus*. The genetic relationship of this parasite found in two host species was also studied. The phylogenetic tree analysis of small-subunit (SSU) rDNA sequences of *S. epinepheli* from both infected hosts was constructed using two algorithms, maximum likelihood (ML) and Bayesian inference (BI). They were placed in the clustered basal to a clade containing four long SSU rDNA sphaerosporid species including *S. truttae*, *S. elegans*, *S. ranae*, *S. fugu* and *Bipteria formosa* with strong bootstrap supports. Histopathologically, renal

intratubular myxozoan spores were associated with tubulonephosis, tubular necrosis, chronic interstitial nephritis and mimic membranoproliferative glomerulonephritis. This myxozoan parasite appears to be a significant pathogen on the basis of pathological changes in the renal tubules and highly distributed in orange-spotted grouper.

Introduction

Myxosporean species play a significant pathogenic role as parasites of the wild and cultured teleost fish in both marine and freshwater habitants with over 2,180 described species (Liu *et al.*, 2010). Additionally there have been numerous reports of myxozoans in elasmobranchs, amphibians, reptiles, and mammals including human immunodeficiency (Moncada *et al.*, 2001; Longshaw *et al.*, 2005). Among them, the genus *Sphearospora* Thélohan, 1892 with polyphyletic 78 described species is found to distribute in different freshwater and marine clades (Lom and Dyková, 2006). Many species belonging to this genus are pathogenic as the coelozoic parasite in the urinary system and usually specific highly to certain hosts. Some species are recognized as serious disease agents in cultured economic fish, for example, *S. dicentrarchi* and *S. testicularis* represent important parasites of wild and cultured European sea bass, *Dicentrarchus labrax*, in the western Mediterranean basin (Fioravanti *et al.*, 2004). However, only one species, *S. ephenepheli*, has been reported to infect brackish and marine fish in South East Asia. It is a renal parasite of wild and cultured malabar grauper, *Epinephelus malabaricus* in Thailand (Supamattaya *et al.*, 1990).

Grouper species, which inhabit subtropical and tropical areas, have become an economically important fish of marine teleost and currently been being

cultured in ASEAN countries (Harikrishnan *et al.*, 2010). In Thailand, grouper productions have been from an artisanal fishery (wild capture) and semi-intensive net-cages aquaculture. Among more than 150 species of grouper, orange-spotted grouper *E. coioides*, malabar grouper *E. malabaricus*, brown marbled grouper *E. fuscoguttatus*, duskytail grouper *E. bleekeri* and six-banded grouper *E. stictus* are the main product of Thailand; especially the first mentioned one is the main marine cultured species in net-cages aquaculture. In the last few years, the concerned phenomenal regarding spherosporosis has been increased significantly in grouper net-cages culture.

Although advanced techniques have been applied in the last few decades to study molecular phylogeny and classical taxonomy, the complete life cycle of many *Sphearospora* species remains unclear (Bermúdez *et al.*, 2010). Moreover, efficacious treatments, prevention and control of myxosporean infection is particularly difficult and lacking (Yokoyama *et al.*, 1990). So far disease outbreaks regarding to the infection with *Sphaerospora* spp. recorded in marine or brackish water fish have been much fewer comparable to those of freshwater fish. The geographic distribution, host specificity and parasitic indication of *S. epinepheli* in economic grouper species in Thailand are indeed rarely reported.

The aims of this present work were to conduct the parasitological survey and the classification of *S. epinepheli* in a new host record, *E. coioides* inferring from both morphological and phylogenetic analysis. Furthermore, the histopathological damages of infected kidney were also demonstrated. The rediscovery of a renal sphearosporesis in orange-spotted grouper, as a new host record, from Thailand was provided by the description of its sporogonic morphology

and phylogenetic analysis inferred from the small subunit ribosomal DNA (SSU rDNA). This finding suggested it is evidently *S. ephenepheli*.

Materials and methods

1. Fish sample

Between 2007–2009 orange-spotted grouper, *E. coioides*, and other four species of economic grouper including *E. malabaricus*, *E. fuscoguttatus*, *E. stictus*, and *E. bleekeri* from Thailand were investigated for parasitic *S. epinepheli* infection. The fish samples ranging from 200–1,200 g were obtained from wild and cultured farms covering the main production areas. The sampling locations included Northern Andaman Sea (Phang-Nga Bay; 5 sampling sites) and Southern Andaman Sea (Satun province; 4 sampling sites) (Fig. 4.1). Alive fish were collected from marine cage culture or purchased from fishermen and moribund fish were kept in dry ice. Fish samples were then transported to the laboratory of the Aquatic Animal Health Research Center (AAHRC), Prince of Songkla University. Standard procedures were used for the examination of myxosporean in internal and external organs especially the kidney since it has been reported as a specific organ of this parasite (Supamattaya *et al.*, 1990). Fresh samples were subsequently used for the morphological and histopathological examination and some infected kidney tissues were collected in cryotube™ (Nunc, Denmark) and stored in liquid nitrogen for the molecular study.

2. Parasite identification and histopathology

Morphology of fresh myxosporean spore was studied under Olympus AX 70 microscope and photographed using Olympus DP 71 cool CCD camera with

differential interference contrast (DIC) optics. The vitality of the mature spore was checked by mixing spores with a 0.4% (v/v) urea (Molnár *et al.*, 2009). Descriptions and measurements of spores were performed following the guideline of Lom and Dyková (2006). Spore measurements were done based on a total of spores which obtained from 5 fish (30 spores/fish). For histology study, the infectious tissues were fixed in 10% (v/v) formalin for 3 days, dehydrated in graded alcohol and embedded using routine procedures. Three–five µm sections were stained with haematoxylin and eosin (H&E), toluidine blue (TB) and periodic acid-Schiff (PAS).
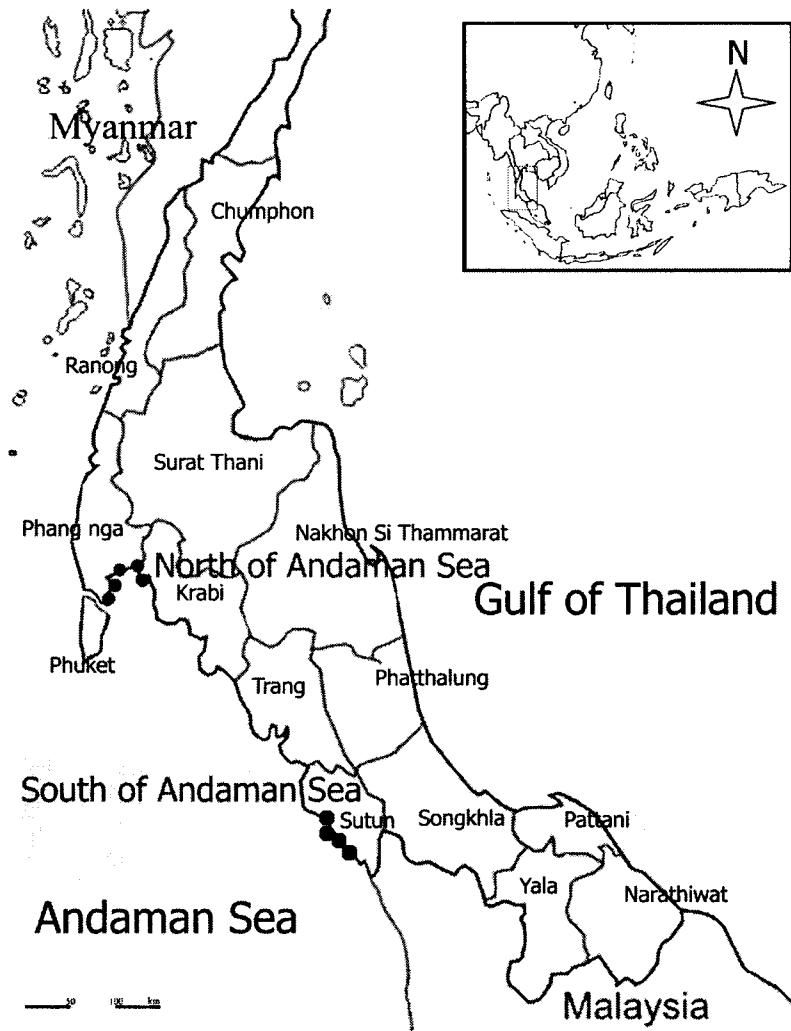
Fig. 4.1 Sampling locations of *S. epinepheli* infected grouper in the Andaman Sea, Thailand.

3. Molecular analysis procedures

Frozen infected kidneys of 3–5 g were thawed and then homogenized in Hank's balanced salt solution (HBSS; Gibco, US) using a sterile plastic Eppendorf pestle. The resultant slurry was collected and centrifuged at 2000xg for 15 min at 4°C. The pellets were resuspended in 1 ml of HBSS and the suspension were transferred into 15 ml polypropylene centrifuge tubes containing discontinuous gradients of Percoll^{TM} (2.5 ml layers of 20% and 40% (v/v) Percoll^{TM} in phosphate buffered saline, PBS pH 7.4; Sigma, US). The tubes were centrifuged at 2000xg for 30 min at 4°C. The resulting pellets of *S. epinepheli* were washed to remove the trace Percoll^{TM} by two repetition of resuspending in 2 ml HBSS followed by centrifugation at 5000xg for 10 min at 4°C.

Pretreatment of proteinase K was applied (U-taynapun *et al.*, 2010) and DNA was then extracted using DNeasy Tissue Kit (Qiagen, CA) according to the manufacturer's instructions. The primer pairs 18e (5′ CTGGTTGATTCTGCCAGT 3′) and 18g (5′ CGGTACTAGCGACGGGCGGTGTG 3′) (Hillis and Dixon, 1991) were used to amplify the 18S rDNA gene of the parasite. The PCR product was isolated from the gel using QIAquick Gel Extraction kit (Qiagen, CA) and cloned into pGEM$^{®}$-T Easy Vector (Promega, US) following manufacturer's instructions. The plasmids containing insert, purified from single clones of the 6 individual samples by spin columns (QIAGEN$^{®}$ Plasmid Purification, Qiagen, CA) were sequenced on automatic sequencer CEQ^{TM} 8000 (Beckman Coulter) using CEQ DTCS Dye kit (Beckman Coulter). Cloning sequence traces were checked for quality and assembled manually using BioEdit 7.0.5.3 (Hall, 1999) and Genetyx (Genetyx, JP). The obtained

sequence was submitted to the National Center for Biotechnology Information (NCBI) GenBank database.

4. Phylogenetic analysis

In order to demonstrate the position of *S. epinepheli* with specific common structure in the phylogram and to obtain homologous sequences, a partial part of 18S rDNA of *S. epinepheli* from both hosts, *E. coioides* and *E. malabaricus*, were compared to those sequences of other myxosporean species available in the GenBank using nucleotide BLAST protocol. Malacosporeana species *Tetracapsuloides bryosalmonae* and *Buddenbrockia plumatellae*, representing a lineage phylogenetically close to maxosporean, were set as outgroups in our analysis. The basal sphaerosporid species sequences were aligned using ClustalW algorithm in BioEdit (Hall, 1999). The result of primary alignment was edited following the secondary structure criterion of long myxozoan 18S rDNA (Holzer *et al.*, 2007) and V4 insertion region of *S. ranae* (Jirků *et al.*, 2007). The structures which could be homologized with certainty were analyzed. The group specific expansion segment which were not presented in all myxozoan taxa were excluded (Holzer *et al.*, 2010). Other ambiguous regions of the alignment output were classified and edited by choosing the guideline from default parameters of Gblocks server, http://molevol.cmima.csic.es/castresana/Gblocks.html (Castresana, 2000). The final alignments of V4 modified insertable sequences in basal sphaerosporid clade and related available myxosporean sequences which guided by Bartošová *et al.* (2010) were aligned with Muscle algorithm in Seaview 4.2.5 (Gouy *et al.*, 2010). We have performed genetic position of *S. epinepheli* in phylogram using two confident algorithms, maximum likelihood (ML) analysis and Bayesian inference (BI).

ML phylogram was examined via PhyML v 3.0.1 (Guindon and Gascuel, 2003) which combines the nearest neighbor interchanges (NNI) and subtree pruning and regrafting (SPR) algorithms. The best-fit parameters model (GTR+I+Γ) were selected using jModelTest v.0.1.1 (Posada, 2008). The 10 random starting BioNJ trees were set for the analysis. Nodes robustness was assessed with 500 bootstrap replicates. BI analyses were constructed using MrBayes v. 3.0b4 (Ronquist and Huelsenbeck, 2003). Clade support was estimated utilizing a Markov chain Monte Carlo (MCMC) algorithm. Parameters in MrBayes were set to 1,000,000 generations and 10,000 trees sampled (sampled every 100th generation), corresponding to the model estimated (GTR+I+Γ) of DNA substitution (nst=6; rates=invgamma; ncat=4) and the default random tree option to begin the analysis. Log-likelihood scores were plotted and only final 25% of generations were discarded as burn-in. The 50% majority rule consensus tree was computed from trees showing likelihoods of stationary. The differences among the individual bootstraps or posterior probabilities from BI computation affected the influential phylogram were presented in tree based drawing of ML analysis.

5. Statistical analysis

Statistical analyses of parasite distribution were performed using SPSS 17 for windows (SPSS Inc., Chicago). All data were calculated into percentage before further analysis. Differences between the presences of the *S. epinepheli* in host fish from the same location were determined by an independent sample *t*-test statistical analysis. The occurrences of infected new recorded host in the same location regarding the season were performed with one-way ANOVA followed by a Tukey's

HSD multiple comparison test. Statistical significance was taken at $P<0.05$. All results are expressed as mean ± S.D.

Results

The seasonal survey of *S. epinepheli*, a fish kidney myxosporean parasite, was demonstrated in five important economic grouper species of Thailand from the main grouper production areas of Andaman Sea during 2007–2009. We found that *E. coioides* is the new host record of this parasite. Moreover, the prevalence infection in the new host was higher than that of the first recorded host *E. malabaricus* (Supamattaya *et al.*, 1990). However, no evidences were authenticated for the infection of *S. epinepheli* in other 3 grouper species, *E. stictus*, *E. fuscoguttatus* and *E. bleekeri*. The morphological analysis, seasonal distribution, histopathological changes and molecular phylogenetic analysis are circumspectly summarized for the new host record of this myxosporean species.

1. Morphological description and specific organ infection

Microscopically, mature spores and developmental stages of parasite were detected specifically in the kidney of infected fish hosts, *E. malabaricus* and *E. coioides* whereas there could not be observed in other organs. The parasite was identified as a myxosporean belonging to the genus *Sphaerospora* (Lom and Dyková, 2006). The spore type found in the present study was corresponded with *S. epinepheli* described by Supamattaya *et al.* (1991) as regarded to the asymmetric morphology of the polar capsules with the polar filaments and details of spore characters. The detailed morphology of *S. epinepheli* from kidney of the new recorded host, *E. coioides* is presented for the first time. This finding was confirmed with data

63

describing the spore from malabar grouper (Table 4.1). In addition, the sutural line was prominent and straight forming a notch at the apex and posterior end of the spore (Fig. 4.2). Spore characterizing parameters from the new host record matched with those isolated form *E. malabaricus* which was first reported (Supamattaya *et al.*, 1991).

Table 4.1 Morphological comparison of *S. epinepheli* in two host record with original description

Fresh spores characteristics[a]	Host species		
	E. coioides (Present work)	*E. malabaracus* (Present work)	Reference data (Supamattaya *et al.*,1991)
Spores	Subspherical to spherical	Subspherical to spherical	Subspherical to spherical
Length	8.8 ± 0.5	8.7 ± 0.5	8.7 ± 0.4
Width	8.3 ± 0.5	8.3 ± 0.6	8.2 ± 0.5
Thickness	13.4 ± 0.6	13.5 ± 0.4	13.4 ± 0.5
Polar capsules (Pc.)	Spherical	Spherical	Spherical
LPc	3.6 ± 0.4	3.6 ± 0.4	3.7 ± 0.3
CPf	6-7	6-7	6-7
LPf	57.23 ± 5.2	56.71 ± 5.5	55.57 ± 4.6
Infection organ	Kidney tubules	Kidney tubules, Glomerulus	Kidney tubules, Glomerulus
Host	*E. coioides*	*E. malabaracus*	*E. malabaracus*

[a] number in μm

LPc, Length of polar capsule; CPf, Coils of the polar filament; LPf, Length of the polar filament
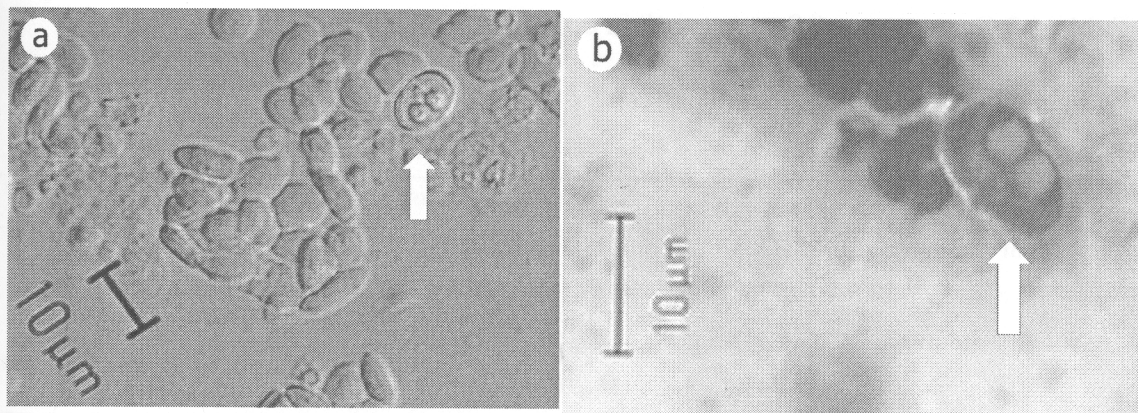
Fig. 4.2 Morphological micrograph of *S. epinepheli* in the new host record, *E. coioides*. **a**; Fresh mature spore (DIC photograph) **b**; Spore in Giemsa staining.

2. Seasonal distribution

The repeat occurrence of *S. epinepheli* species was found in malabar grouper from Andaman Sea as well as in the new fish host record (Table 4.2). The overall parasite infection was higher in the *E. coioides* (24.82%) than *E. malabaricus* (9.05%) during our research period (30 months). In the new host, the highest parasite occurrence of 33.62% was found in the northern Andaman Sea while the southern Andaman Sea was only 16.20%. Comparison of infection in *E. malabaricus* and *E. coioides* (Fig. 4.3) revealed that the north of Andaman Sea is the only location exhibiting statistically significant differences upon different seasons ($P<0.05$). In the south of Andaman Sea, the occurrence of this parasite was slightly higher in *E. coioides* than that detected in *E. malabaricus* in every sampling period which was significantly different in rainy season 2008 ($P<0.05$).

Table 4.2 Occurrence of *S. epinepheli* in economic grouper species from two

locations of the Andaman Sea

	E. malabaricus	E. coioides	E. fuscoguttatus	E. stictus	E. bleekeri
North of Andaman Sea	31/331 (9.37%)	118/351 (33.62%)	0/292	0/288	0/276
South of Andaman Sea	30/343 (8.74%)	58/358 (16.20%)	0/148	0/225	0/147
Total	61/674 (9.05%)	176/709 (24.82%)	0/440	0/513	0/423

The incidence of infection in *E. coioides* in the Andaman Sea was not related to the season changes. However, the infection in rainy season of all observed locations was slightly higher than that in dry season although not statistically significant. By mean of comparison regarding locations, the north of Andaman Sea and the south of Andaman Sea disclosed the significant difference of the percentage of host infected with *S. epinepheli*. The north of Andaman Sea has higher infection rate than other locations even all sampling times. The isolated parasite was 31.81% (dry season, 2008) to 36.82% (rainy, 2009) in the Northern Andaman Sea while the infection in the south of Andaman sea was between 12.78 –22.01%.
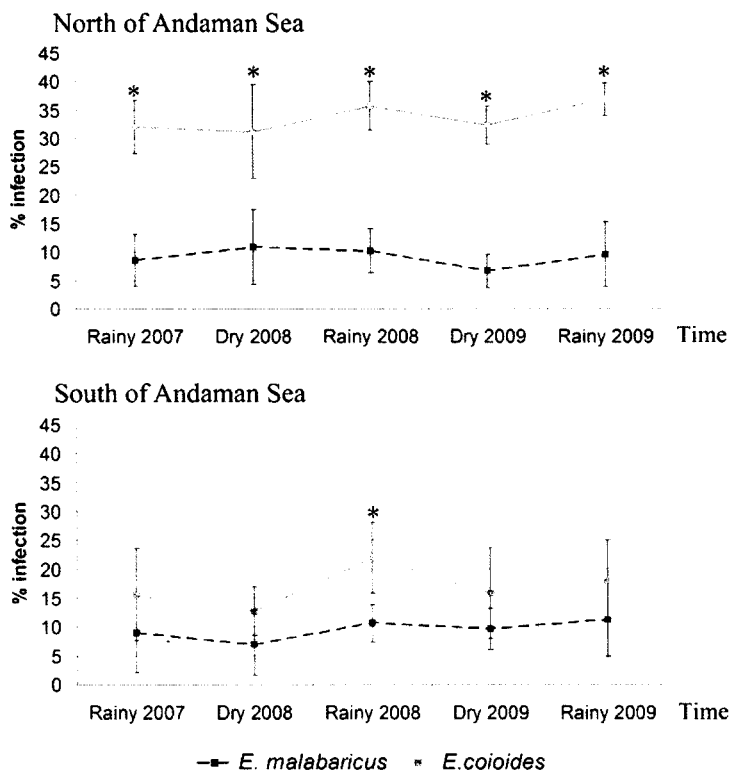
Fig. 4.3 Seasonal occurrence of *S. epinepheli* infection in two host record from the Andaman Sea, *; Significant difference of infection rates in the same time period (*P*<0.05)

3. Histopathology and host immune response

Orange-spotted groupers infected by *S. epinepheli* showed heavy infection and severe pathological damage in kidney, which is specific target organ of infection (Fig. 4.4a). Various stages of the parasite were observed in renal tubules (Fig. 4.4b and 4.4d). In some cases, the spores were presented in glomerular capillary loops but displayed mild or non pathological change. The parasitic penetration was not observed in the Bowman's space (Fig. 4.4c). Large amounts of pseudoplasmodia attached to brush border of renal tubular epithelial cell, while mature spores were predominantly found in the center of tubular lumens (Fig. 4.4e). Many tubules filled with a large number of spores and pseudoplasmodia where the tubular epithelium

became necrotic or underwent necrosis (Fig. 4.5a and 4.5b). The infected proximal tubules showed significant dilation. Moreover, it exhibited severe cytoplasmic vacuolation and pyknotic nuclei of low columnar epithelial cells (Fig. 4.5c and 4.5d). High degree of cellular degeneration and necrosis were observed. In early stages, proximal tubules architecture could still be recognized and some small pseudoplasmodia appeared in brush border. After parasitic accretions, the distal tubules were obstructed and vacuolation attaching to parasitic pseudoplasmodia were observed in epithelial cells. Finally, epithelial cell membrane, brush border and whole renal tubules were totally destroyed and disappeared. Only intact spores, cellular debris and surrounded mononuclear phagocytic cells were observed. Occasionally in heavy necrotic tissue, a few melanomacrophages were presented especially in the interstitium. Therefore, degenerated appearances of renal tubules as a result of this parasite infection are variable from gradual tissue destruction to atrophy renal parenchyma in chronic stage (Fig. 4.5f). In the PAS staining, all infected proximal tubules with remained parasites are commonly associated with mucus hypersecretion characterized by higher positive PAS stain on brush border than in normal cells distinctively (Fig. 4.5e). Histopathologically, inflammatory responses of the fish host were only immunological cell infiltration and a few melanomacrophage centers. The common immunological host response to the myxosporean group such as melanization and eosinophilic granular cell (EGC1) were not evident in this study.
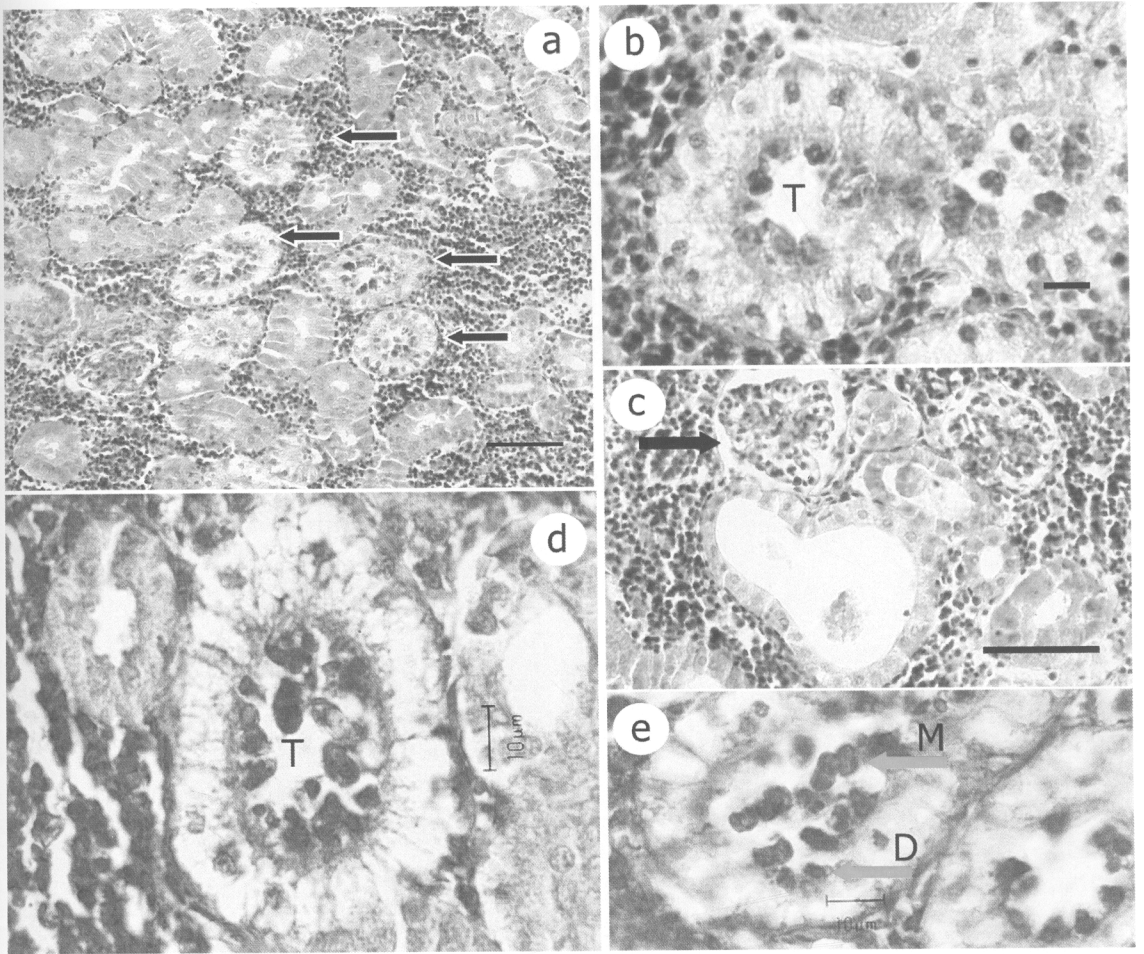
Fig. 4.4 General indication of *S. epinepheli* infected the kidney of orange-spotted grouper, *E. coioides* (**a-e**). **a**; Infected renal tubules showed histopathological changes in their architecture (black arrow). **b**; Low columnar epithelial cells displayed vacuolation in infected renal tubule (T). **c**; The parasitic penetration was not observed within the Bowman's space (arrow) and no pathological change in glomerulus. **d**; High magnification was elucidated the location site of parasite development in renal tubule (T). **e**; Developmental plasmodia (D) were generated inside the brush border connected with tubule columnar epithelial cell and mature spore (M) were related to proximal tubule. Sections were stained with H&E (**a-c**) and toluidine blue (**d** and **e**). Scale bars (**a-c**): 10 μm.
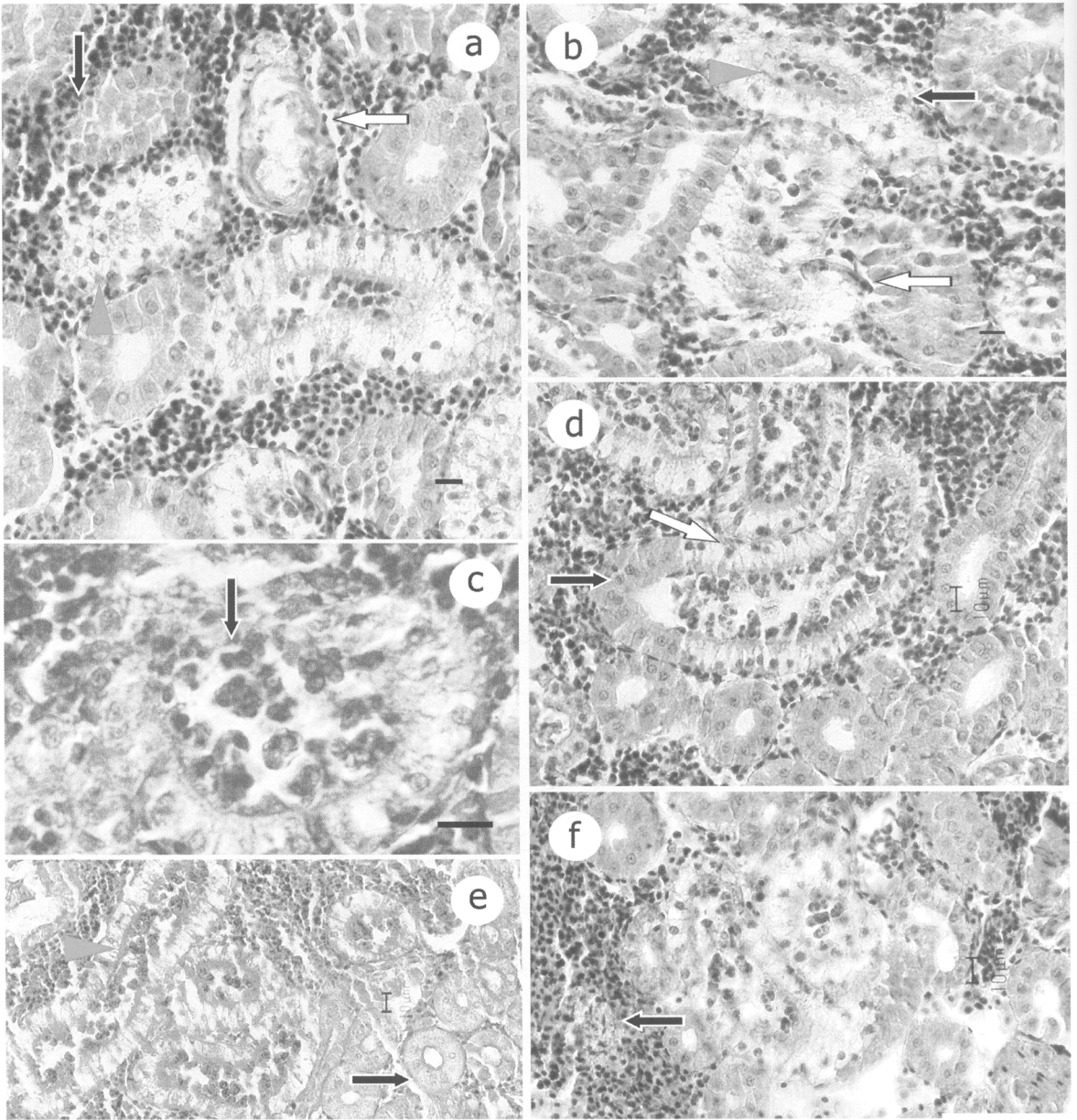
Fig. 4.5 Histopathological damage of *E. coioides* kidney infected by *S. epinepheli* (**a-f**). **a**; The heavy infection showed the decay of brush border (red arrow head) and renal tubule (white arrow) with mononuclear phagocytic cells infiltrated (black arrow). **b**; Renal tubule occluded by various sporogonic stages (red arrow head) and degenerated (white arrow) and pyknotic nuclei (black arrow) of low columnar epithelial cell. **c**; the evidence of tubule epithelium destroying by parasite. **d**; Low columnar epithelial cells showed

vacuolation particularly to which attached parasitic pseudoplasmodia (white arrow), while other cells are normal (black arrow). **e;** The infection tubule (red arrow head) show the thick mucosubtract layer more than normal tubule (black arrow) and it was burrowed and cover associated immature spore. **f;** Renal parenchyma became atrophy lately in chronic stages and inflammatory response from the host, melanomacrophage centre (black arrow). Sections are H&E (a, b, d and f) PAS (e) and toluidine blue (c). Scale bars (a-c): 10 μm

The main inflammatory response was mononuclear phagocytic cells infiltrated throughout renal parenchyma which involved renal corpuscle and tubules. However evidences of invasion or damage of tubular epithelium and the histopathological changes in brush border were clearly observed as well as dilatation of infected tubules.

4. Molecular data and phylogenetic analysis

The nucleotide sequences of 18S rDNA of six *S. epinepheli* collected from each host, *E. malabaricus* and *E. coioides*, from two sampling locations were obtained and determined. The sequences revealed two distinct sequences of *S. epinepheli* type SEM (GenBank Accession Number: HQ871152) from *E. malabaricus* and type SEC (GenBank Accession Number: HQ871153) from *E. coioides*. Both sequence types were submitted to GenBank and displayed a 99.9% homology of nucleotide sequence. The BLAST analysis of *S. epinepheli* with SSU rDNA myxosporean sequences available in GenBank revealed the highest homology to *Bipteria formasa* (GenBank Accession Number: FJ790309) which also showed

71

97% sequence identity with 70% of SSU rDNA of *S. epinepheli*. The preprimary alignment of SSU rDNA *S. epinepheli* sequence from both hosts with other member sequences of genus *Sphaerospora* and other myxosporeans showed two long independent inserts in the V4 region that represents numerous bases in conserved areas of the SSU rDNA differed from those of most myxozoans. The phylogenetic trees constructed using ML and BI revealed the same gross topology and showed that *S. epinepheli* is deeply embedded in the basal sphaerosporid clade (Fig. 4.6). Parametric bootstrapping (ML) and posterior probabilities (BI) of interested clusters within these lineages and at the base of the tree are generally high. Some branches were swapped within clades, however, this did not significantly change the apparent evolution relationship. Both topology analysis demonstrated the *S. epinepheli* in the monophyletic group which containing four species of marine urinary *Sphaerospora* and one *Bipteria* species. In the phylogram, ML constructed tree was used to base tree with the three major clusters including 1) the cluster of basal *Sphaerospora*, 2) predominantly freshwater taxa and 3) the predominantly marine species cluster with high bootstrap value support. Our interested *S. epinepheli* taxa were presented in basal sphaerosporid subclade which all members contributing to this subclade inhabit the marine fish parasite. However this group was manifestly separated from marine myxosporean cluster by exhibiting a common of large expansion segment in variable region. Up to date, 13 species of *Sphaerospora* Thélohan, 1892 have been sequenced and their positions are in variable clades of phylogram, suggesting to the paraphyletic genus. In addition, phylogenetic analysis from both algorithms showed the predominant of *Sphearospora* spp. including *S. epinepheli* in the basal sphaerosporid

clade, as a primitive cluster of myxosporea clade with high bootstrap values support.
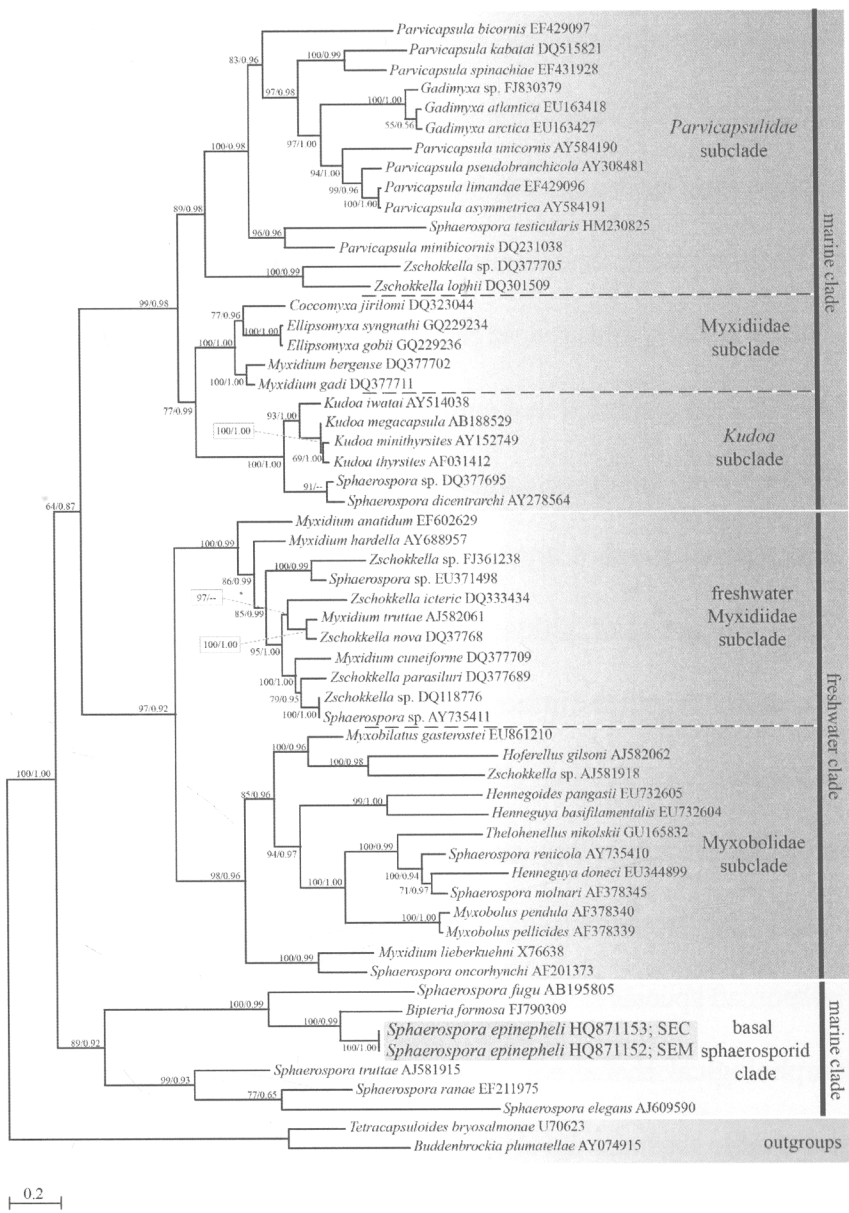
Fig. 4.6 Maximum likelihood tree (-In= 41635·62655) of the SSU rDNA sequence of selected myxozoans species was shown the genetic position of *S. epinepheli*. Malacosporeans; *Tetracapsuloides bryosalmonae* and *Buddenbrockia plumatellae* were set as outgroups. Nodal supports are indicated for ML (bootstrap, n=500) and BI (posterior probabilities, 1,000,000 generations) with less than 50% support are not shown. GenBank Accession Number of each taxon are listed. The distance scale is shown under the tree. - represents the differences node output of BI from ML tree.

Discussion

Two economic grouper species, *E. malabaricus* and *E. coioides*, out of five species were infected with *S. epinepheli*. *E. coioides* appeared to be a new host record. This finding was authenticated by inferring from multi-biological tools underneath the opaque host specificity of myxosporean. The majority of *Sphaerospora* species usually showed high degree of host specificity (Lom and Dyková, 2006) and prefer developing in a single organ or specific to a host tissue type (Liu *et al.*, 2010). However, many researchers have made the critical comments on inaccuracy of using spore morphology and host record in discriminating between myxosporean species (Hogge *et al.*, 2004; Iwanowicz *et al.*, 2008). The morphology variation of myxosporean which infect multiple hosts has led to erroneously description as the same species (Molnár *et al*, 2002; Hallett *et al.*, 2006; Griffin *et al.*, 2009). The combination of morphology and molecular analysis, with an investigation of host range and tissue tropism, plays important roles in the classification of complicated myxosporean species (U-taynapun *et al.*, 2010).

Morphological characters of our reported *S. epinepheli* from both fish hosts are closely resemble those in the original description. The resemblance of fresh spores isolated from both hosts was corroborated. Moreover, the mature spores presented as a drawing line by Supamattaya *et al.* (1991) was definitely the same as our observations. The similar spore morphology and organ infection of the different hosts were found in *S. epinepheli* as well as presented in previous reports of *S. ranae* in *Rana dalmatina* and *R. temporaria* (Jirků *et al.*, 2007). Eszterbauer and Székely (2004) suggested that in most cases of the variable host infected myxosporean, their locations (organ and/or tissue tropism) within the new fish host remained unchanged. Our results suggested that the high degree of host specificity of *S. epinepheli* is

recently restricted to specific to two species of the economic *Epinephelus* spp. A relative narrow host spectrum was also reported in other species of the basal sphearosporid group, *S. elegans* and *S. truttae*, parasitizing only related fish species of the family Dasterosteidae and Salmonidae, respectively (Lom and Dyková, 2006).

The incidence of *S. epinepheli* infection in *E. malabaricus* and *E. coioides* as a percentage of infection rate was 9.05% and 24.82%, respectively. Our result could indicate that *S. epinepheli* prefers infecting the orange-spotted grouper. This may be due to some parameters which promote the parasite susceptibility in host-parasite interaction (Nuismer and Otto, 2005); however, those parameters have to be figured out. Even though seasonal patterns of *S. epinepheli* occurrence from both fish hosts were not related to the incidence of infection, the data showed higher infection in rainy season than dry season. The population dynamics in *E. malabaricus* was similar to the previous report 20 years ago (Supamattaya *et al.*, 1991).

The severity of kidney damage in *E. coioides* infected by *S. epinepheli* was similar to those reported in *E. malabaricus*. Histopathological changes demonstrated the harmful effect of this parasite infection. Spores and developmental stages of *S. epinepheli* were often found in large numbers which partially obstructed the renal tube. This is a typical characteristic of coelozoic myxosporean which are mostly found in the coelom. The infected glomerulus of *E. malabaricus* showed extremely dilated glomerulus capillaries, reduced number of podocyte and congestive developmental stages. However the mature spores that were found in Bowman's space could not be observed in *E. coioides*. In contrast, the infected renal tubules of both fish hosts revealed that intraluminal stages of parasite induced many vacuoles and pyknotic nuclei in tubular epithelial cells. Chen *et al.* (2001) have reported that spores of *Sphaerospora* spp. a coelozoic parasite of kidney in cobia, *Rachycentron*

canadum could be detected causing mass mortality with dilation, hypertrophy and hyperplasia of renal tubules. Some other myxosporean species which affect their hosts in a similar pattern are *Myxidium hardella*, the parasite infecting turtle, *Hardella thurjii* kidney resulting in tubular necrosis and chronic interstitial nephritis (Garner *et al.*, 2005). Trivial host immune responses have been detected in *S. epinepheli* infection. The infected renal tubules were besieged by mononuclear phagocytic cell from surrounding renal parenchyma and a few melanomacrophage centers were found. In some cases of infection, spores were found in destroyed renal tubules suggesting the host immune responses. Inability of tissue reactions or host responses to myxosporean infections have been mentioned by many other authors (Alvarez-Pellitero *et al.*, 2007; Sitja-Bobadilla, 2008).

As pointed out by many researchers (Molnár *et al.*, 2009; Adriano *et al.*, 2009 Bartošová *et al.*, 2009; Jirků *et al.*, 2007; Liu *et al.*, 2010), molecular phylogenetic analysis have become a novel standard of taxonomic tools for the classification of complicated myxosporean. In this study, 18S rDNA analysis of *S. epinepheli* from both fish hosts exhibited the inserted long variable regions causing longer sequence than expected length. However, this result is close to the previous reports in sphaerorid species (Holzer *et al.*, 2004; Bartošovà *et al.*, 2010). The investigation of the main variable region length showed the present of 2 areas with extensive inserts in the V4 region (Jirků *et al.*, 2007). Our phylogram analysis indicated the polyphyletic character in the *Sphaerospora* genus. The phylogenetic position of both *S. epinepheli* isolated from *E. malabaricus* and *E. cioiodes* were placed together with other long SSU rDNA *Sphaerospora* spp. in the clade of basal sphaerosporid which were separated from freshwater and marine myxosporean clade with high bootstrap value supports. This is consistent with previous reports (Holzer *et*

al., 2007, 2010; Bartošovà *et al.*, 2010; Jirků *et al.*, 2007). On the other hand, *S. epinepheli* was placed in a close relationship with *B. formosa*, a gallbladder parasite of marine fish. Up to date, only 18S rDNA of *Bipteria* genus is available in GenBank. However the previous report discussing about *B. formosa* suggested that the molecular data is related to *S. fugu* and the members belonging to sphaerosporid clade (Karlsbakk and Køie, 2009). Modern phylogenetic clustering, conducted based on ML and BI algorithms, revealed the related evolution of myxosporean species in sphaerosporid clade, nevertheless, the hosts of this parasite clade are variable including marine teleost fish and frog. All species from basal sphaerosporid were found only in the urinary system; kidney tubules, glomerulus and gallbladder. It might be that the relationships between myxosporean species containing long SSU rDNA are obscure, since sequence data from the type taxa of this clade is still scarce.

In conclusion, spore morphology, genetic analysis and histological validity in the present study have demonstrated that coelozoic *Shaerospora* spp. in the kidney tubules of *E. coioides* is that of *S. epinepheli* which was reported to infect in *E. malabaricus*. The new host record of *S. epinepheli* was firmly asserted and acceptable via the individual conceptions of *Sphaerospora* genus. They are polyphyletic, with species deposited in different phylogenetic clusters including freshwater, marine and basal sphaerorid clade. Further studies will be focused on the rapid diagnosis and a survey on infection in different fish culture conditions and habitat which are important for clarification of pathological characters of this parasite in grouper aquaculture.

References

Adriano, E. A., Arana, S., Alves, A. L., Silva, M. R. M., Ceccarelli, P. S., Henrique-Silva, F. and Maia, A. A. M. 2009. *Myxobolus cordeiroi* n. sp., a parasite of *Zungaro jahu* (Siluriformes: Pimelodiade) from Brazilian Pantanal: Morphology, phylogeny and histopathology. Vet. Parasitol. 162 : 221–229.

Alvarez-Pellitero, P., Palenzuela, O. and Sitjà-Bobadilla, A. 2007. Histopathology and cellular response in *Enteromyxum leei* (Myxozoa) infections of *Diplodus puntazzo* (Teleostei). Parasitol. Int. 57 : 110–120.

Bartošová, P., Fiala, I., Hypša, V. 2009. Concatenated SSU and LSU rDNA data confirm the main evolutionary trends within myxosporeans (Myxozoa: Myxosporea) and provide an effective tool for their molecular phylogenetics. Mol. Phylogenet. Evol. 53 : 81–93.

Bartošová, P., Freeman, M. A., Yokoyama, H., Caffara, M. and Fiala, I. 2010. Phylogenetic position of *Sphaerospora testicularis* and *Latyspora scomberomori* n. gen. n. sp. (Myxizoa) within the marine urinary clade. Parasitology 15 : 1–13.

Bermúdez, R., Losada, A. P., Vázquez, S., Redondo, M. J., Álvarez-Pellitero, P. and Quiroga, M. 2010. Light and electron microscopic studies on turbot *Psetta maxima* infected with *Enteromyxum scophthalmi*: histopathology of turbot enteromyxosis. Dis. Aquat. Org. 89 : 209–221.

Castresana, J. 2000. Selection of conserved blocks from multiple alignments for their use in phylogenetic analysis. Mol. Biol. Evol. 17 : 540–552.

Chen, S. C., Kou, R. J., Wu, C. T., Wang, P. C. and Su, F. Z. 2001. Mass mortality associated with a *Sphaerospora*-like myxosporidean infestation in juvenile

cobia, *Rachycentron canadum* (L.), marine cage cultured in Taiwan. J. Fish Dis. 24 : 189–195.

Eszterbauer, E. and Székely, C. 2004. Molecular phylogeny of the kidney-parasite *Sphaerospora renicola* from common carp (*Cyprinus carpio*) and *Sphaerospora* sp. from goldfish (*Carassius auratus auratus*). Acta Vet. Hung. 52 : 469–478.

Fioravanti, M. L., Caffara, M., Florio, D., Gustinelli, A. and Marcer, F. 2004. *Sphaerospora dicentrarchi* and *S. testicularis* (Myxozoa: Sphaerosporidae) in farmed European seabass (*Dicentrarchus labrax*) from Italy. Folia Parasitol. 51 : 208–210.

Garner, M. M., Bartholomew, J. L., Whipps, C. M., Nordhausen, R. W. and Raiti, P. 2005. Renal myxozoanosis in crowned river turtles *Hardella thurjii*: Description of the putative agent *Myxidium hardella* n. sp. by histopathology, electron microscopy, and DNA sequencing. Vet. Pathol. 42 : 589–595.

Gouy, M., Guindon, S. and Gascuel, O. 2010. SeaView Version 4: A multiplatform graphical user interface for sequence alignment and phylogenetic tree building. Mol. Biol. Evol. 27 : 221–224.

Griffin, M. J., Khoo, L. H., Torrans, L., Bosworth, B. G., Quiniou, S. M., Gaunt, P. S. and Pote, L. M. 2009. New data on *Henneguya pellis* (Myxozoa: Myxobolidae), a parasite of blue catfish *Ictalurus furcatus*. J. Parasitol. 95 : 1455–1467.

Guindon, S. and Gascuel, O. 2003. A simple, fast, and accurate algorithm to estimate large phylogenies by maximum likelihood. Syst. Biol. 52 : 696–704.

Hall, T. A. 1999. BioEdit: a user-friendly biological sequence alignment editor and analysis program for Windows 95/98/NT. Nuclic Acids Symp. Ser. 41 : 95–98.

Hallett, S. L., Atkinson, S. D., Holt, R. A., Banner, C. R. and Bartholomew, J. L. 2006. A new myxozoan from feral goldfish (*Carassius auratus*). J. parasitol. 92 : 357–363.

Harikrishnan, R., Balasundaram, C. and Heo, M.-S. 2010. Molecular studies, disease status and prophylactic measures in grouper aquaculture: economic importance, disease and immunology. Aquaculture 309 : 1–14.

Hillis, D. M. and Dixon, M. T. 1991. Ribosomal DNA: molecular evolution and phylogenetic inference. Q Rev Biol 66 : 411–453.

Hogge, C., Campbell, M. and Johnson, K. 2004. Discriminating between a neurotropic *Myxobolus* sp. and *M. cerebralis*, the causative agent of salmonid whirling disease. J. Aquat. Anim. Health 16 : 137–144.

Holzer, A. S., Sommerville, C. and Wooten, R. 2004. Molecular relationships and phylogeny in a community of myxosporeans and actinisporeans based on their 18S rDNA sequences. Int. J. Parasitol. 34 : 1099–1111.

Holzer, A. S., Wootten, R. and Sommerville, C. 2007. The secondary structure of the unusually long 18S ribosomal RNA of the myxozoan *Sphaerospora truttae* and structural evolutionary trends in the Myxozoa. Int. J. Parasitol. 37 : 1281–1295.

Holzer, A. S., Wootten, R. and Sommerville, C. 2010. *Zschokkella hildae* Auerbach, 1910: Phylogenetic position, morphology, and location in cultured Atlantic cod. Parasitol. Int. 59 : 133–140.

Iwanowicz, L. R., Iwanowicz, D. D., Pote, L. M., Blazer, V. S. and Schill, W. B. 2008. Morphology and 18S rDNA of *Henneguya gurlei* (Myxosporea) from *Ameiurus nebulosus* (Siluriformes) in North Carolina. J. Parasitol. 94 : 46–57.

Jirků, M., Fiala, I. and Modrý, D. 2007. Tracing the genus *Sphaerosppora*: rediscovery, redescription and phylogeny of the *Sphaerospora ranae* (Morelle, 1929) n. comb. (Myxosporea, Sphaerosporidae), with emendation of the genus *Sphaerospra*. Parasitology 134 : 1727–1739.

Karlsbakk, E. and Køir, M. 2009. *Bipteria formosa* (Kovaleva et Gaevskaya, 1979) comb. n. (Myxozoa: Myxosporea) in whiting *Merlangius merlangus* (Teleostei: Gadidae) from Denmark. Folia Paraitol. 56 : 86–90.

Liu, Y., Gu, Z. M. and Luo, Y.L. 2010. Some additional data to the occurrence, morphology and validity of *Myxobolus turpisrotundus* Zhang, 2009 (Myxozoa: Myxosporea). Parasitol. Res. 107 : 67–73.

Lom, J. and Dyková, I. 2006. Myxozoan genera: definition and notes on taxonomy, life-cycle terminology and pathogenic species. Folia Parasitol. 53 : 1–36.

Longshaw, M. Frear, P. A. and Feist, S. W. 2005. Descriptions, development and pathogenicity of myxozoan (Myxozoa: Myxosporea) parasite of juvenile cyprinids (Pisces: Cyprinidae). J. Fish Dis. 28 : 489–508.

Molnár, K., Eszterbauer, E., Székely, C., Dán, A. and Harrach, B. 2002. Morphological and molecular biology studies on intramuscular *Myxobolus* spp. of cyprinid fish. J. Fish Dis. 25 : 643–652.

Molnár, K., Székely, C., Hallett, S. L. and Atkinson, S. D. 2009. Some remarks on the occurrence, host-specificity and validity of *Myxobolus rotundus* Nemeczek, 1911 (Myxozoa: Myxosporea). Syst. Parasitol. 72 : 71–79.

Moncada, L. I., López, M. C., Murcia, M. I., Nicholls, S., León, F., Guío, O. L. and Corredor, A. 2001. *Myxobolus* sp., Another opportunistic parasite in immunosuppressed patients? J. Clin. Microbiol. 39 : 1938–1940.

Nuismer, S. L. and Otto, S. P. 2005. Host-Parasite interaction and the evolution of gene expression. PLoS Biol. 3, 1283–128.

Posada, D. 2008. jModelTest: Phylogenetic model averaging. Mol. Biol. Evol. 25 : 1253–1256.

Ronquist, F. and Huelsenbeck, J. P. 2003. MrBayes 3: Bayesian phylogenetic inference under mixed models. Bioinformatics 19 : 157–1574.

Sitja-Bobadilla, A. 2008. Fish immune response to Myxozoan parasites. Parasite 15 : 420–425.

Supamattaya, K., Fischer-Scherl, T., Hoffmann, R. W. and Boonyaratpalin, S. 1990. Renal sphaerosporosis in cultured grouper *Epinephelus malabaricus*. Dis. Aquat. Org. 8 : 35–38.

Supamattaya, K., Fischer-Scherl, T., Hoffmann, R. W. and Boonyaratpalin, S. 1991. *Sphpaerospora epinepheli* n. sp. (Myxosporea: Sphaerosporidae) observed in grouper (*Epinephelus malabaricus*). J. Eukaryot. Microbiol. 38 : 448–454.

U-taynapun, K., Penprapai, N., Bangrak, P., Mekata, T., Itami, T. and Tantikitti, C. 2010. *Myxobolus supamattayai* n. sp. (Myxosporea: Myxobolidae) from Thailand parasitizing the scale pellicle of wild mullet (*Valamugil seheli*). Parasitol. Res. in press. 10.1007/s00436-010-2223-1.

Yokoyama, H., Ogawa, K. and Wakabayashi, H. 1990. Chemotherapy with fumagillin and toltrazuril against kidney enlargement disease of goldfish caused by the myxosporean *Hoferellus carassii*. Fish Pathol. 25 : 157–163.

5. DEVELOPMENT OF RAPID DIAGNOSIS FOR PARASITIC *Sphaerospora epinepheli* (MYXOSPOREA) IN GROUPER (*Epinephelus* spp.): THE COMPARISON BETWEEN TURBIDITY-BASED REAL TIME LAMP AND QUANTITATIVE PCR

Abstract

The rapid diagnosis real time turbidity-based loop-mediated isothermal amplification (real time LAMP) to detect *Sphaerospora epinepheli*, a sphaerosporesis disease causing pathogen in economic groupers *Epinephelus coioides* and *E. marabaricus*, was developed. The optimal temperature, and primer sets used for real time LAMP was determined using total DNA of *S. epinepheli* as a template. The results showed that the reaction contains loop primers which amplified at 63°C giving highest amplification efficiency. The assay performance of the developed real time LAMP was tested and compared to that of the real time PCR (qPCR). The detection limit including specificity and sensitivity of these two methods was compared. Only DNA of *S. epinepheli*, while none of other myxosporean, could be amplified by these two systems. Sensitivity analysis indicated that at least 5 copies of the recombinant plasmid with inserted target DNA is the detectable ability of real time LAMP and qPCR. Moreover, these two methods were tested for their potential utilization to detect *S. epinepheli* in fishes which were diagnosed by microscopically detection. Our results demonstrated that real time LAMP and qPCR assays can be applied as a diagnostic standard protocol for *S. epinepheli* detection in infected juvenile grouper. However, real-time LAMP assay will be more suitable for use routinely as a comprehensive *S. epinepheli* and other myxosporean pathogens detection system in the field because of its speed, simplicity, specificity and low cost.

Introduction

Asia is the largest producer of cultured seafood products in the world as well as the biggest producer of groupers, a high-value marine fish. The top of the list of grouper aquaculture production are China and Taiwan followed by Indonesia and Thailand. In 2005, Asia produced a total of 62,088 tons representing 24% of total world grouper production (FAO, 2007). Among grouper species, *Epinephelus coioides* and *E. marabaricus* are the important commercial fishes which have been widely cultured in the Indo-Pacific (Liao and Leaño, 2008). However, the rapid increase of culture density and environmental deterioration results in the occurrence of several disease epizootics. Among these, parasitic diseases such as myxosporean infection cause the serious impact on the economic loss of cultured and wild groupers.

Myxosporeans are parasitic metazoan parasite and their infections wildly distribute in several fish species (Lom and Dyková, 2006). Although most myxosporean species have been reported as an unserious parasite in aquaculture and wild fish, the numbers of species of the genus *Myxobolus*, *Enteromyxum*, and *Sphaerospora* are described as the important parasitic pathogens. Sphaerosporesis disease caused by *Sphaerospora* spp. is such a problem with growing importance on economic fish cultures worldwide. Some species such as *S. dicentrarchi* and *S. testicularis* are responsible for important economic losses in European sea bass, *Dicentrarchus labrax* in Mediterranean zone (Bartošova *et al.*, 2010). Similarly, *S. epinepheli* is a significant pathogen in orange spotted grouper and malabar grouper in Southeast Asia. Its geographic distribution has been recorded in both India and West Pacific Ocean. Moreover, study on the pathology of *S. epinepheli* revealed its strong pathogenicity effects on fish host kidney including the renal tubulonephosis,

tubular necrosis and chronic interstitial nephritis. The research on these diseases in Thailand, however, is still scarce.

Conventionally, the identification of the myxosporean is performed microscopically based on morphological characteristics. This method is very time consuming and results are not always conclusive. In addition, microscopic diagnosis requires tissue dissection from the fish such as kidney or liver which cannot avoid so fish loss. Due to the limitation of sensitivity and simplification of myxosporean species identification technique which requires substantial experience, it is indeed complicated to achieve important information of myxosporean in cultured grouper. This data will help overcome protecting fish seed from parasitic infection and enhance the net cage culture. The development of high sensitivity diagnosis for myxosporean has grown concurrent with the outbreak and spread of the disease in fish and intermediate host populations (El-Matbouli and Soliman, 2005). Recently, various molecular diagnotic assays for myxosporean detection have been developed including the PCR based detection systems. For rapid identification of these pathogens, PCR, nested PCR and qPCR have therefore been developed to classify various species based on the detection of small subunit ribosomal DNA. These techniques are highly specific and conquer sensitivity limitations of classical diagnosis. Among these methods, qPCR has been promoted as the best tool because of its high sensitivity and high specificity. However, there are some inherent disadvantages of qPCR methods that require either a high-precision amplification instrument or an elaborate complicated method for detection of amplified products (Parida *et al.*, 2004) or long operation time. Thus, a simple, quick and reliable quantitative detection method is urgently needed.

A loop-mediated isothermal amplification (conventional LAMP) developed by Notomi *et al.* (2000) is an efficient and specific method for amplification of nucleic acid templates. The LAMP method produces large amounts of the target DNA as well as an insoluble by-product, magnesium pyrophosphate during the reaction allowing possibility to perform a real time measurement of turbidity using an inexpensive photometer (Mori *et al.*, 2001; Sudhakaran *et al.*, 2008). Nowadays, a quantitative real time LAMP using isothermal conditions has been developed. For the diagnosis of human and veterinary animal health, real time LAMP was used to verify the various pathogens (Christopher *et al.*, 2010). Moreover it has been developed to analyze and monitor other purposes involving bacterial community in environment and plant crop protection strategies (Aoi *et al.*, 2006; Bekele *et al.*, 2011).

In this study, a real time LAMP method for rapid detection of *S. epinepheli*, parasite of economic grouper species, *E. malabaricus* and *E. epinepheli*, in Thailand was developed and evaluated. It is important to establish a monitoring method which targets sphaerosporesis in seed grouper for aquaculture and juvenile state in nature because this parasite plays an important role in destroying fish health. The following result is the dysfunction of fish kidney. Moreover, we evaluate two measurement tools for *S. epinepheli* quantification – turbidity real time LAMP, and fluorescence based qPCR. The potential use of both methods on detecting parasitic pathogen in grouper blood samples was also tested.

Materials and Methods

1. Source of *S. epinepheli* spores and DNA sample

Kidney samples of grouper, *E. malabaricus* and *E. coioides* infected with *S. epinepheli* were obtained from fish farms and fishermen in the Andaman Sea area, Thailand. Wet-mount diagnosis of kidney tissues and blood stage parasite were examined by light microscopy and indentified following the taxonomic guideline of Lom and Dyková (2006) and Supamattaya *et al.* (1991). Parasite was isolated from fish tissue using discontinuous Percoll™ gradients technique (2.5 ml layers of 20% and 40% (v/v) Percoll™ in phosphate buffered saline, PBS pH 7.4; Sigma, US) and centrifuged at 2,000*xg* for 30 min at 4°C. The spores were washed twice with PBS. The purified spores were treated with proteinase K (U-taynapun *et al.*, 2010) before being extracted using DNeasy Tissue Kit (Qiagen, CA) according to the manufacturer's instructions. Extracted DNA samples were quantified spectrophotometrically at 260 nm and stored at -20°C until use.

2. Primer design for LAMP and qPCR

Species-specific primers for LAMP were designed based on the SSU rDNA of *S. epinepheli* (GenBank Accession Number HQ871152 and HQ871153). The target gene sequence was analyzed and primers were generated using the LAMP primer design software: Primer Explorer V.4 (http://primerexplorer.jp/lamp1.0.0/ index.html, Fujitsu, Japan). Each primer set, consisting of six primers; F3, B3, LF, LR, FIP and BIP, was designed according to the guideline provided.

Primers; S.epiF and S.epiR used in the qPCR study were designed via the Primer3 web interface (Rozen and Skaletsky, 2000) within the same sequences

data for designing the real time LAMP primers. The oligonuleotide primers used for the amplification, real time LAMP and qPCR are shown in Table 5.1.

Table 5.1 Primer used for the real time LAMP and qPCR diagnosis of *S. epinepheli* 18S rRNA gene

Primer name	Position	Sequence 5'->3'
Specific primes for real time LAMP		
S.epi-FIP		GCATGTGTTGTACCAAGAGTTATGT-CGCTCGTAG TTTGATAGCA
S.epi-BIP		TTGTGGTTCCCTATACCTCGG-CGCAAATCACATA CCCTTGT
S.epi-F3	685-730	GTGGTGTATCGCATTGTTG
S.epi-B3	874-892	CGTACCCACGATACATTGT
S.epi-LF	744-765	GTATGGATAATGCTACAGCCGG
S.epi-LB	819-842	TATGGGGTTCACACATCACATTAG
Specific for qPCR		
S.epiF	814-831	CTCGGTATGGGGGTTCACA
S.epiR	987-1005	AAATACCCCAACAAGCCT

3. Turbidimetry real time LAMP reaction

Real time LAMP was performed in 25 µl of total reaction mixture volume containing a loopamp DNA amplification kit (Eiken Chemical, Japan) according to the manufacturer's instructions. Briefly, 5.5 µl of the target DNA (>5 copies) was mixed with 1 µl (40 pmol) of each S.epi-FIP and S.epi-BIP, 1 µl (5 pmol) of S.epi-F3 and S.epi-B3 primers, 1 µl (20 pmol) of S.epi-LF and S.epi-LR, 12.5 µl of reaction mix (2X), 1 µl Bst DNA polymerase. The reaction temperature was optimized with 59°C, 61°C, 63°C and 65°C using a real time turbidimeter (Loopamp LA-200, Teremecs, Japan) by mean of measuring the increase in turbidity derived from the magnesium pyrophosphate, a by-product of LAMP reaction. Reaction

mixture was incubated at the optimal temperature for 80 min and monitoring every 6 s by spectrophotometric measurement at 650 nm.

4. SYBR Fluorescent based qPCR reaction

Primers were synthesized for detecting *S. epinepheli* in both recorded host fish and used to develop a detection system for this pathogen. Primers were used to amplify 191 bp fragment. Quantitative PCR: 1 μl of target DNA was added to 12.5 μl of SYBR Green master mix (iQ SYBR Green Supermix, BioRad Laboratories, Hercules, CA) and 50 pmol of each forward and reverse primers were added along with a sufficient volume of nuclease free water to make a 25 μl of reaction mixture. Quantitative PCR employed with the ABI 7300 instrument and proceeded with a 94°C melt step for 4 min, and then 40 cycles of 94°C for 20 s and 65°C for 50 s with green fluorescence read at the end of each cycle. A melt curve was determined at the end of each qPCR run.

5. Sensitivity determination of real time LAMP and qPCR assay

To quantify the target DNA of *S. epinepheli* using the real time LAMP and qPCR method, the recombinant vector of *S. epinepheli* SSU rDNA with 2,066 bp inserted fragment (pGEM-epinepheli) was constructed by using the pGEM T-Easy Vector System (Promega, CA) following the manufacturer's protocol. The target DNA was amplified using PCR with the 18e-18g universal primer (Hillis and Dixon, 1991). To evaluate the quantitative sensitivity of both methods, the standard 10-fold-dilutions of pGEM-epinepheli was created by measuring DNA concentration using nanodrop UV spectrophotometer ND-1000 (NanoDrop Technologies Inc., USA) and then a standard curve, ranging from copies of $5–5 \times 10^6$ SSU rDNA was constructed.

For the standard curve of each method, copy number was plotted against the time at the turbidity signal increased above the Tp (the time taken to generate a positive result; O.D. > 0.1) and threshold value (Tv > 0.2) for real time LAMP and qPCR, respectively. Each assay was carried out three times.

6. Specificity determination of real time LAMP and qPCR assay

To evaluate whether these two developed methods could specifically amplify only *S. epinepheli*, DNA of other myxosporean species observed in the Andaman Sea and related areas such as connected river basis were used as templates. The tested parasites included five species; 1) *M. supamattayai* from blue spotted mullet, 2) *Henneguya* sp. from Asian sea bass, 3) *H. duadi* from Gourami, 4) *Zschokkella* sp. from marine cat fish and 5) *Ceratomyxa* sp. from orange spotted grouper. The DNA samples of groupers, exhibiting non infected by *S. epinepheli*, *E. coioides* and *E. malabaricus* were used to test as non-specific amplification. The accuracy of specificity tests were determined by repeating three times with the same samples.

However, the amplified DNA from total DNA of purified *S. epinepheli* spore obtained from both diagnosis methods was sequenced to confirm and recheck the detected products. The qPCR product, 191 bp. which generated using specific primer (SepiF and SepiR) and PCR product (207 bp.) amplified by F3 and B3 primer of specific LAMP primer set were cloned into the vector pGEM-T Easy (promega, USA) following the manufacturer's instruction. The purified plasmid was sequenced on a CEQ™ 8000 automatic sequencer (Beckman Coulter) using CEQ DTCS Dye Kit (Beckman Coulter). The sequence of detected product was blasted with original *S. epinepheli* sequence (GenBank Accession Number HQ871153).

7. Applicability of real time LAMP and qPCR assay

In application for the field diagnosis, both assays were conducted to determine *S. epinepheli* in blood stage and early sporogenesis in wild juvenile grouper that was used as fish seed for net cage aquaculture. Twenty-six orange spotted groupers were collected from Phang-Nga Bay, where the occurrence of this parasite was detected massively. All fish were diagnosed using microscopic test, six grouper were *S. epinepheli*-infected in blood stage or parasitic sporogonic stage within their kidneys (positive) while twenty were negative. Relative quantitative of *S. epinepheli* template was interpolated from plasmid DNA standard curve, based on Tp (the time taken to generate a positive result) of the real time LAMP and Ct value of qPCR.

Results

1. Optimization of real time LAMP assay condition for *S. epinepheli* detection

To determine the optimal temperature and reaction time, real time LAMP was performed using total DNA of *S. epinepheli* as a template. The temperatures, 59, 61, 63 and 65°C were selected for the optimum temperature study. The results indicated that the temperature giving the highest amplification efficiency is 63°C, which is also optimum for the activity of *Bst* DNA polymerase. Moreover, at this temperature, the most rapid amplification was achieved within 30 min for the initiation of amplification as determined by the changes in the turbidity resulted from the accumulated magnesium pyrophosphate (Fig. 5.1a).

91
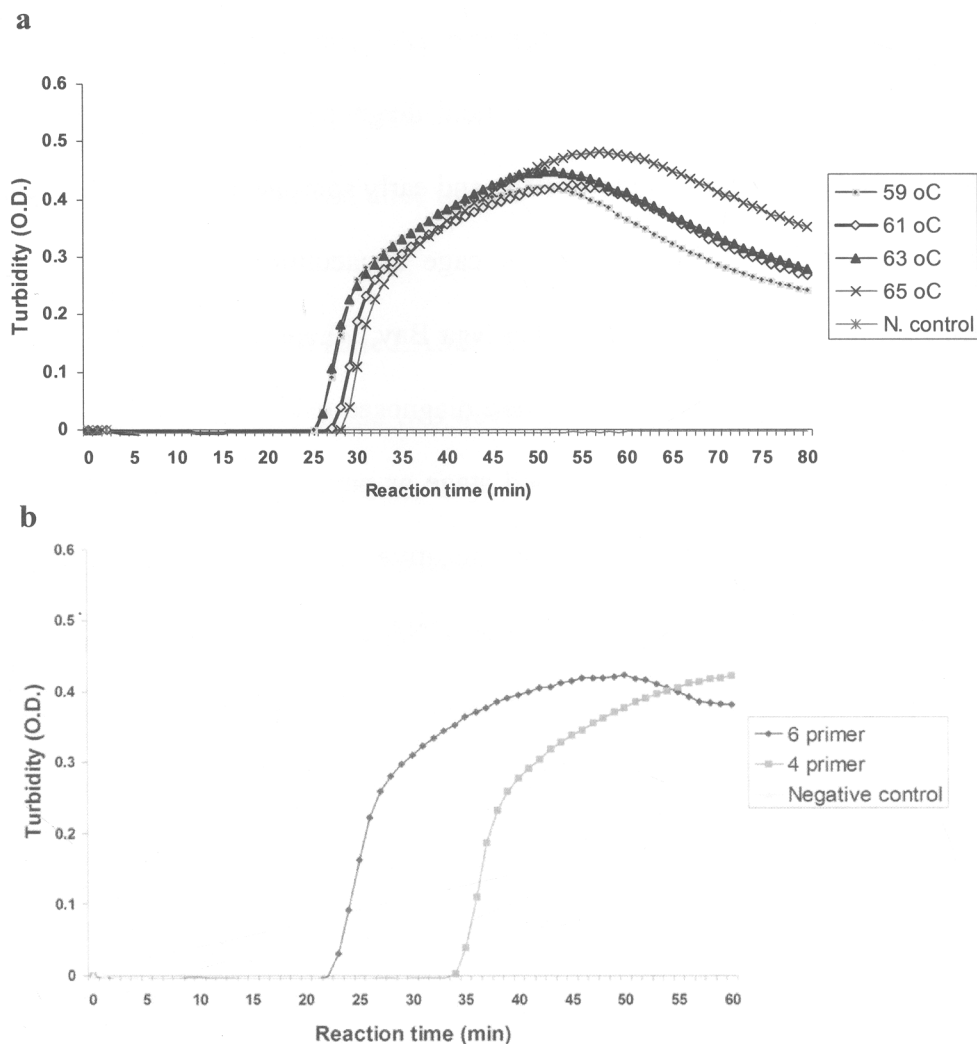
Fig. 5.1 Optimization of the diagnosis reaction for *S. epinepheli* real time LAMP assay; **a**: temperature optimization at 59°C, 61°C, 63°C and 65°C, **b**: sensitivity test of reaction by using 4 primers and 6 primers set.

The real-time kinetics of the real time LAMP reaction with or without loop primers was studied at 63°C by monitoring turbidity as described above. The time required for initiation of amplification was 24 or 35 min with or without loop primers, respectively (Fig. 5.1b). This finding suggested that the use of loop primers accelerated the amplification by reducing 1/3 or 30% of the detection time compared to those obtained without loop primers. The continuous amplification of the target

sequence in a stepwise gradient manner also occurred as observed by increased turbidity compared to that of the negative control, containing no template, where the accepted turbidity were fixed at 0.1 O.D. recording the optical density at 650 nm. Although, amplification was efficient at all tested temperatures and primer sets tested, 63°C for 60 min of reaction time with six primers was selected as optimal conditions for further experiments. However, the product amplified by F3 and B3 primer of specific LAMP primer set and qPCR product were sequenced and checked with the sequence of original *S. epinepheli* (GenBank Accession Number HQ871153).

2. Comparison of sensitivity (detection limits) between real time LAMP and qPCR assay

The sensitivity comparison of frontier rapid detection assay, of parasitic *S. epinepheli*, between real time LAMP and qPCR methods was determined. The serial 10-fold dilutions of pGEM-epinepheli vector that had previously been prepared were used to generate the standard curve as described above. The accelerated real time LAMP assay was able to amplify 50 copies of recombinant *S. epinepheli* vector in 37 min but having a detection limit when using 5 copies of parasitic SSU rDNA (Fig. 5.2a). The comparative sensitivities of the real time LAMP and qPCR assays revealed that both methods showed the same detection limit, of 5 copies of template tested, as revealed by the presence of a 201-bp amplicon in qPCR (Fig. 5.2c). However, both assays displayed high correlation coefficient linearity, $R^2 = 0.9934$ and 0.9835 in real time LAMP and qPCR, respectively when plotting DNA copies against the time to positive detected signal (Fig. 5.2b and 5.2d).
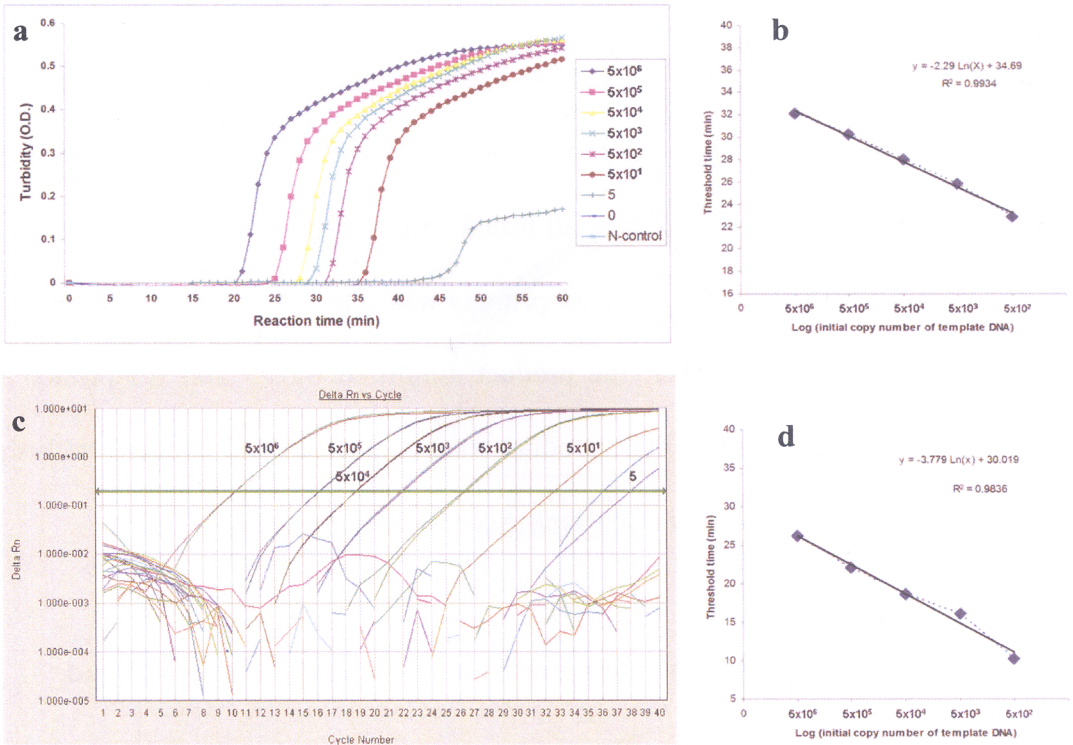
Fig. 5.2 Comparison of the sensitivity between real time LAMP and qPCR assay for quantitative amplification of pGEM-S. epinepheli recombinant vector; **a** and **c** are plasmid standards form real time LAMP and qPCR respectively, **b** and **d** are standards curve generated by real time LAMP and qPCR, respectively.

3. Specificity of real time LAMP and qPCR

The specificity of the real time LAMP and qPCR primers for SSU RNA gene of *S. epinepheli* was established by checking the reactivity with other myxosporean species distributed in related basins. The analysis was carried out with 4 myxosporean species; 1) *Henneguya* sp. parasitizing Asian sea bass, *Lates calcarifer*, 2) *H. daoudi* parasitizing in three spot gourami, *Trichogaster trichoterus*, 3) *Myxobolus supamattayai* parasitizing mullet, *Valamugil seheli*, 4) *Zschokkella* sp. parasitizing marine catfish, *Plotosus canius* and uninfected fish hosts, *E. coioides* and *E. malabaricus* to determine the specificity of both methods. The diagnostic report

showed that both assays developed in this study are highly specific to detect only *S. epinepheli* without any cross-reaction (Fig. 5.3).
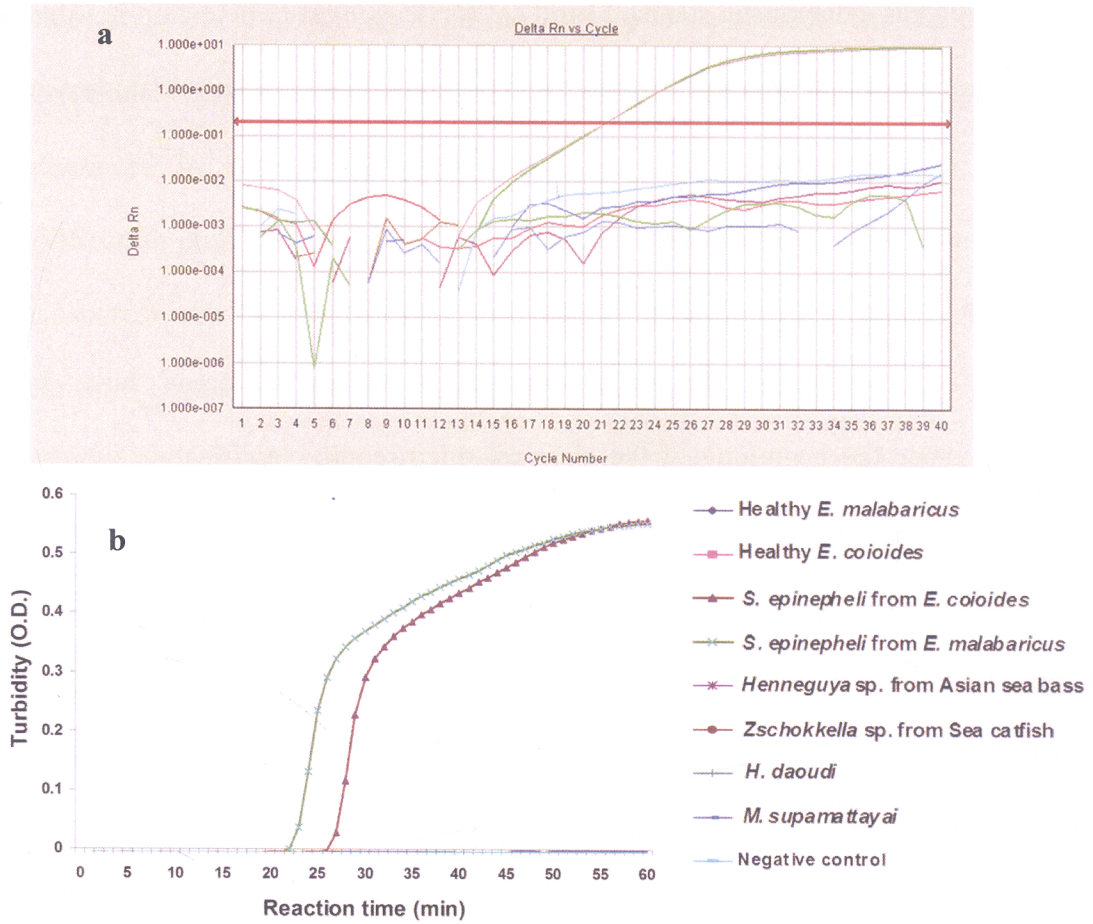
Fig. 5.3 Specificity of diagnosis assays, **a**: qPCR assay and **b**: real time LAMP method. Cross reaction studies with other myxosporan in related habitat of *S. epinepheli* and negative control.

4. Direct detection of *S. epinepheli* in infected wild grouper

The potential utilization of real time LAMP and qPCR assay were tested for application in the field diagnosis of *S. epinepheli* in juvenile orange spotted grouper. The total 5 positive and 20 negative fish specimens for *S. epinepheli* infection diagnosed by microscopically detection were analyzed. As expected, all 5 infected samples showed the positive detection results from both assays (Table 5.2a). The results obtained by these two methods were also similar in negative

microscopically samples, 7 from total 20 samples gave the positive diagnosis (Table 5.2b). These results indicated that our developed real time LAMP and qPCR assays can be applied as a diagnostic standard protocol for *S. epinepheli* detection in infected juvenile grouper which are more sensitive and accurate than the classical microscopic technique.

Discussion

A range of diagnostic techniques for myxosporean have been developed since the beginning of the classical microscopic classification which are conventional nucleic detection, PCR based techniques. Numerous PCR, widely-known assays, were developed and applied to identify specific target gene of various myxosporean, mostly SSU rDNA. However, conventional PCR diagnostic detection based on visualizing after electrophoresis can be problematic, with occasional false positives, particularly through amplification of low concentration of target template. Thus, various modified PCR diagnostic methods for myxosprean have been developed and reported by several researchers worldwide. Different modified PCR based and other nucleic detection assays such as nested PCR, PCR-restriction fragment length polymorphism (PCR-RFLP) and *in situ* hybridization are powerful techniques to employ. Nonetheless, these methods still have limitations towards their sensitivity limit and requisition high marginal costs as well as investment in expensive equipments. More recently, alternative detection tools, for example a low density oligonucleotide array system based on LSU rRNA gene sequence (Wylezich *et al.*, 2010) and terminal-RFLP (T-RFLP) analysis based on the SSU rDNA (Felten *et al.*, 2011) have been developed to identify complex pathogen species. However, modern diagnostic methods require long operating time for identification.

Conventional LAMP technique, that is simple with high sensitivity is a powerful tool to facilitate genetic testing for the rapid diagnosis of infectious diseases (Gahlawat *et al.*, 2009), without using expensive equipment. On the other hand, conventional LAMP could not evaluate infection of the parasite quantitatively. Furthermore in case of un-amplification and low turbidity product level, the amplification products need to be confirmed with the electrophoresis. The amount of myxosporean can be quantified by real time PCR assays using Taqman and SYBR chemistry (True *et al.*, 2009; Grabner and El-Matbouli, 2009). However the cost of the experiments using qPCR is more expensive and requires qualified technicians. The disadvantages of using inexpensive methods to quantify *S. epinepneli* led us to develop the real time LAMP. Also the cost of the LoopAmp turbidimeter is low whereas the real time PCR assays require fluorogenic probes (Taqman qPCR) and an expensive fluorometer (Parida *et al.*, 2004; Mekata *et al.*, 2009).

Table 5.2 Real time LAMP and qPCR diagnosis of *S. epinepheli* infected orange spotted grouper seed collected from nature; a, microscopic positive samples and b, microscopic negative samples.

a: microscopic positive samples

Sample No.	Microscopic detection		Real time LAMP		qPCR	
	Spore in kidney	Blood stages	kidney	Blood	kidney	Blood
1	(+)	(+)	(+)	(+)	(+)	(+)
2	(-)	(+)	(+)	(+)	(+)	(+)
3	(+)	(-)	(+)	(+)	(+)	(+)
4	(-)	(+)	(+)	(+)	(+)	(+)
5	(-)	(+)	(+)	(+)	(+)	(+)

b: microscopic negative samples

Sample No.	Microscopic detection		Real time LAMP		qPCR	
	Spore in kidney	Blood stages	kidney	Blood	kidney	Blood
1	(-)	(-)	(-)	(-)	(-)	(-)
2	(-)	(-)	(-)	(-)	(-)	(-)
3	(-)	(-)	(+)	(+)	(+)	(+)
4	(-)	(-)	(-)	(-)	(-)	(-)
5	(-)	(-)	(-)	(-)	(-)	(-)
6	(-)	(-)	(-)	(-)	(-)	(-)
7	(-)	(-)	(+)	(+)	(+)	(+)
8	(-)	(-)	(-)	(-)	(-)	(-)
9	(-)	(-)	(-)	(-)	(-)	(-)
10	(-)	(-)	(-)	(+)	(-)	(+)
11	(-)	(-)	(-)	(-)	(-)	(-)
12	(-)	(-)	(-)	(-)	(-)	(-)
13	(-)	(-)	(+)	(+)	(+)	(+)
14	(-)	(-)	(-)	(+)	(-)	(+)
15	(-)	(-)	(-)	(-)	(-)	(-)
16	(-)	(-)	(-)	(-)	(-)	(-)
17	(-)	(-)	(+)	(+)	(+)	(+)
18	(-)	(-)	(-)	(-)	(-)	(-)
19	(-)	(-)	(-)	(+)	(-)	(+)
20	(-)	(-)	(-)	(-)	(-)	(-)

(-); Negative detection, (+); positive detection

S. epinepheli-specific standard curve was generated using 10-fold dilutions of 5 to 5×10^6 copies/μl of purified recombinant plasmid (pGEM-epinepheli) and the reactions were made in duplicate. The mean Tt for the plasmid standards was generated using the specific software provided with the loopamp real-time turbidimeter. Standard curve equations were calculated using regression analysis comparing the average Tt to the standard copy number. Cross reactivity analysis showed that the primers were specific to *S. epinepheli*, morevover, neither other myxosporean species tested nor both uninfected fish host DNA templates, *E. coioides* and *E. malabaricus* were amplified. Sensitivity analysis showed the detectable ability of real time LAMP at least 5 copies of the DNA template, as sensitive as those of the qPCR method developed parallel in this study. Too low the amount of template, 5 copies, might however cause some errors regarding Tc and Ct values in real time LAMP and qPCR, respectively. We recommend the lowest template concentration approximately to 50 copies that could be used to quantitative analysis of *S. epinepheli* infection in both diagnostic assays.

Both developed real time LAMP and qPCR were applied for detecting SSU rDNA of *S. epinepheli* in fish samples from naturally infection. According to our result, these two assays are suitable for diagnosing the sphaerosporesis in grouper. Normally, fish seeds collected from the nature are continually cultured in net cage until they reach the optimum size. Therefore, these applications would be useful for screening the *S. epinepheli* infected juvenile grouper in order to avoid distribution and transmission of the disease causing parasite across locations. Because of the higher sensitivity, simple and lower diagnostic cost of the real time LAMP assay, we anticipate that it will be more effective than qPCR in detection of asymptomatic grouper seed for cage culture.

In the present study, the tools for rapid detection of *S. epinepheli* including real time LAMP and qPCR were tested for the assay performance. These validated real time LAMP assay, especially loop primers added, proved highly robust to clear out performance same as an optimized qPCR assay in the proof of sensitivity concept assay. However, we believe that the genome specific real time LAMP assay will be routinely used as a comprehensive *S. epinepheli* and other myxosporean pathogens detection system in field diagnostic laboratories because of its speed, simplicity, specificity and low cost.

References

Aoi, Y., Hosogai, M. and Tsuneda, S. 2006. Real-time quantitative LAMP (loop-mediated isothermal amplification of DNA) as a simple method for monitoring ammonia-oxidizing bacteria. J. Biotechnol 125 : 484-491.

Bartošová, P., Freeman, M. A., Yokoyama, H., Caffara, M. and Fiala, I. 2010. Phylogenetic position of *Sphaerospora testicularis* and *Latyspora scomberomori* n. gen. n. sp. (Myxizoa) within the marine urinary clade. Parasitology 15 : 1–13.

Bekele, B., Hodgetts, J., Tomlinson, J., Boonham, N., Nikolić, P., Swarbrick, P. and Dickinson, M. 2011. Use of a real-time LAMP isothermal assay for detecting 16SrII and XII phytoplasmas in fruit and weeds of the Ethiopian Rift Valley. Plant Pathol. 60 : 345–355.

Christopher, M.A., Amod Kulkarni, C., Brinchmann, M.F., Korsnes, K. and Kiron, V. 2010. Detection of *Francisella piscicida* in Atlantic cod (*Gadus morhua* L) by the loop-mediated isothermal amplification (LAMP) reaction. Vet. J. 184 : 357–361.

El-Matbouli, M. and Soliman, H. 2005. Rapid diagnosis of *Tetracapsuloides bryosalmonae*, the causative agent of proliferative kidney disease (PKD) in salmonid fish by a novel DNA amplification method, loop-mediated isothermal amplification (LAMP). Parasitol. Res. 96 : 277–284.

FAO. 2007. Fisheries statistics database. Food and Agriculture Organization of the United Nation, Rome, Italy. Available: http://www.fao.org/fishery/ statistics/ programme/publications/all/en [accessed March, 2, 2009].

Felten, A. V., Meyer, J. B., Défago, G. and Maurhofer, M. 2011. Novel T-RFLP method to investigate six main groups of 2,4-diacetylphloroglucinol-producing pseudomonads in environmental samples. J. Microbiol. Methods 84 : 379–387.

Gahlawat, S.K., Ellis, A.E. and Collet, B. 2009. A sensitive loop-mediated isothermal amplification (LAMP) method for detection of *Renibacterium salmoninarum*, causative agent of bacterial kidney disease in salmonids. Fish Dis. 32 : 491–497.

Grabner, D. S. and El-Matbouli, M. 2009. Comparison of the susceptibility of brown trout (*Salmo trutta*) and four rainbow trout (*Oncorhynchus mykiss*) strains to the myxozoan *Tetracapsuloides bryosalmonae*, the causative agent of proliferative kidney disease (PKD). Vet. Parasitol. 165 : 200–206.

Hillis, D. M. and Dixon, M. T. 1991. Ribosomal DNA: molecular evolution and phylogenetic inference. Q Rev Biol 66 : 411–453.

Liao, I. C., and Leaño, E. M. 2008. The aquaculture of groupers. Taiwan : Asian Fisheries Society, Manila, Philippines, World Aquaculture Society, Louisiana, USA, The Fisheries Society of Taiwan, Keelung, Taiwan and National Taiwan Ocean University, Keelung, Taiwan.

Lom, J. and Dyková, I. 2006. Myxozoan genera: definition and notes on taxonomy, life-cycle terminology and pathogenic species. Folia Parasitol. 53 : 1–36.

Mekata, T., Sudhakaran, R., Kono, T., Supamattaya, K., Linh, N. T. H., Sakai, M. and Itami, T. 2009. Real-time quantitative loop-mediated isothermal amplification as a simple method for detecting white spot syndrome virus. Lett. Appl. Microbiol. 48 : 25–32.

Mori, Y., Nagamine, K., Tomita, N. And Notomi, T. 2001. Detection of loop-mediated isothermal amplification reaction by turbidity derived from

magnesium pyrophosphate formation. Biochem. Biophys. Res. Commun. 289 : 150–154.

Notomi, T., Okayama, H., Masubuchi, H., Yonekawa, T., Watanabe, K., Amino, N. and Hase, T. 2000. Loop-mediated isothermal amplification of DNA. Nucleic Acids Res. 28 : E63.

Parida M., Posadas, G., Inoue, S., Hasebe, F. and Morita, K. 2004. Real-time reverse transcription loop-mediated isothermal amplification for rapid detection of West Nile virus. J. Clin. Microbiol. 42 : 257–263.

Rozen, S. and Skaletsky, H.J. 2000. Primer3 on the WWW for general users and for biologist programmers. In: Krawetz, S. and Misener, S. (eds) Bioinformatics Methods and Protocols: Methods in Molecular Biology. New York : Humana Press.

Sudhakaran, R., Mekata, T., Kono, T., Supamattaya, K., Linh, N.T.H., Sakai, M. and Itami, T. 2008. Rapid detection and quantification of infectious hypodermal and hematopoietic necrosis virus in whiteleg shrimp *Penaeus vannamei* using real-time loop-mediated isothermal amplification. Fish Pathol. 43 : 170–173.

Supamattaya, K., Fischer-Scherl, T., Hoffmann, R. W. and Boonyaratpalin, S. 1991. *Sphaerospora epinepheli* n. sp. (Myxosporea: Sphaerosporidae) observed in grouper (*Epinephelus malabaricus*). J. Eukaryot. Microbiol. 38 : 448–454.

True, K., Purcell, M. K. and Foott, J. S. 2009. Development and validation of a quantitative PCR to detect *Parvicapsula minibicornis* and comparison to histologically ranked infection of juvenile Chinook salmon, *Oncorhynchus tshawytscha* (Walbaum), from the Klamath River, USA. J. Fish Dis. 32 : 183–192.

U-taynapun, K., Penprapai, N., Bangrak, P., Mekata, T., Itami, T. and Tantikitti, C. 2010. *Myxobolus supamattayai* n. sp. (Myxosporea: Myxobolidae) from Thailand parasitizing the scale pellicle of wild mullet (*Valamugil seheli*). Parasitol. Res. in press. 10.1007/s00436-010-2223-1.

Wylezich, C., Nies, G., Mylnikov, A. P., Tautz, D. and Arndt, H. 2010. An evaluation of the use of the LSU rRNA D1-D5 domain for DNA-based taxonomy of eukaryotic protists. Protist 161 : 342–352.

6. *Myxobolus supamattayai* n. sp. (MYXOSPOREA; MYXOBOLIDAE) FROM THAILAND PARASITIZING THE SCALE PELLICLE OF WILD MULLET (*Valamugil seheli*)

Abstract

A new myxosporean species, *Myxobolus supamattayai* n. sp. was isolated from wild mullet (*Valamugil seheli*) from the Andaman Sea, Thailand and described based on its morphology and molecular data. The myxosporean produced black plasmodia like unique clinical sign on the skin with sporogonic stages and mature spores. Polysporous plasmodia, up to 2.5 mm in diameter, were found in epithelium tissue in the scale pocket. The spores measured 6.6 (6.2–7.0) µm in length, 6.5 (6.2–6.7) µm in width, smooth, round board to ellipsoidal in valvular view. Spores were enclosed with intracapsular process which represents 5–7 and 11–12 in amount revealed in light microscopy and ultrastructure, respectively. The polar capsules were pyrifrom and of equal size, measuring 3.5 (3.4–3.6) µm in length and 2.0 (1.9–2.2) µm in width, with 4–5 turns of polar filament arranged perpendicularly to longitudinal axis of the polar capsule. In conclusion, this new species is entirely different from those of previously described, however this finding was assured by the partial sequence of SSU rRNA gene (1,666 bp) analysis that differed from all known species of *Myxobolus* Bütschli, 1882. The phylogenetic tree of the sequence data sets including those of freshwater and marine of *Myxobolus* spp. and the sister group (*Henneguya* spp.) was constructed to establish the relationship of this new species in *Myxobolus* clade and to explore it's relations between their sister groups. Phylogenetic analysis indicated that a monophyletic group with *Myxobolus* spp.

which infected mullet represents the newly formed species. These results suggested the presumably nearby evolution prospecting of *Myxobolus* species that were found in the same host.

Introduction

The genus *Myxobolus* of the phylum *Myxozoa* contains more than 792 species; some are the most important parasitic pathogens of economic fish such as *M. cerebralis*, causative of the whirling diseases in salmon. Most members of *Myxobolus* are histozoic parasite of fresh water fish, however, about 30 species live in marine or estuarine water. Some of them have coelozoic plasmodia of far less compact structure than histozoic trophozite (Lom and Dyková, 2006). Although there are numerous detailed descriptions of species of the genus *Myxobolus* from teleost of the nearly all geographical areas, information about this genus in Southeast Asia, mainly *Myxobolus* as a parasitizing in economic marine fish such as Asian sea bass, grouper and mullet, remains scare. Mullet species is one of the most important economic fish of Southeast Asia, particularly in southern Thailand. Culture of mullet has been increased in Thailand in recent years, which is performed in cage-polyculture systems along with Asian seabass, grouper and red snapper. In addition, wild caught mullet has been decreasing while the demand is very high. Coinciding with the growing economic value of this fish, its increasing parasite loads are likely to affect the aquaculture industry.

The taxonomic methodology for identification of myxosporea species have been principally based on spore morphology to primary classification of the species character until the acceptance of molecular data with reference to phylogenetic tree in taxonomic myxosporea (Liu *et al.*, 2010). These classical

morphological methods are very difficult to determine the validity identification of similar morphological myxosporea especially from identical tissue of the taxonomically closely related host species (Székely et al., 2009). Although, host and tissue specific are of great help in differentiating morphologically similar spores, there are some myxosporea, such as M. rotundus, classified from 27 cyprinid fish species and from different sites in the fish body (Eiras et al., 2005; Molnár et al., 2009; Zhang et al., 2010). However, the recent reports have described as a specific parasite of common bream using molecular data and the actinosporean stage develops in oligochaete, Tubifex tubifex (Molnár et al., 2009; Székely et al., 2009). The wide host range and multiple infection sites are still yet to be explored. Unfortunately, spores of many species of the genus Myxobolus vary similar to each other, many species descriptions in long discovery of this genus are not definite and many are inconsistent with their documentation (Dyková et al., 2002). The combination of morphology and molecular based classification, with the consideration of host range and tissue specificity provides a precise approach to distinguish valid species from identified taxa (Molnár et al., 2009). A list of parasites of the wild mullet species has been introduced including 15 species of the genus Myxobolus (Bahri and Marques, 1996; Bahri et al., 2003; Kent et al., 2001), which can be found in various organs of their host fish. Only M. episquamalis and M. exiguus were observed in the scales of mullet (Egusa et al., 1990; Pulsford and Matthews, 1982). However, most of the mullet parasite, Myxobolus spp., were described based on their morphology while 6 species have been studied for both morphology and phylogeny (Bahri et al., 2003). The recent classification model, designed for gaining more sufficient and reliable resolution, requires morphological information along with molecular analysis. The morphological data have been obtained from the fine structures of the genus

Myxobolus appearances followed from typical myxozoa pattern including shape of spore, polar capsule polar filament turns and ultra-structural studies. The SSU rRNA gene sequences, typically 18S rDNA, has indicated a proof of molecular classification (Fiala, 2006).

In the present study, *M. supamattayai* n. sp. a new species belonging to the genus *Myxobolus*, found in wild mullet (*Valamugil seheli*) from the Andaman Sea, Thailand, was described. Light microscopic, ultra-structure study and phylogenetic analysis using SSU-rDNA was performed to determine the evolutionary relationships of this particular species among genus *Myxobolus,* to assess the reliability of spore morphology based classification.

Materials and Methods

1. Fish samples and sampling

The samples were collected in 2007 and 2008, 143 specimens of *V. seheli* ranging in weight of 30–120 g from two different areas on the coast of the Andaman Sea in Satun province (station 1; 6° 50′ 33″ N, 99° 46′ 19″ E, station 2; 6° 47′ 03″ N, 99° 49′ 44″ E), Thailand. These fish samples were caught using floating seine and beach seine, which are fishing tool of an artisanal fishery. According to the previous work from our group, the black cyst scale is the hallmark of host infected with interesting *Myxobolus* species thus the mullets exhibiting this symptom were separated to the restrictive tank. The infected and uninfected fish with or without symptoms were transported alive in aerated seawater to the Aquatic Animal Health Research Center, Prince of Songkla University, Thailand immediately after collection. Moribund fish were killed using over dose of clove oil, packed in a plastic bag and kept in temperature controlled freezer boxes during the transportation. Standard

procedures of myxosporean examination; internal organs, body surface and body fluid were used to diagnose myxosporean infection in the collected fishes.

2. Morphology analysis

Morphological measurement of species description was obtained among 50 spores according to Lom and Arthur (1989) and Lom and Dyková (2006). Fresh spores and Giemsa stained spores were analyzed to identify their morphology and photographed. Species descriptions were based on several *Myxobolus* populations from more than one host specimens. Spores were observed under Olympus AX 70 microscope and photographed using Olympus DP 71 cool CCD camera with differential interference contrast (DIC) optics.

For ultra-structure studies by electron microscopy, fresh plasmodia were dissected from infected fish skin and fixed in 3% (v/v) glutareldehyde in cacodylate buffer (pH 7.4) at 4°C for 6 h. Samples were postfixed in 1% (w/v) osmium tetraxide using the same buffer. Transmission electron microscopy samples were dehydrated through graded acetone series before embedding in Epon-812, ultra-thin sectioned, and stained with uranyl acetate and lead citrate. They were examined under a JEOL transmission electron microscopy (JEM-123) at 80 kV. The images were digitally recorded for further analysis.

3. Genomic DNA extraction

The DNA extraction method was modified from Salim and Desser (2000). Briefly, spores were centrifuged and pelleted at 8,000g for 10 min, washed twice with PBS and resuspended in 200 μl of 2% (v/v) proteinase K in STE buffer (pH 8.0) containing 1% (w/v) SDS. Spores were incubated overnight at 30°C. The

spore suspension was boiled for 10 min and then plunged into liquid nitrogen, the same process was repeated for 3 times. The suspension was examined using light microscopy to verify whether most spores released their sporoplasms. The DNA was subsequently extracted with phenol/chloroform/IAA (25:24:1, v/v/v) method, incubated overnight and precipitated with 70% ethanol. The DNA pellet was obtained after centrifugation at 12,000g for 15 min at 4°C, followed by washing with 70% ethanol, air-dried and resuspended with 20–30 µl of double distilled water. The DNA samples were kept at -20°C until use.

4. PCR amplification and purification of the 18S rDNA

The 18S rDNA of the *Myxobolus* parasite was amplified with MX 5 (5′ CTGCGGACGGCTCAGTAAATCAGT 3′) and MX 3 (5′ CCAGGACATCTTAG GGCATCACAGA 3′), which binds to the conserved regions in the 5′ and 3′ end, respectively (Andree *et al.*, 1998). The PCR was performed in a 50 µl reaction containing 2 µl of template DNA (100–150 ng of genomic DNA), 100 pmol of each of forward and reverse primer, 250 mM dNTP, 5 µl of 10X PCR buffer and 1 µl of 5 units/µl Taq DNA polymerase (Invitrogen). Amplifications were conducted with a MJ Research DNA Engine 100 (MJ Research) using the following cycling protocol; an initial denaturation step of 95°C for 5 min; 40 cycles of 95°C/1 min-60°C/1 min-72°C/1 min and a final extension of 10 min at 72°C. The PCR products were electrophoresed on 1.5% agarose gel (Vivantis) in TAE buffer for approximately 30 min at 100 V. The expected band of the 18S rDNA fragments of *Myxobolus* were directly cut from the gel and further purified with QIAquick Gel Extraction kit (Qiagen). The purified DNA was immediately used as inserted DNA in cloning system.

5. DNA Cloning of PCR Products and Sequencing

The 18S rDNA gene of *Myxobolus* species was cloned into pGEM®-T Easy Vector using the pGEM®-T Easy Vector Systems cloning kit (Promega) and transformed into *Escherichia coli* TOP10 cells, according to the manufacturer's instructions. The plasmids were purified from positive clones, selected upon the blue/white color screening method, using the QIAprep Spin Miniprep Kit (Qiagen). Inserted parasitic genes in the plasmid was confirmed before sequencing by PCR using either the same primers as those used in the original amplification (MX 5 and MX 3) or the primers that flanked the insertion site (T7 and SP6). The purified plasmids containing insert were sequenced on automatic sequencer CEQ™ 8000 (Beckman Coulter) using CEQ DTCS Dye Kit (Beckman Coulter) according to the manufacture's protocol. In addition, the internal part of 18S rDNA was sequenced using the internal forward (5′ CCAGTAGCGTATCTCAAAGTTGC 3′) and reverse (5′ CCCGTGTTGAGTCAAATTAAGC 3′) primers which were designed based on conserved sequences within the SSU-rDNA gene of this species.

6. Phylogenetic analysis

The 18S rDNA sequence of *M. supamattayai* n. sp. was compared to those of other species available in the GenBank using nucleotide BLAST protocol (Altschal *et al.*, 1990). Taxa included in the alignments were based on similarities from BLAST results including congeners of the novel species and representatives from each of the major clades reported in previous studies (Fiala, 2006). Out-group species was selected from several other platysporinid genera, *Ceratomyxa shata*. In addition 38 selected taxa of platysporinid rDNA sequence from the genus *Myxobolus*

and related species, mostly *Henneguya* spp., used in the analysis were restricted to the same length of the sequence of those isolated from hosts living in all habitats; fresh water, brackish and marine. CLUSTAL X algorithm (Thompson *et al.*, 1994) was used for initial sequence alignment with default setting for gap opening/extension penalties and regions of ambiguous sequence alignments were manually edited using the BioEdit sequence alignment editor (Hall, 1999). We used neighbor-joining (NJ), Maximum parsimony (MP) and Maximum likelihood (ML) methods to infer phylogenetic relationships among the *Myxobolus* spp. and its sister group. There were a total of 2,220 positions in the final dataset. Phylogenetic analyses of the NJ method and MP method were conducted using the MEGA V. 4.0 program (Kumar *et al.*, 1993). For the NJ method, evolutionary distances were analyzed using the Kimura two-parameter (K2P) evolution sequence model (Kimura, 1983). The evolutionary history was concluded using the NJ method. Statistical consensus trees inferred from 1,000 replications bootstrapping were taken to present the evolutionary history of the taxa analyzed. The MP tree was obtained using the Close-Neighhbor-Interchange (CNI) algorithm (Nei and Kumar, 2000) with search level 3 in which the initial trees were obtained with the random addition of sequence (100 replications). Parsimonious trees were shown with the percentage of replicate trees in which the associated taxa clustered together in the bootstrap test (1,000 replicates). All alignment gaps/missing data were set as the complete deletion in both analysis methods. We used MEGA 4 for these analyses including the primary tree based drawing of NJ tree.

The SeaView V 4 program (Gouy *et al.*, 2010) was executed using the GTR model for ML analysis. The selecting models were evaluated by using jModelTest (Pasada, 2008). The BioNJ (Gascuel, 1997) algorithm was selected for starting trees. Nearest-Neighbor interchange (NNI) and Subtree Pruning and

Regrafting (SPR) were used for tree searching operation. The data sets were built with 500 bootstrap replications for the ML reconstruction.

Results

1. Morphology and clinical signs

Several cyst-like plasmodia, with diameter up to 2.5 mm, containing numerous sporogonic stages and mature spores were observed in the epithelium tissue above the scale. Twenty five of 143 specimens (17.48%) were infected with parasites classified, based on the spore morphology, as a myxosporean belonging to the genus *Myxobolus* Bütschli, 1882 (Lom and Dyková, 2006). All characteristics of the genus *Myxobolus* were observed in the spores' stage of these parasites found in macroscopical lesions localized in the epithelium scales pocket. Black cystic formations as parasite plasmodia were detected in only target organ while no other tissues or organs contained visible parasites revealed by light microscopy. The majority of the parasitized fish showed more than 100 cyst-like structures in different locations, mostly in pectoral to anal fin of the under lateral line body area (Fig. 6.1a).
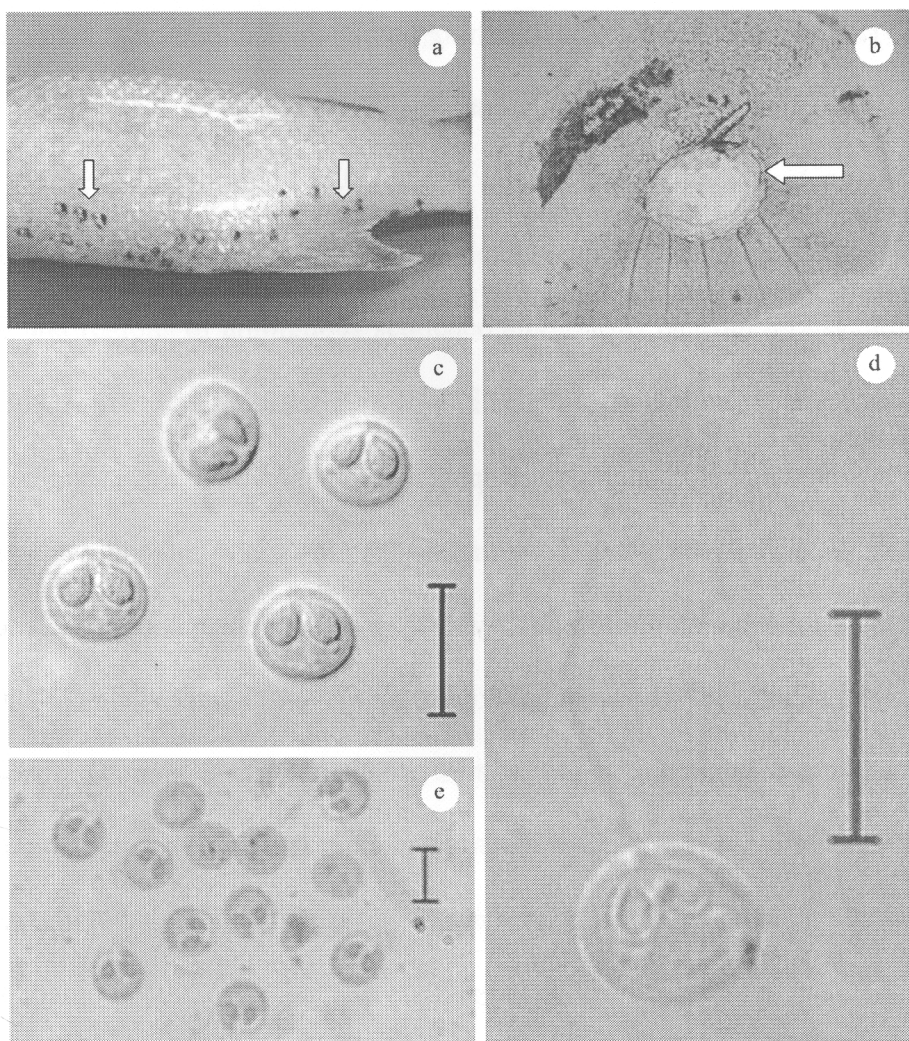
Fig. 6.1 *Myxobolus supamattayai* n. sp. in mullet (*Valamugil seheli*) from the coast of the Andaman Sea. **a** Cysts of *M. supamattayai* n. sp. on the infecting mullet scales (arrows). **b** Pathology of *M. supamattayai* n. sp. on the scales (arrow). **c** Fresh mature spore (DIC photography). **d** Spore in Giemsa staining. **e** Fresh spore with ejected polar filament. All scale bars are in μm.

Myxobolus supamattayai n. sp.

Vegetative stages: More developed plasmodia contained late sporogonic stages and mostly mature spores. Black, polysporous, like spot to ellipsoidal shape histozotic cyst-like plasmodia measuring up to 2.5 mm in diameter were found in epithelium tissue above the scales. The scales were destroyed as a plasmodium hole pocket (Fig. 6.1b). The scale missing and little ulcerated patches on

114

the skin were occasionally found particularly in severe infected fish. Numerous plasmodia could be found in each infected fish; however, only one plasmodium per scale could be observed. In addition, this was not found in other organs.

Morphology of spores (based on 50 mature spores): Spores with typical character of the genus *Myxobolus* were observed. The mature spores were round board to ellipsoidal in frontal view. Most of them are round with several edges marking (normally 5–7) whereas a few is variable in shape. Spore size was 6.6 (6.2–7.0) μm in length, 6.5 (6.2–6.7) μm in wide. The spherical two polar capsules were equal in size and close together in the plane of sutural line at the apical end which measured 3.5 (3.4–3.6) μm in length and 2.0 (1.9–2.2) μm in width. Polar filaments formed four to five coils opening at the spores anterior nearby the sutural line. The coil arrangement was almost perpendicular to the sutural line. Polar filaments extruding from mature spores of fresh material evaluated 10.5 (10–11) μm in length (Fig. 6.1e). Small intercapsular appendix was located between the polar capsules at the anterior end of the spore and discernible vacuole-like body in the sporoplasm of the spore. Spore morphology observations under the light microscopy using Giemsa staining were shown in Fig. 6.1c and 6.1d.

Type host: bluespot mullet (*Valamugil seheli*)

Type locality: The coast of the Andaman Sea, Satun province, Thailand (6° 47′ 03.68″ N, 99° 49′ 44.60″ E)

Site of infection: Epithelial tissue located in the centre of the scale

Prevalence: up to 17.48% (25/143)

Type material: Slides with stained spore (syntype) and fomalin preserved of infected host fish (*V. seheli*) have been deposited in the collection of the

Princess Maha Chakri Sirindhorn Natural History Museum, Prince of Songkla University, Songkhla, Thailand. (Accession Number: PSUZC-20090216.01)

Etymology: The species name (*M. supamattayai*) is in homage to Assoc. Prof. Dr. Kidchakan Supamattaya, one of the pioneers in the study of aquatic animal disease in Thailand and the first director of this project (Myxosporidia disease and biodiversity of parasite in economic marine fish of Thailand), who passed away in 2008.

Electron microscopy (EM)

Fine structure of mature spores presented the complete developing cells comprising two shell valves, mono-nucleated sporoplasm and two polar capsules (Fig. 6.2a and 6.2b). The spore body formed by two smooth shell valves, each one with two caudal projection for releasing the polar filament. The internal of sutural line, the overlapping of two spore valves, contained 11–12 intracapsular process. The two equal polar capsules were pyriform, elongated and little converged at the apex of the spore. The polar capsules with a polar filament, basal straight central shaft and coils of 4–5 turns were visible. Polar capsules composed of thin electron-dense external wall along with thick and lighter inner. The apical channel for the polar filament discharge showed close contact with caudal projection in valves. The sporoplasmic cell was located in the posterior pole of the spore and the cytoplasm contained three distinct organelles; mono nuclei close to each other, low density electron dense body, like a cell vacuole and sporoplasmosomes. These spherical shaped vesicles were membrane bounded, contained an electron dense and homogenous matrix. The nucleus was found in sporoplasm cell whereas other cells in mature spore could not show the basis of complete cell structure. A semi-schematic illustration of the spore, based on TEM observations, was shown in Fig. 6.3.
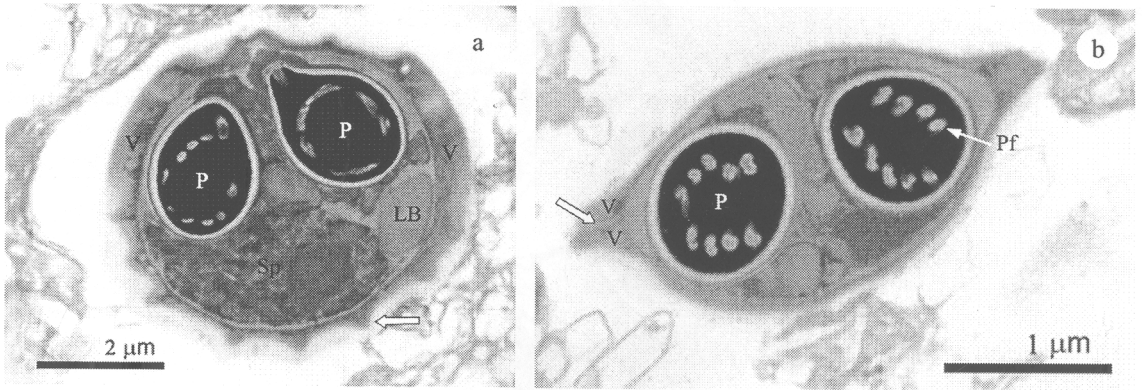
Fig. 6.2 Transmission electron micrographs of the mature spore of *M. supamattayai* n. sp. **a** The detail of spore longitudinal ultra-thin section showing the valves (V) with internal capsular process (arrow), the two polar capsules (P) and sporoplasm (Sp) with one nucleus and low density electron dense body (LB), like a vacuole. **b** The detail of spore sectioned transversally showing the valves (V) and sutural line (arrow), two polar capsules (P) with 4-5 polar filament turns.
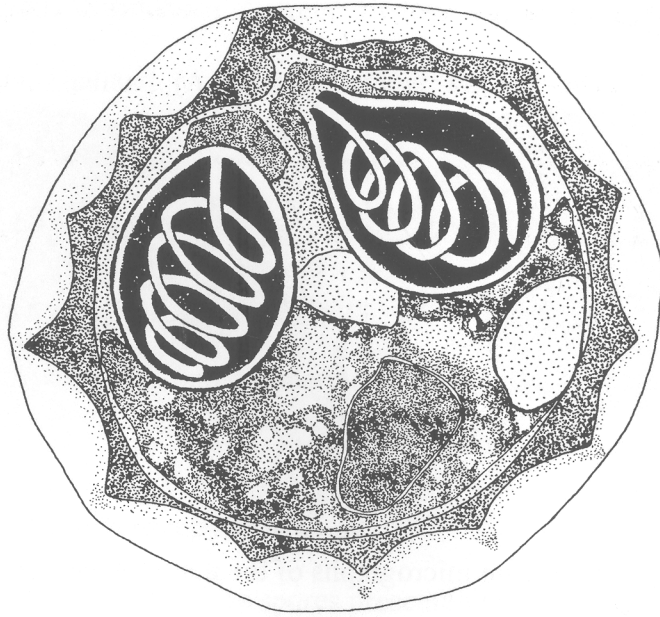
Fig. 6.3 Semi-schematic illustration of a longitudinal view of a mature spore of the *M. supamattayai* n. sp., a parasite of blue spot mullet, *Valamugil seheli* showing species-specific characters including spore size and shape, two equal polar capsules with 4-5 polar filament turns, uni-nucleated sporoplasm, vacuole with sporoplasmosome and 11-12 intercapsular process in sutural line.

2. Molecular characterization and phylogenetic tree

Overall SSU rDNA sequences were determined for 12 samples (6 samples form each sampling site). All the sequence samples showed 99.9% homology to the rDNA nucleotide sequences. The amplified and sequenced 18S rDNA gene of *M. supamattayai* n. sp. was 1,617 nucleotides in length excluding the region corresponding to MX 5-MX 3 primers while the G+C content was 43.0%. The sequence was deposited at the National Center for Biotechnology GenBank (Accession Number: HQ166720). The 18S rDNA gene of this *Myxobolus* species isolated from mullets revealed the sequence identity with other parasite species in the

same host are, 88% with *M. muelleri*, 90% with *M. episqamalis*, 91% with *M. bizerti*, 88% with *M. exiguous*, 87% with *M. ichkeulensis* and 88% with *M. spinacurvatura*. The nucleotide sequences of *M. supamattayai* n. sp. was obviously differed, more than 25% of 1,666 base pair, from those of all other *Myxobolus* species available in the GenBank.

Phylogenetic analysis was conducted with neighbor-joining (NJ) algorithm resulting in a single most parasimonnious tree (Fig. 6.4), while the member species in each clade of the maximum parsimony (MP) tree and maximum likelihood (ML) tree remained the same. Some branches were swapped within clades, but this did not significantly change the apparent evolution relationship. The clades of *Myxobolus* species were divided into three main clades that were strongly supported by bootstrap values. However the demise of *Myxobolus* clades distinctly interfere from the clade of *Henneguya* species. The all phylogenetic topology analysis tree demonstrated that the mullet parasitic *Myxobolus* species containing seven species (*M. supamattayai* n. sp., *M. muelleri, M. episqamalis, M. bizerti, M. exiguous, M. ichkeulensis and M. spinacurvatura*) correspond to a monophyletic group (clade A.). This is separated into a distinct clade, strongly supported by high bootstrap values. The representation of marine *Myxobolus* clade, infected mullet fish host, partitioned within the clade formed by the *Henneguya* species which was separated from other *Myxobolus* clades (B. and C.) composed of 18 species which are involved in freshwater fish parasites.
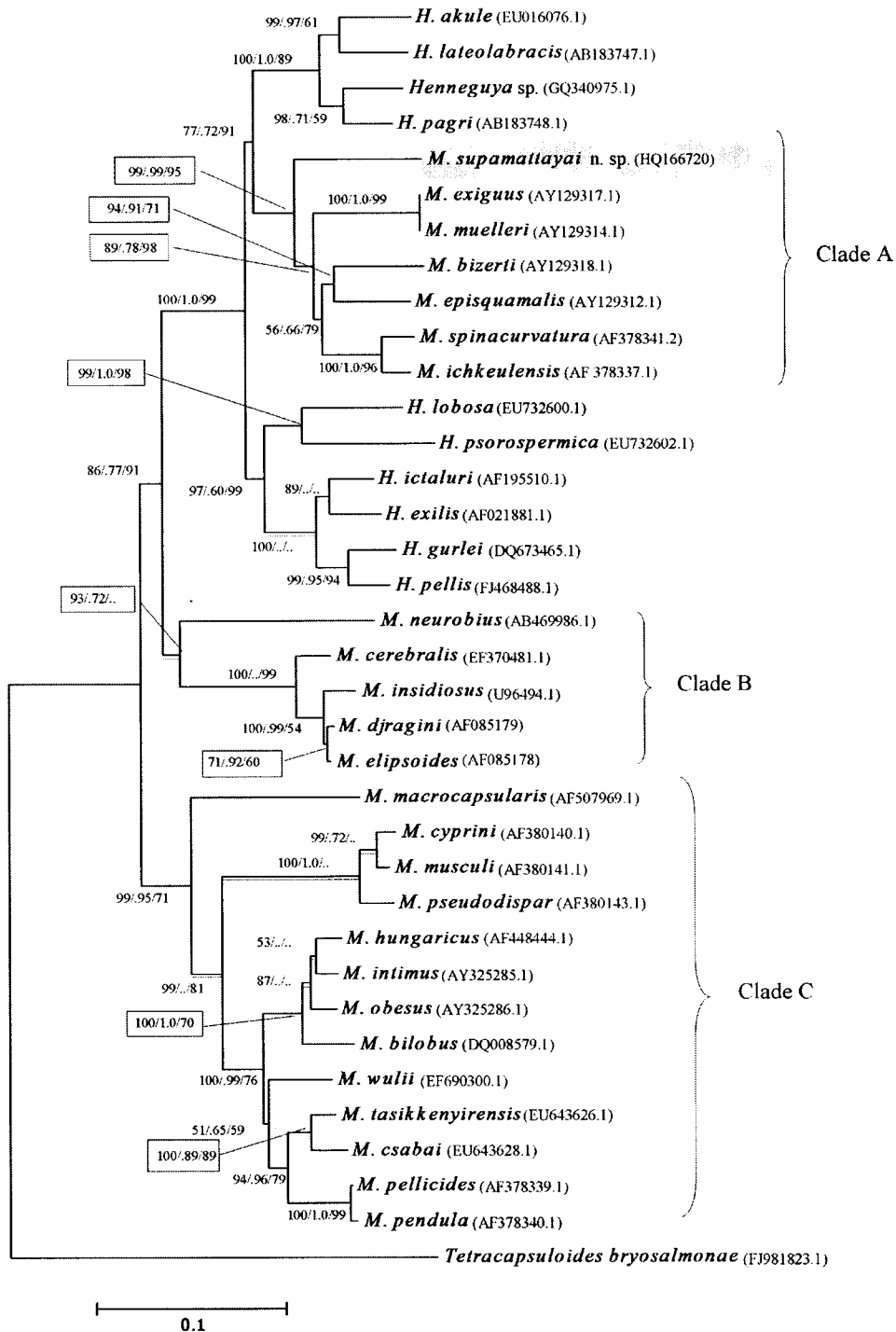
119

Fig. 6.4 Phylogenetic tree of the 18S rDNA sequence of myxosporeans. The tree generated by neighbor-joining (NJ), maximum likelihood (ML) and maximum parsimony (MP) analyses of the 18S rDNA sequence, root at *C. shasta*. Numbers at nodes indicate bootstrap confidence levels presented as percentage for NJ, ML and MP, respectively. GenBank Accession

Numbers of each species are given in parenthesis. The distance scale is shown beside the tree. Myxosporean identified in the present study is given in gray background. The dashed lines indicate the differences between the three trees, taking NJ as basic topology.

Discussion

1. Morphological and ultra-structure taxonomic classification:

The light morphology of the spores described in the present work corresponds to those of the genus *Myxobolus*, myxozoa parasite. Myxozoa species are very common parasites of fish. Many researchers demonstrated that more than one species of myxosporea parasite infect the same host fish. Although few studies on the host specificity are reported, recent data indicated that most species are strictly host specific or only capable of developing in closely related fish host (Tajdari *et al.*, 2005). According to previously described species, 15 species belonging to the *Myxobolus* genus have demonstrated to infect mullet (Bahri and Marques, 1996). *Myxobolus* species infecting mullet have been reported on various geological regions including west coast of Tunisian, Mediterranean coast, in the Atlantic at Ria de Aveiro in the northern Portugal, South Florida coast, Australia and Japanese coast (Diamanka *et al.*, 2008; Maeno *et al.*, 1990; Rothwell *et al.*, 1997; Umur *et al.*, 2010). All characteristics of this new species were also compared to confirm morphological similarities to the spores of different species of the genus *Myxobolus* described previously (see Table 6.1). Two species, *M. episqamalis* and *M. exiguous*, occurring on the host scales, which are the parasite infected in epithelial tissue over scale of species, are similar to that of *M. supamattayai* n. sp. However, *M. episqamalis* differ from our founded new species because of the less elongated shape of the spore and

polar capsule, smaller in overall dimensions and the type and color of the plasmodia. Conversely, *M. exiguous* has a bigger spore size and longer length of polar filament than those of *M. supamattayai* n. sp. Although, spore shape of *M. parvus* (Bahri and Marques, 1996) showed higher similarity to the spore of *M. supamattayai* n. sp., the first one has a bigger polar capsule. *M. bizerti* and *M. ichkeulensis* have the larger spore and polar capsule, more polar filament coils in the polar capsule and longer polar filament length indeed than those observed from *M. supamattayai* n. sp. The shape of spore and polar capsule of *M. spinacurvatura* is larger than that found in *M. supamattayai* n. sp. even if it also occurs in the epithelial tissue over scale (Lom and Dyková, 1994). The ellipsoidal spores of *M. branchialis* are longer space and in overall dimensions besides the polar capsule are bigger. *M. cheni* occurs on muscles and fins, in addition, the shape of spores are larger and more ellipsoid. *M. achmarovi*, *M. cephalis* and *M. rohdei* occur on mesentery, gill filament and kidney, respectively, and these all species have larger spore and polar capsule than those of *M. supamattayai* n. sp. The morphological data of spores of *M. mugcephalus*, parasitizing in gill arches was insufficient for comparison, however, it can be discriminated from *M. supamattayai* n. sp. by its smaller and more round board spore shape. *M. muelleri*, a high variable morphology detailed parasite can be separated from *M. supamattayai* n. sp. by a number of considerable features. Spores seem much more oval than those of *M. supamattayai* n. sp., and bigger polar capsule and 6–8 coil turns to the polar filament in *M. muelleri* distinguish it from our species that contains only 4–5 colis.

Moreover, the ultra-structural morphology of the spores described in the present study also confirms that this parasite belongs to the genus *Myxobolus* Bütschli, 1882 according to previous studies and the key for determination of

myxosporean genera (Lom and Dyková, 2006). The ultra-structure data of mature spore of *Myxobolus* species infected mullet remains scarce. However, fine structure of *M. exiguus* and *M. epiaquamalis* infecting in scales of grey mullet and flathead mullet has been described (Pulsford and Matthews, 1982; Bahri and Marques, 1996). *M. supamattayai* n. sp. is fundamentally similar to both *Myxobolus* species mentioned above which infect in mullet and is similar throughout other myxosporean though there is a minor difference observed in the size and structure. The presented mature spores, polar capsule were plugged with a stopper, which was covered by a cap-like structure at its apical end. These characters were similar to those recorded for the genus *Myxobolus* (Ali *et al.*, 2007) and also from other myxosporean genera such as *Sphaerospora* (Supamattaya *et al.*, 1991) and *Zschokkella* (Lom and Dyková, 1996). The sporoplasm cell of genus *Myxobolus* is commonly characterized by a single binucleated sporoplasm (Pulsford and Matthews, 1982; Bahri and Marques, 1996). In contrast, this presented species showed only one nucleus in the mature spore of sporoplasm cell. However, uninucleated sporoplasm has been reported in some *Myxobolus* species such as *M. stomun* (Ali *et al.*, 2003). Dense spherical inclusions, sporoplasmosomes were identified in the sporoplasm of the present species, which seem to be the common features of *Myxobolus* species and other myxosporean (Abdel-Ghaffar *et al.*, 2008).

Table 6.1 Comparison of spore characteristics between *Myxobolus* species infecting

mullet. The mean and standard deviation or range of spore is provided

Species	Host	Localization	Spore		Polar capsule		Polar filament	
			Length (μm)	Width (μm)	Length (μm)	Width (μm)	Length (μm)	Number of coils
M. bizerti Bahri and Marques 1996	*M. cephalus*	Gill filaments	14.25±0.22	14.25±0.22	6.5±0.54	5.75±0.27	45-50	6-7
M. episqamalis Egusa et al., 1895	*M. cephalus*	Scales	7.5-9.5 8.5±0.51	6-7.5 6.5±0.51	3.8-5 4±0.42	2-3 2±0.15	25-44	5-6
M. exiguus Bahri et al., 2003	*L. ramada*	Intestine	9.5±0.51	7.5±0.51	3.5±0.13	2.25±0.26	22-30	ND
M. ichkeulensis Bahri and Marques 1996	*M. cephalus*	Gill arches	13.5±0.54	12.5±0.54	5.5±0.54	4.25±0.27	45-63	7-8
M. muelleri Bahri et al., 2003	*L. ramada*	Mesenteric vessels	10.5±0.51	8.5±0.51	4.5±0.31	2.5±0.21	22-40	6-7
M. spinacurvatura Maeno et al. 1990	*M. cephalus*	Mesentery Brain Gill filaments	10.5-12.5 12±0.63	9-11 10±0.57	3.5-5 4.75±0.67	2.5-3.5 2.75±0.59	22-43	4-5
M. parvus Shulman, 1962	*M. cephalus*	Gill lamellae	6.6-7	5.5-6	4-4.2	3.8-4.2	ND	ND
M. cheni Shulman, 1962	*M. cephalus*	Muscles Fins	8-8.5	6-6.5	4.5-5	2	ND	ND
M. mugcephalus Landsberg and Lom, 1991	*M. cephalus*	Gill filaments	4.8	5.2	ND	ND	ND	ND
M. rohdei Lom and Dykova, 1994	*M. cephalus*	Kidney	9.8-11.6	8.4-9.1	3.7-5	2.5-3.1	ND	ND
M. platanus Eiras et al., 2007	*M. platanus*	spleen	10.7 (10-11)	10.8 (10-11)	7.7 (7-8)	3.8 (3.5-4)	ND	5-6
M. goensis Eiras and D'Souza, 2004	*M. cephalus*	Gill raker	9.7 (9.5-10.5)	6.6 (6-7.5)	5.3 (4.5-6) 2.4 (2-3)	2.4 (2-3) 1.8 (1.5-2)	ND	5 3
M. branchialis Bahri and Marques, 1996	*M. cephalus*	Gill filaments	7.6-8	6.8-8.5	4.4-4.8	2.5-4.1	ND	ND
M. achmerovi Bahri and Marques, 1996	*M. cephalus*	Mesentery	12-14	9-10	ND	2.3-3.5	ND	ND
M. cephalis Bahri and Marques, 1996	*M. cephalus*	Gill arches	14-15	10-11	4-5	3-4	ND	ND
M. supamattayai n. sp. Persent work	*V. seheli*	Scales	6.2-7.0 6.6±0.32	6.2-6.7 6.5±0.21	3.4-3.6 3.5±0.13	1.9-2.2 2.0±0.09	12-15	4-5

2. Phylogenetic tree analysis by SSU rDNA approach

Species of the genus *Myxobolus* has been found in several clades over a broad analysis of the Myxozoa (Kent *et al.*, 2001). Modern phylogenetic analysis classifications of myxosporean have been described into two major clades that are fresh water and marine species (Fiala, 2006). SSU rDNA is widely used for studying phylogenetic relationships among taxa (Avise, 2004). Moreover, it is the only molecular marker available for the broad range of *Myxobolus* species at present. Therefore, SSU rDNA sequences have been used as the main information source for reconstruction of *Myxobolus* evolutionary history. Obtained discrepancies between SSU rDNA gene phylogeny and taxonomy, based on the morphological data, may suggest that the molecular phylogeny is not congruent with the true phylogeny or may indicate that the characters of spore morphology are homoplasious. Consequently, molecular data of other genes, for instance, large subunit ribosomal DNA (LSU rDNA) or intergenic transcribed spacer (ITS), are required to confirm the myxosporean rDNA phylogeny (Fiala, 2006). However, phylogenetic analyses of SSU rDNA suggest that pore morphology is of minor importance in phylogenetic relationships of myxosporean clades (Andree *et al.*, 1999; Canning and Okamura, 2003; Eszterbauer, 2004; Holzer *et al.*, 2004). Since the occurrence of different spore morphology in the same clade even when similar another species in other clade due to convergence, it seems that *Myxobolus* evolution may not depend on the change of spore shape. Moreover, separation of the minor clade of marine *Myxobolus* spp., infecting mullet, from other *Myxobolus* species in *Myxobolus* clade was established in the present study.

Our comparative molecular genetic analysis included sequences from 36 species of expanded myxosporean to the extent of SSU rDNA sequence availability. The intention of these analysis was to verify the differentiation of *M. supamattayai* n. sp., first from infected blue spot mullet *Myxobolus* species followed by the possibly in its closest relatives. Phylogenetic analyses formed one large clade that includes one of out group species, *Ceratomyxa shasta*. This large clade was further divided into more sub-clades, one of which represented all of the infecting mullet *Myxobolus* species, as marine myxozoa, including *M. episquamalis*, *M. muelleri*, *M. spinacurvatura*, *M. ichkeulensis*, *M. bizerti*, *M. exiguus* and *M. supamattayai* n. sp.

In summary, *M. supamattayai* n. sp. does not correlate to any other *Myxobolus* spp. previously reported to infect mullet or another species among the genus *Myxobolus*. It tends to be differentiated from all known species of *Myxobolus* spp. by the presence of morphology, ultra-structure and phylogenetic analysis.

References

Abdel-Ghaffar, F., El-Toukhy, A., Al-Quraishy, S., Al-Rasheid, K., Abdel-Baki, A. S., Hegazy, A. and Bashter, A. R. 2008. Five new myxosporean species (Myxozoa: Myxosporea) infecting the Nile tilapia *Oreochromis niloticus* in Bahr Shebin, Nile Tributary, Nile Delta, Egypt. Parasitol. Res. 103 : 1197–1205.

Ali, M. A., Abdel-Baki, A. S., Sakran, T., Entzeroth, R. and Abdel-Ghaffar, F. 2003. Light and electron microscopic studies of *Myxobolus stomum* n. sp. (Myxosporea: Myxobolidae) infecting the blackspotted grunt *Plectorhynicus gaterinus* (Forsskal, 1775) in the Red Sea, Egypt. Parasitol. Res. 91 : 390–397.

Ali, M. A., Abdel-Baki, A. S., Sakran, Th., Entzeroth, R. and Abdel-Ghaffar, F. 2007. *Myxobolus lubati* n. sp. (Myxosporea: Myxobolidae), a new parasite of haffara seabream *Rhabdosargus haffara* (Forsskal, 1775), Red Sea, Egypt: a light and transmission electron microscopy. Parasitol. Res. 100 : 819–827.

Altschul, S. F., Gish, W., Miller, W., Myers, E. W. and Lipman, D. J. 1990. Basic local alignment search tool. J. Mol. Biol. 215 : 403–410.

Andree, K. B., MacConnell E. and Hedrick, R. P. 1998. A nested polymerase chain reaction for the detection of genomic DNA of *Myxobolus cerebralis* in rainbow trout *Oncorhynchus mykiss*. Dis. Aquat. Org. 34 : 145–154.

Andree, K. B., Székely, C., Molnár, K., Gresoviac, S. J. and Hedrick, R. P. 1999. Relationships among members of the genus *Myxobolus* (Myxozoa: Bilvalvulidae) based on small subunit ribosomal DNA sequences. J. Parasitol. 85 : 68–74.

Avise, J. C. 2004. Molecular Marker, Natural History, and Evolution. Massachusetts : Sinauer Associates Inc. Publishers,

Bahri, S. and Marques, A. 1996. Myxosporean parasites of the genus *Myxobolus* from *Mugil cephalus* in Ichkeul lagoon, Tunisia: description of two new species. Dis. Aquat. Org. 27 : 115–122.

Bahri, S., Andree, K. B. and Hedrick, R. P. 2003. Morphological and phylogenetic studies of marine *Myxobolus* spp. from mullet in Ichkeul Lake, Tunisia. J. Eukaryot. Microbiol. 50 : 463–470.

Canning, E. U. and Okamura, B. 2003. Biodiversity and evolution of the Myxozoa. Adv. Parasitol. 56 : 43–131.

Diamanka, A., Fall, M., Diebakate, C., Faye, N. and Toguebaye, B. S. 2008. Identification of *Myxobolus episquamalis* (Myxozoa, Myxobolidae) in flathead mullet *Mugill cephalus* (Pisces, Teleostei, Mugilidae) from the coast of Senegal (eastern tropical Atlantic Ocean). Acta Adriat 49 : 19–23.

Dyková, I., Fiala, I. and Nie, P. 2002. *Myxobolus lentisuturalis* sp. n. (Myxozoa: Myxobolidae), a new muscle-infecting species of the Prussian carp, *Carassius gibelio* from China. Folia Parasitol. 49 : 253–258.

Egusa, S., Maeno, Y. and Sorimach, M. 1990. A new species of Myxozoa, *Myxobolus episquamalis* sp. n. infecting the scales of the mullet, *Mugil cephalus* L. Fish Pathol. 25 : 87–91.

Eiras, J. C., D'Souza, J. 2004. *Myxobolus goensis* n. sp. (Myxozoa, Myxosporea, Myxobolidae), a parasite of the gills of *Mugil cephalus* (Osteichthyes, Mugilidae) from Goa, India. Parasite 11 : 243–248.

Eiras, J. C., Molnár, K. and Lu, Y. S. 2005. Synopsis of the species of *Myxobolus* Butschli, 1882 (Myxozoa: Myxosporea: Myxobolidae). Syst. Parasitol. 61 : 1–46.

Eiras, J. C., Abreu, P. C., Robaldo, R. and Júnior, J. 2007. *Myxobolus platanus* n. sp. (Myxosporea, Myxobolidae), a parasites of *Mugil platanus* Günther, 1880 (Osteichthyes, Mugilidae) form Lagoa dos Patos, RS, Brazil. Arq Bras Med Vet Zootec 59 : 895–898.

Eszterbauer, E. 2004. Genetic relationship among gill-infecting *Myxobolus* species (Myxosporea) of cyprinids: molecular evidence of importance of tissue-specificity. Dis. Aquat. Organ. 58 : 35–40.

Fiala, I. 2006. The phylogeny of Myxosporea (Myxozoa) based on small subunit ribosomal RNA gene analysis. Int. J. Parasitol. 36 : 1521–1534.

Gascuel, O. 1997. BIONJ: An improved version of the NJ algorithm based on a simple model of sequence data. Mol. Biol. Evol. 14 : 685–695.

Gouy, M., Guindon, S., Gascuel, O. 2010. SeaView Version 4: A multiplatform graphical user interface for sequence alignment and phylogenetic tree building. Mol. Biol. Evol. 27 : 221–224.

Hall, T. A. 1999. BioEdit: a user-friendly biological sequence alignment editor and analysis program for Windows 95/98/NT. Nucleic Acids Symp. Ser. 41 : 95–98.

Holzer, A. S., Sommerville, C. and Wooten, R. 2004. Molecular relationships and phylogeny in a community of myxosporeans and actinosporeans based on their 18S rDNA sequences. Int. J. Parasitol. 34 : 1099–1111.

Kent, M. L., Andree, K. B., Bartholomew, J. B., El-Matbouli, M., Desser, S.S., Devlin, R. H., Feist, S. W., Hedrick, R. P., Hoffmann, R. W., Khattra, J., Hallett, S. L., Lester, J. G., Longshaw, M., Palenzuela, O., Siddall, M. E. and Xiao, C. 2001. Recent advances in our knowledge of the Myxozoa. J. Eukaryot. Microbiol. 48 : 395–413.

Kimura, M. 1983. The Neutral Theory of Molecular Evolution. Cambridge, UK : Cambridge University. Press.

Kumar, S., Tamura, K. and Nei, M. 1993. MEGA: Molecular Evolutionary Genetics Analysis, version 1.01. The Pennsylvania State University, Pennsylvania : University Park.

Liu, Y., Gu, Z. M. and Luo, Y.L. 2010. Some additional data to the occurrence, morphology and validity of *Myxobolus turpisrotundus* Zhang, 2009 (Myxozoa: Myxosporea). Parasitol. Res. 107 : 67–73.

Lom, J. and Arthur, J. R. 1989. A guideline for preparation of species description in Myxosporea. J. Fish Dis. 12 : 151–156.

Lom, J. and Dyková, I. 1994. Studies on protozoan parasites of Australian fishes III. Species of the genus *Myxobolus* Bütschli, 1882. Eur. J. Protistol. 30 : 431–439.

Lom, J. and Dyková, I. 1996. Notes on the ultrastructure of two myxosporean (Myxozoa) species, *Zschokkella pleomorpha* and *Ortholinea fluviatitis*. Folia Paraitol. 43 : 189–202.

Lom, J. and Dyková, I. 2006. Myxozoan genera: definition and notes on taxonomy, life-cycle terminology and pathogenic species. Folia Parasitol. 53 : 1–36.

Maeno, Y., Sorimach, M., Ogawa, K. and Egusa, S. 1990. *Myxobolus spinacurvatura* sp. n. (Myxosporea: Bivalvulida) parasitic in deformed mullet, *Mugil cephalus*. Fish Pathol. 25 : 37–41.

Molnár, K., Székely, C., Hallett, S. L. and Atkinson, S. D. 2009. Some remarks on the occurrence, host-specificity and validity of *Myxobolus rotundus* Nemeczek, 1911 (Myxozoa: Myxosporea). Syst. Parasitol. 72 : 71–79.

Nei, M. and Kumar, S. 2000. Molecular Evolution and Phylogenetics. New York : Oxford University Press.

Posada, D. 2008. jModelTest: Phylogenetic model averaging. Mol. Biol. Evol. 25 : 1253–1256.

Pulsford, A. and Matthews, R. A. 1982. An ultrastructure study of *Myxobolus exiguus* Thelohan, 1895 (Myxosporea) from grey mullet, *Crenimguil labrosus* (Risso). J. Fish Dis. 5 : 509–526.

Rothwell, J. T., Virgona, J. L., Callinan, R. B., Nicholls, P. J. and Langdon, J. S. 1997. Occurrence of cutaneous infections of *Myxobolus episquamalis* (Myxozoa: Myxobolidae) in sea mullet, *Mugill cephalus* L, in Australia. Aust. Vet. J. 75 : 349–352.

Salim, K. Y. and Desser, S. S. 2000. Descriptions and phylogenetic systematics of *Myxobolus* spp. from cyprinids in Algonquin Park, Ontario. J. Eukaryot. Microbiol. 47 : 309–318.

Supamattaya, K., Fischer-Scherl, T., Hoffmann, R. W. and Boonyaratpalin, S. 1991. *Sphpaerospora epinepheli* n. sp. (Myxosporea: Sphaerosporidae) observed in grouper (*Epinephelus malabaricus*). J. Eukaryot. Microbiol. 38 : 448–454.

Székely, C., Hallett, S. L., Atkinson, S. D. and Molnár, K. 2009. Complete life cycle of *Myxobolus rotundus* (Myxosporea: Myxobolidae), a gill myxozoan of common bream *Abramis brama*. Dis. Aquat. Organ. 85 : 147–155.

Tajdari, J., Matos, E., Mendonça, I. and Azevedo, C. 2005. Ultrastrutural morphology of *Myxobolus testicularis* sp. n., parasite of the testis of *Hemiodopsis microlepis* (Teleostei: Hemiodontidae) from the NE of Brazil. Acta Protozool. 44 : 377–384.

Thompson, J. D., Higgins, D. G. and Gibson, T. J. 1994. CLUSTAL W: Improving the sensitivity of progressive multiple sequence alignment through sequence weighting, position-specific gap penalties and weight matrix choice. Nucleic Acids Res. 22 : 4673–4680.

Umur, Ş., Pekmezci, G. Z., Beyhan, Y. E., Gürler, A. T. and Açici, M. 2010. First record of *Myxobolus muelleri* (Myxosporea: Myxobolidae) in flathead grey mullet *Mugil cephalus* (Teleostei, Mugilidae) from Turkey. Ankara Üniv Vet Fak Derg 57 : 205–207.

Zhang, J. Y., Wang, J. G., Li, A. H. and Gong, X. N. 2010. Infection of *Myxobolus turpisrotundus* sp. n. in allogynogenetic gibel carp, *Carassius auratus gibelio* (Bloch), with revision of *Myxobolus rotundus* (s.l.) Nemeczek reported *from C. auratus auratus* (L.). J. Fish Dis. 33 : 625–638.

7. SEASONAL OCCURRENCE AND ULTRA-STRUCTURE OF DEVELOPMENTAL STAGE OF *Myxobolus supamattayai* (MYXOZOA), A PARASITE OF WILD MULLET (*Valamugil seheli*) FROM THAILAND

Abstract

The myxosporean, *Myxobolus supamattayai* infected the epithelium tissue in the scale pocket of bluespot mullet, *Valamugil seheli* has been first described in 2010. More information on their geographic distribution, ultra-structure of spore development and molecular identification were investigated. The parasite occurred in restricted areas, Andaman Sea, but not in other bluespot mullet in Gulf of Thailand and Songkhla Lake. The prevalence infection of parasite in large wild mullet size (>15 cm) showed non variation between rainy and dry seasons of 2007–2009. We found parasite infection between 12.5–16.66%. Among small mullet (<15 cm), the prevalence in both sampling sites presented high infection in rainy season, up to 26.09% and dropped to 2.94–12.5% in dry season. In addition, morphometric taxonomy and geographic related *Myxobolus* sp. in Southeast Asia are complicated. Therefore semi-nested PCR diagnosis was developed for simplificative identification. The assay specificity was tested with four myxosporean species within same distributed areas and non infected fish host sample. The detection limit was evaluated with SSU rDNA of *M. supamattayai* recombinant plasmid and show detected concentration up to 10^3 copy/reaction. For the complete biological data, the first ultra-structure description of developmental stage of *M. supamattayai* was presented. The parasite possess spherical to ellipsoidal polysporus plasmodium. The primary stage of

spore has an oval-shape body. The valves are first observable organ in developmental process, they have two long opposite lateral possessions. The spore has two sub-spherical polar capsules with a polar filament. A mononucleate sporoplasm that contains several sporoplasmosomes presented in the posterior end of the spore and between the two polar capsules.

Introduction

Myxobolus, the largest genus of Myxozoa with over 792 species, is a common histozoic parasite of freshwater fish. However more than 30 described species were isolated from marine fish. Some are important pathogens of economic fish. The importance of this parasite has interestingly increased in recent years with the overabundant of intensive aquaculture. Moreover, the myxosporean is the scientifically interesting organism. Their geographic distribution, genetic evolution, life cycle, taxonomy and parasitism role including developmental process have been extensively reported. The ultra-structural investigation of cyst-like plasmodium and developmental stage of the parasite to elucidate some aspects of the parasitic biology and host-parasite interaction is yet available for the vast majority of myxosporean species (Redondo *et al.*, 2003; Abdel-Ghaffar *et al.*, 2008). There is a lot of information on the ultra-structure of different freshwater myxosporean species. However, detailed descriptions of the developmental stage of marine myxosporean involving in the host-parasite relationship are scarce.

Myxobolus spp. infections in mullet are long history with described 16 species in variable geographical areas including the west coast of Tunisia, Mediterranean coast, Atlantic Ocean in Portugal and Florida coast, Australia, Japan and Andaman Sea, Thailand (Maeno *et al.*, 1990; Rothwell *et al.*, 1997; Bahri *et al.*,

2003; Diamanka *et al.*, 2008; Umur *et al.*, 2010; U-taynapun *et al.*, 2010). These parasites could be found in various organs of their host. In Thailand, mullet is a high economical value fish and mostly from artisanal fishery. However, wild mullet population have been decreasing due to overfishing, environmental pollution and diseases. Coinciding with the growing demand for this fish, the myxosporean parasite loads in wild and extensive culture are also increasing.

Myxobolus supamattayai, latest discovery of myxosporean species from wild mullet *Valamugil seheli* in the Andaman Sea, Thailand was originally described by U-taynapun *et al.* (2010) from the epithelial tissue over the scale. Available detailed data on this species are limited. The morphology, ultra-structure of mature spore and phylogeny were presented in our previous study. However, the geographic occurrence of this parasite, ultra-structural developmental stage, pathology and scanning electron micrograph of the spore are required to gain more insight in understandings the parasitic biology and epidemiology. The present study therefore aimed to study the geographic occurrence and completed fine structure of developmental stage including damaged scale evidences to support the validity of *M. supamatayai*.

Materials and Methods

1. Fish samples

The total of 1,063 mullets collected from 5 sampling locations in the southern Thailand, 438 mullets from Andaman Sea, 463 from Gulf of Thailand and 162 from Songkhla Lake, were caught between October, 2007 and May, 2009. The designed locations consisted of two sampling sites in Gulf of Thailand coast; Songkhla province (1), Nakhon Si Thammarat province (2), one station of Songkhla

Lake (3) and 2 sampling sites in Andaman Sea coast; Satun province (4) and Phang-Nga Bay (5). The sampling sites and recorded myxosporean locations are shown in Fig. 7.1. The mullets with black cyst scale were selected because this phenomenon is the hallmark of host infected with interesting *Myxobolus* species. Immediately after collection, the fish were transported alive to the Aquatic Animal Health Research Center, Prince of Songkla University. Dead fish were packed in plastic bag and sent to the laboratory in freezable controlled temperature box.
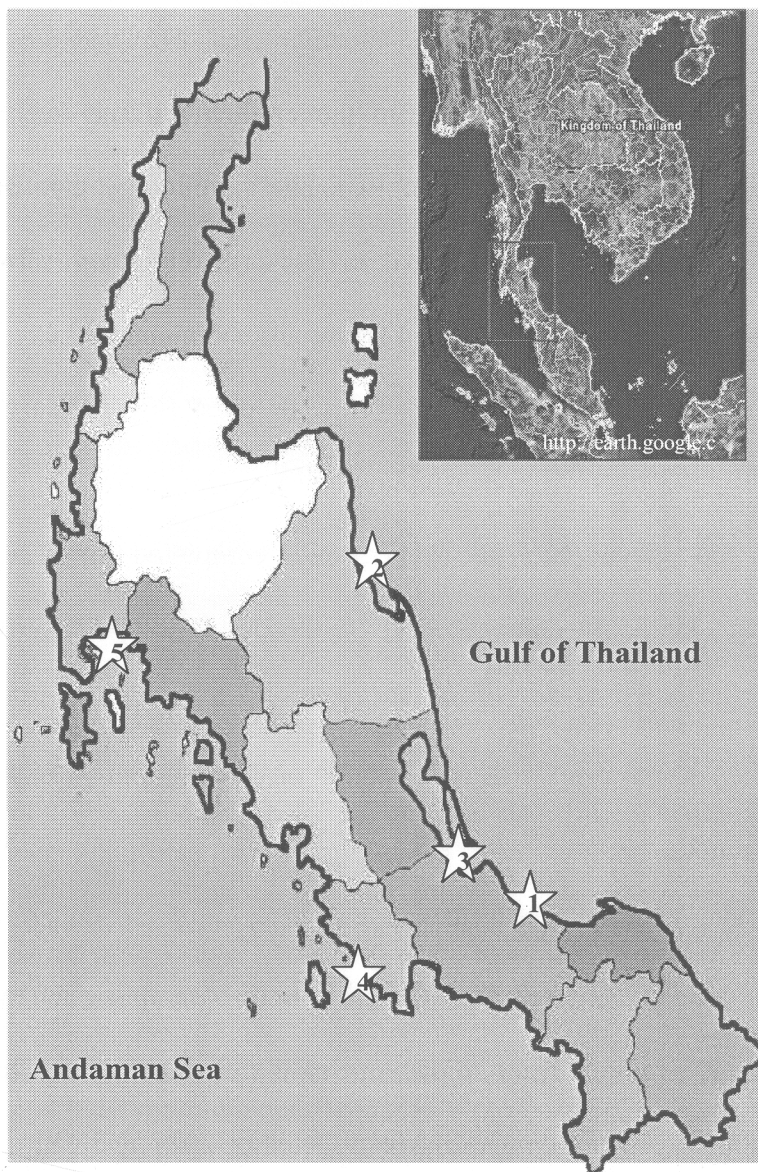

Fig. 7.1 The sampling sites in this study. The sites where myxosporean were recorded are signified by stars.

2. Molecular diagnosis

The parasite samples from all infected fish were confirmed with molecular analysis. Genomic DNA of *M. supamattayai* was extracted from fresh plasmodia. Spores were digested with 2% (v/v) proteinase K (U-taynapun *et al.*, 2010) and incubated at 35°C overnight. The DNA was extracted using DNeasy tissue kit (Qiagen, CA) according to the manufacturer's instructions. The DNA samples were kept at -20°C until use.

The primer set of PCR was designed based on the sequence of SSU rDNA of *M. supamattayai* (GenBank accession number HQ166720). The semi-nested PCR reaction was performed in 15 µl reaction mixture containing 2 µl of genomic DNA (approximately 100-150 ng), 0.1 µM first forward; MX5 5′ CTGCGGACG GCTCAGTAAATCAGT 3′ (Andree *et al.*, 1998), 0.5 µM of each specific primer (MsuF; 5′ TGTGGCGTTATTATCAAAAGCTAA 3′, MsuR; 5′ AAGGAAACGGC ATTGCTAGA 3′) in 1x PCR mixture (Gotaq® Green master Mix, Promega). Thermocycling was performed in the Mycycler™ (Biorad) for 35 cycles consisting of 95°C for 40 sec, 60°C for 45 sec, 72°C for 1 min preceded by an initial denaturation at 95°C for 3 min and followed by final extension at 72°C for 5 min. The specificity of this primer set was confirmed with genomic DNA of 4 species of other myxosporean which available in related habitat from Thailand. The tested species included *Henneguya* sp. from Asian seabass (*Lates calcarifer*), *Sphaerospora epinepheli*, *Zschokkella* sp. from striped sea catfish (*Plotosus lineatus*). PCR products were visualized using 1.5% (w/v) ethidium bromide-stained agarose gel electrophoresis.

To evaluate the sensitivity of semi-nested PCR diagnosis, a plasmid containing 18s rDNA fragment of *M. supamattayai* was constructed. The target 18S rDNA fragment was amplified using PCR with the universal myxosporean primers

(MX5; 5′ CTGCGGACGGCTCAGTAAATCAGT 3′ and MX3; 5′ CCAGGACATC TTAGGGCATCACAGA 3′) (Andree *et al.*, 1998) and then cloned into pGEM-T Easy vector (Promega, USA) according to the manufacturer's protocol. The concentration of obtained recombinant plasmid (pGEM-M) was evaluated using a Nanodrop UV spectrophotometer ND-1000 (NanoDrop Technologies Inc., USA). Ten-fold serial dilutions of myxosporean plasmid (pGEM-M) from 10^7 to 10^1 copy/μl were used as standards for the analysis.

3. Morphological methods

Cyst-like plasmodia were dissected from the skin of infected mullets. Spore classification was performed from fresh spores according to Lom and Dyková (2006) and U-taynapun *et al.* (2010). The vitality of spore was classified by adding spores into a 0.4% (w/v) urea solution and they were regarded as mature when at least 90% extruded polar filaments into the solution (Molnár *et al.*, 2009). Spore morphological characters were observed under an Olympus AX 70 microscope and photographed using Olympus DP71 cool CCD camera with differential interference contrast (DIC) optics.

Electron microscopy, fresh plasmodia were dissected from infected fish skin. Samples were fixed with 3% (v/v) glutareldehyde in cacodylate buffer (pH 7.4) at 4°C, after 12 h; they were then postfixed with 1% (v/v) osmium tetraxide in the same buffer. For, transmission electron microscopy (TEM), samples were dehydrated through acetone series before embedding in Epon-812. Ultra-thin section was stained with 1% (w/v) toluidine blue. They were examined in the JEOL transmission electron microscopy (JEM-123) at 80 kV accelerating. For scanning electron microscopy (SEM), isolated spores and infected scales were fixed and postfixed followed the

above mentioned fixative procedure. Samples were dehydrated through graded ethanol series and dried under critical point dryer (CPD: Hitachi). The dry sample was coated with 15 nm gold partical in a polaron sputter coater. They were viewed under JEOL scanning electron microscopy (JSM-5200) at 15 kV accelerating. The images were digitally recorded and transferred to a computer for further analysis.

Results

1. Geographical and seasonal occurrence

The geographical and seasonal survey of *M. supamattayai* from both coastal lines of Thailand; Gulf of Thailand, Songkhla Lake and Andaman Sea, during 2007–2009 were demonstrated. A total of 61 from 1,063 mullets were verified for parasitic infection. The parasite was only found in Andaman Sea, which was 12.8% (32 of 250) mullets from Satun province and 14.6% (29 of 198 mullet) from Phang-Nga province. There was no evidence of *M. supmattayai* infection observed in both sampling sites of Gulf of Thailand (two locations) and Songkhla Lake. The percentage of infection in relation to the geographical site of Andaman Sea, Gulf of Thailand and Songkhla Lake was shown in Table 7.1. For seasonal study, fish samples were collected annually for two year in order to relate the incidence of infection with seasonal changes. The incidence of infection in small fish (<15 cm length) was related to the seasonal changes. The dry season, parasite occurrence in small mullet was 2.94–7.89% and 4.76–9.52% recorded in Satun and Pang-Nga province, respectively, while the occurrence was significantly higher in rainy season with 13.51–19.23% (Satun province) and 22.22–26.09% (Phang-Nga province). Conversely, there was no observed relationship between the incidence of infection in

large mullet (>15 cm length) and seasonal changes on Andaman Sea, infection between 12.5–16.66 % (Fig. 7.2).

Table 7.1 Incidence of *M. supamattayai* infection in mullet (*V. seheli*) at different sampling time[a]

Location/Time	Period of time[b]			
	Rainy 2007 Oct.-Dec.	Dry 2008 Mar.-May	Rainy 2008 Oct.-Dec.	Dry 2009 Mar.-May
Gulf of Thailand				
Nakhon Si Thammarat	0/57	0/65	0/55	0/51
Songkhla	0/53	0/58	0/61	0/63
Songkhla Lake	0/42	0/40	0/36	0/44
Andaman Sea				
Satun	10/58 (17.24%)	8/69 (11.59%)	9/63 (14.29%)	5/60 (8.33%)
Phang-Nga Bay	9/46 (19.57%)	5/50 (10.0%)	10/57 (17.54%)	5/45 (11.11%)

[a] Examined from squash preparation of fresh tissues

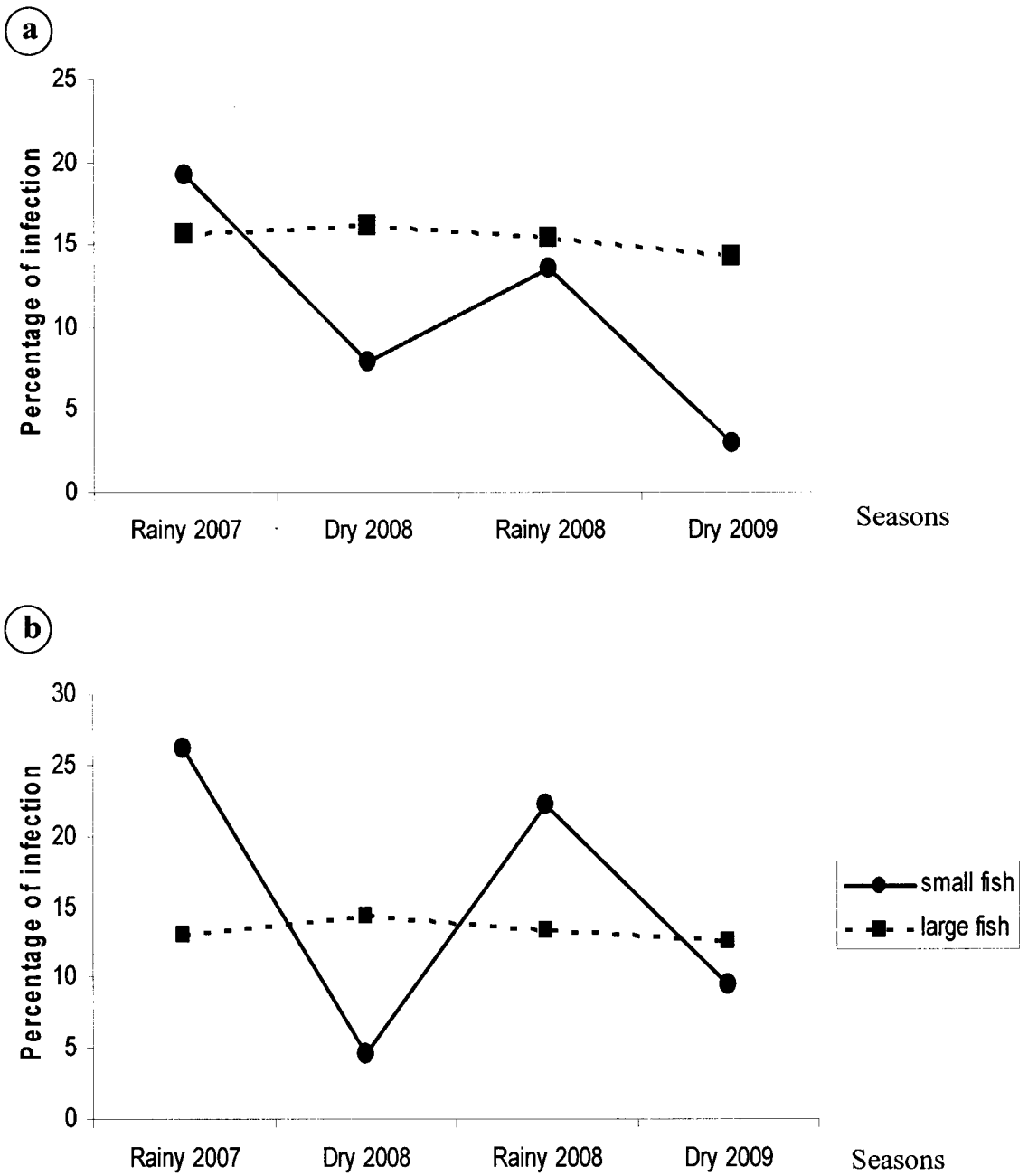[b] Number of infected fish per number of total fish

Fig 7.2 Seasonal occurrence of *M. supamattayai* in small (<15 cm.) and large fish (>15 cm) from Phang-Nga Bay (**a**) and Sutun province (**b**) were presented.

2. Molecular detection and identification

A simple and reliable assay based on one step semi-nested PCR was developed for the detection and identification of *M. supamattayai* in the bluespot mullet myxosporeosis. The detection system consistsed of three primers for amplifications, that are two forward primers; MX5 (myxosporean universal primer) and MsuF (specific forward primer), and one specific reverse primer (MsuR). The result of diagnosis was shown up to two PCR product sizes depending on the concentration of parasitic DNA template. PCR products amplified using MX5/MsuR and MsuF/MsaR, sized 1,200 and 900 bp, respectively (Fig. 7.3a). Negative semi-nested PCR results were presented when using genomic DNA of non-pathogenic bluespot mullet (Fig. 7.3b, lane 6), as well as those of the control without template DNA (Fig. 7.3b, lane7). The sensitivity and specificity test of the detection method was also demonstrated and the result was shown in Fig. 7.3a and 7.3b. It was obvious that the semi-nested PCR could detect a very little amount as little as 10^3 copies of parasite DNA (pGEM-M) in the reaction. The DNA of *Henneguya* sp. from Asian seabass (*L. calcarifer*), *Sphaerospora epinepheli* and *Zschokkella* sp. from striped marine catfish (*P. lineatus*) revealed no cross-amplifications (Fig. 7.3b) indicating the high specificity of the method.
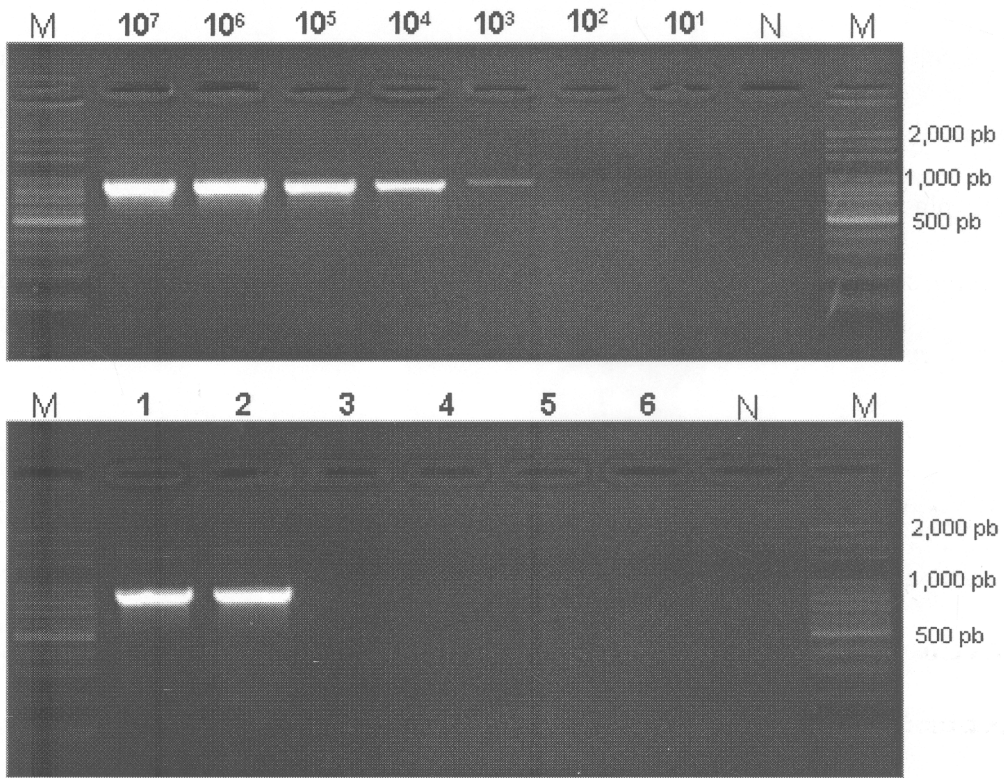
Fig. 7.3 Sensitivity and specificity of semi nested PCR assay for *M. supamattayai*

a. sensitivity of reaction assay. **b**. specificity test of *M. supamattayai* detection assay; lanes 1 and 2 are M. supamattayai obtained from Phang-Nga bay and Sutun province, lanes 3–5 are other myxosporean species which occur in related area, lenes 3: *Henneguya* sp. from Asian sea bass (*L. calcarifer*), lanes 4: *Sphaerospora epinepheli* from orange spotted grouper and *Zschokkella* sp. from striped sea catfish (*P. lineatus*). lanes 6 is genomic DNA of non-pathogenic bluespot mullet and lanes 7, negative control.

3. Ultra-structural data

Transmission electron micrograph of *M. supamattayai* presented the detail of various proliferative and sporogonic stages within the black-plasmodium connected to epithelial host tissue. The plasmodium was enveloped by a thin layer epithelial host membrane with one pinocytotic channel (Fig. 7.4a). The plasmodium

wall was composed of two distinct layers, ectoplasm and endoplasm. A collagen layer, which separates those layers, was presented as well as some fibroblasts in ectoplasm (Fig. 7.4b). Pinocytotic channel extended from the inner host membrane into the plasmodium and was encircled by large ectoplasmic cell. Asynchronous developing stage, the generative cells, early stages of sporogony and mature spore were observed in the whole of endoplasm zone (Fig. 7.5c).

Sporogenesis

Generative cells, representing the recognizable stages, were found in the endoplasm. The early stages of generative cells were spherical or ovoid in shape and contained multi-cellular sporoblast (Fig. 7.4d). The development stages of sporogenesis were initiated by the enclosure of the generative cell by an enveloping cell. This was followed by a series of division of the former, which gave rise to cells participating in the spore formation. After two enveloping cell were proceeded generating to valvogenic cell, three sporonts were developed to sporoplasmic and two valvogenic cell in the intrinsic region of the sporoblast (Fig. 7.4e–i). The progeny cells resulting from early sporogenesis achieved differentiation into capsulogenic, valvogenic and sporoplasmic cells. Each spore-producing unit consisted of two capsulogenic cells and sporoplasm surrounded by two valvogenic cells. Maturation of spore processing performed a structure progress towards capsulogenic development.
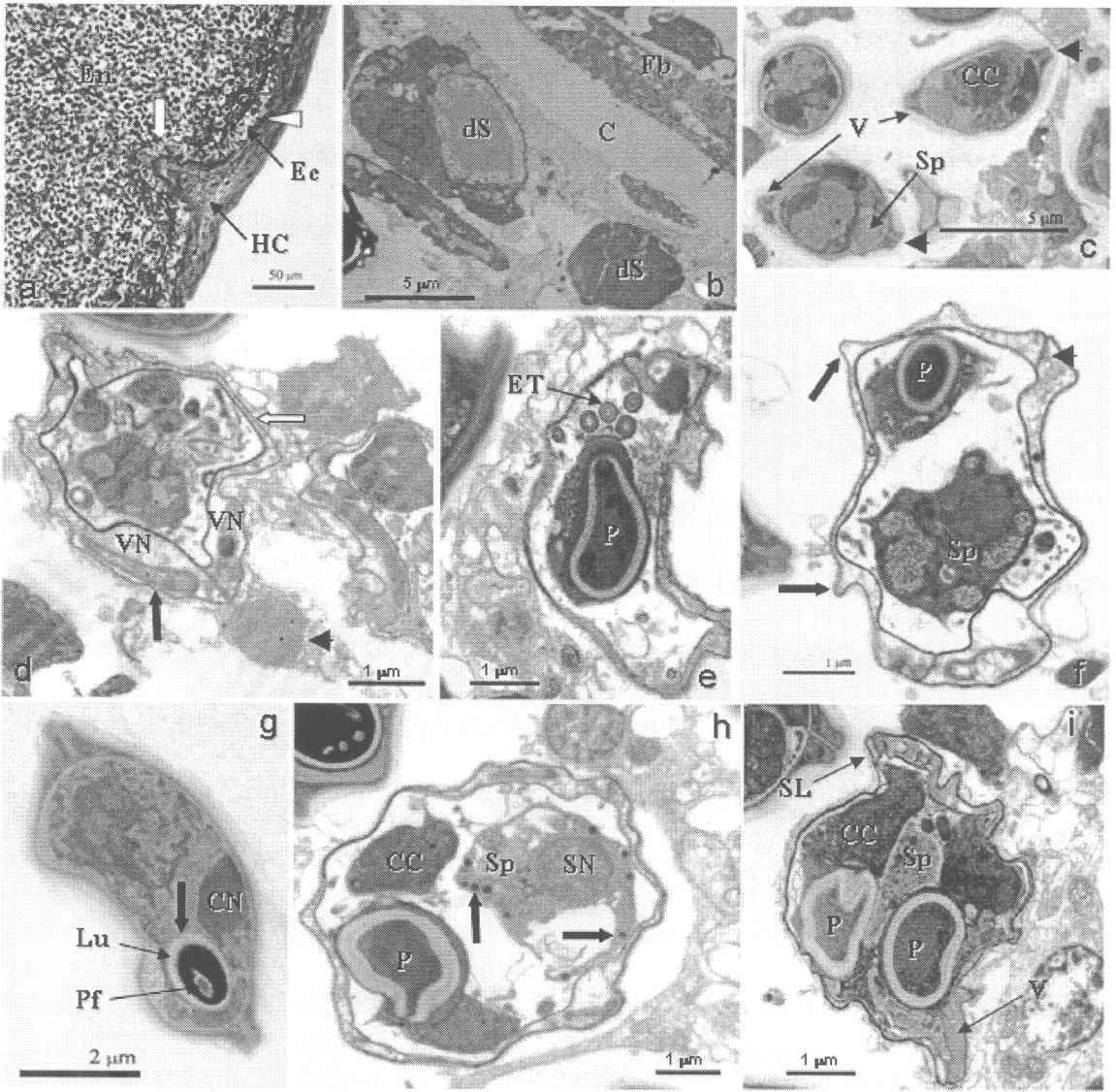
Fig. 7.4 (a-i) Transmission electron micrographs of the developmental stages of myxosporean, *M. supamattayai* **a**. Semi-thin section of a plasmodium, showing large pinocytotic channel (white arrow) with plasmodium membrane (white arrow head) that contacted with host cell (HC). Plasmodium wall demarcated into out ectoplasm (Ec) and inner endoplasm (En) containing generative cells. **b**. Ultrathin section of the plasmodium periphery enlargement (box in a), showing the collagen fibers wall (C) and fibroblast cell (Fb). Developmental spore (dS) were observed internally. **c**. Longitudinal section through early development stage of spores, which

showed capsulogenic cell (CC), sporoplasm (Sp), two valvogenic cell (V) and connected together at the sutural line (arrow head). **d.** Ultrastructural details of a plasmodium showing the differential stages of spore development around endoplasm areas. Immature spore section (white arrow) showed two valvogenic cells (VC) (black arrow), with flattened nucleus (VN) and developmental cell inside the spore, while an adjoining cell was in an early stage of pansporoblast (arrow head). **e.** Immature spore showed the external tube (ET) and maturing polar capsule (P). **f.** Detail of the valvogenic cell development, showing sutural line (arrow head) and external plasmalemma (arrow) in external layer of the cell, while the internal one was smooth and dense. **g.** Longitudinal section of immature spore showing developmental stage of capsulogenic cell consist of immature polar capsule and capsulogenic nucleus (CN). The polar capsule was composed of an electron dense outer layer (black arrow), a central translucent (Lu) and inner dense core with polar filament (Pf). **h.** Detail of sporoplasm (Sp), which contained one sporoplasmic nucleus (SN) and sporoplasmosomes (black arrow). **i.** Ultrastructural details of five cell in spore-producing unit contain two capsulogenic cell (CC) with polar capsule (P), sporoplasm (Sp) and two valvogenic cell (VC), which connected together at the sutural line (SL).

Capsulogenesis

Capsulogenic cells were clearly distinguished from other differentiated cells as they contained large numbers of distended cistenae of endoplasmic reticulum and capsular primordium inside of electron dense capsule. An early stage of capsulogenesis is the capsular primordium, which is observed as ovoidal structure in cytoplasm of the capsulogenic cells. The differentiation of capsulogenic cells, capsular primordium was prolonged by the external tube. Large aggregates of external tubes were found close to the capsular primordium or immature polar capsule (Fig. 7.4e). Continually, the polar filament developed and invaginated toward the polar capsules, the external tube disappeared. Finally, the capsular primordium increased the size and the polar filament was presented in the coil shape within the capsular cortex. The wall of polar capsule was formed by an electron dense outer layer, an inner electron translucent layer and terminated with capsular plug, which was shielded by a cap-like cover (Fig. 7.4a and 7.4d).

Sporoplasm

The sporoplasmic cell was located in the posterior end of the spore and between the two polar capsules. During the sporoplasm maturation, mono-nucleus was districtive with the large accumulation of glycogen bodies and a lot of electron-dense sporoplasmosomes in cytoplasm. The nucleus of generated sporoplasm contained scattered nuclear chromatin but not clearly observable nucleolus (Fig. 7.4h).

Valvogenesis

Valvogenesis is the first development process in sporomaturation. It is initiated when valvogenic cells enlarge to compass the generative cells of capsulogenic and sporoplasmic cells and rapidly adhere from their ridges through the continuous septate junction. The posterior end of the valvogenic cells protrudes forming elementariness of the sutural line process (Fig. 7.4c and 7.4d). Their nuclei were flattened and laterally located on one side of spore end nearly the continuous septate junction and dense in early phase of development after that attenuating in more developed phases (Fig. 7.4c and 7.4g). During sporogenic phase, the external plasmalemma were thin and protrude, like a horn, while the internal one was dense and showed an usual outline in close contact with other inner cells (Fig. 7.4g).

Scanning electron morphology

SEM study showed the round shaped and smooth surface of *M. supamattayai* spore. Spore ridge is absence, with smooth edge observed at sutural line (Fig. 7.5a). Position of discharging orifices (arrow) of polar filament in the anterior end of spore is in raised position in sutural line (Fig. 7.5b).
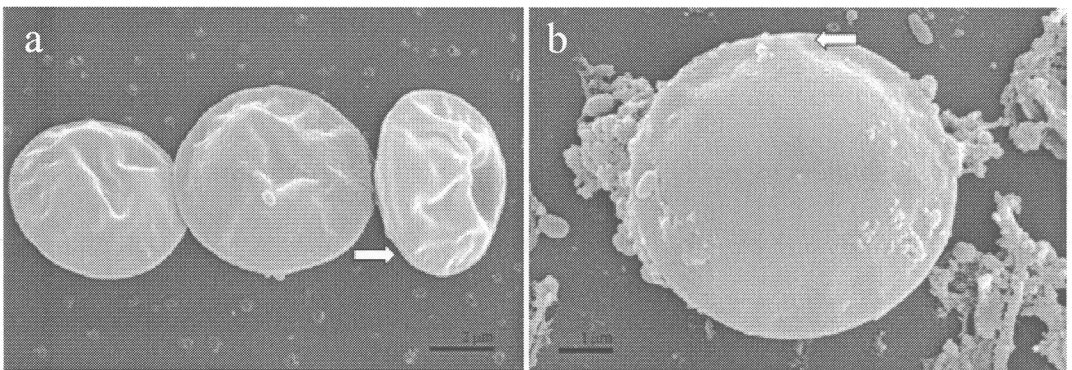

Fig. 7.5 Scanning electron microscopy images of *M. supamattayai*. **a.** Frontal view scanning eletron micrography with sutural line (arrow). **b.** Position of discharging orifices (arrow) of polar filament in the anterior end of spore.

4. Pathogenesis

Gross lesions were manifested in severely infected fish as well as consistent color changes of epithelial tissue over the damaged scales. Plasmodia were black and located on the end of epithelial tissue which destroys the scale resulting in the plasmodium hole-pocket. Remarkable site specificity was observed at the infection of plasmodia, where the localization was always restricted to the epithelial in center part of the scale. Occasionally, we found the missing scale and little ulcerated patches on skin in severely infected fish. Scanning electron micrograph showed characters of annihilability and porous hole in the plasmodium pocket of host scales (Fig. 7.6b and 7.6c).

In addition, scales under the plasmodia were thin and scatteringly found little penetrable holes in center of scales. Edge of plasmodium pockets showed level of scales damaged and displayed expandable plasmodium areas (Fig. 7.6d). The normal mullet scale was show in Fig. 7.6a.

Even though there is no report on mortality or violent diseases caused by parasites in wild bluespot mullet, the infection of *M. supamattayai* in this fish from Thailand could have a commercial impact. Although consumers are not aware of the heavy infected fish because the prevalence is not evident, this parasite may cause losses. The regular infection of this parasite in the fish is harmful to skins' functions and fish health. In the case of heavy infection, it may facilitate secondary bacterial infection.
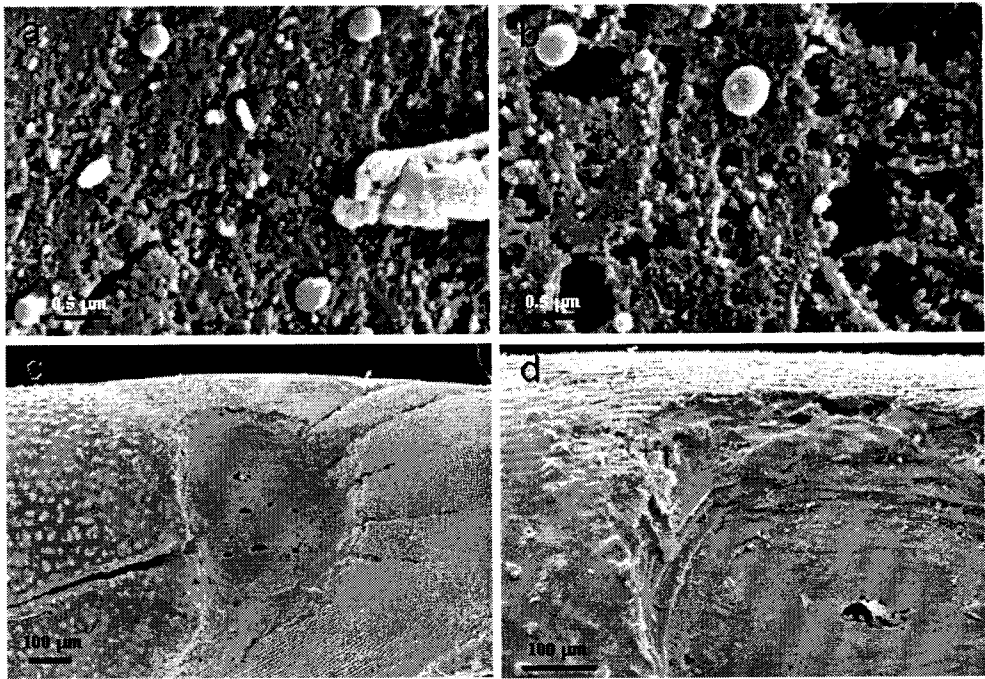
Fig. 7.6 Scanning electron micrographs of infected fish scales showing scales pathology. **a.** The surface of normal fish scale. **b.** Scale under parasitic plasmodium showing the porous scale. **c.** Hole pocket of parasite plasmodium. **d.** Detailed structure of hole pocket border showing border step and expandable size of the plasmodium.

Discussion

1. Geographical and seasonal occurrence

The myxosporean parasite isolated from fish caught from the Andaman Sea probably belongs to the same species, *M. supamattayai*, because the spore morphology and genetic data of SSU rDNA are similar. The infection pattern of this species is widespread similar with other myxobolus species infected in mullet which were found worldwide. For instance, the dispersion of *M. episquamalis* that infected in Australia mullet, *Mugil cephalus* (Rothwell *et al.*, 1997) and the worldwide disease of mullet *M. cephalus* caused by several myxobolus species (Bahri and Marques,

1996; Umur *et al.*, 2010; U-taynapun *et al.*, 2010). Our study suggested that *M. supamattayai* occurs in restricted areas, Andaman Sea. Moreover, the prevalence of infection and disease was significantly higher in rainy season in both stations of the Andaman Sea. The relatively high prevalence of *M. supamattayai* infection in rainy season may be related to the low salinity level of sea water diluted with freshwater runoff similar to the report of Urawa *et al.* (2006) which suggested that the infection level of parasitic *M. kisutchi* in Chinook salmon, *Oncorhynchus kisutch* related to freshwater level in the Columbia River basin. In contrast to the prevalence of *M. episquamalis* in mullet, *M. cephalus* at the Clarence River, Australia, that was higher in a marine environment than a brackish environment (Rothwell *et al.*, 1997). There might be involved the abundance of intermediate host for the parasite (Holzer *et al.*, 2006) and some other biological requirement with regarded to the infection.

2. Molecular detection and identification

Microscopy has been the basis of the diagnosis of parasitic myxozoa infection. Parasitic morphological classification was mainly depended on the size of mature spore by direct light microscopy or Giemsa staining. This procedure is cheap and simple, but it is a labor intensive procedure and requires well-trained technician. Many reports have demonstrated a greater sensitivity and specificity to detect myxosporean and other pathogens by the PCR based diagnostic method such as direct PCR, semi-nested PCR and quantitative PCR (Andree *et al.*, 1998; Bomfim *et al.*, 2008; Holzer *et al.*, 2004, 2006; Yokoyama *et al.*, 2010; Zakeri *et al.*, 2002). In the present study, we developed one step PCR diagnosis using three primers based on the concept of simple technique, low cost and high accuracy purposes. The semi-nested PCR assay of *M. supamattayai* was developed for species-specific detection of target

myxosporean parasite in wild bluespot mullet. The diagnosis was composed of three primers derived from the 18S rDNA sequence which could be used to directly detect parasite in mullet sample as an alternative to applied diagnostic method, such as the infection of *M. supamattayai* in secondary host. During the standardization of the method, we found that the specific primers (MsuF and MsuR) could be used in a conventional PCR with just one round of amplification using target template DNA sample. However, we believe that for a field work or small number of samples a semi-nested of amplification by using optimal concentration of one universal primer and specific primer set would improve sensitivity and accuracy.

3. Ultra-structure:

The ultra-structure data of development state and mature spore of *Myxobolus* species infected mullet is scarce. However, fine structure of *M. exiguus* and *M. epiaquamalis* which infect in scales of grey mullet and flathead mullet was described, respectively (Pulsford and Matthews, 1982 and Bahri and Marques, 1996). Sporogenesis of *M. supamattaya*i was principally similar to those of both *Myxobolus* species infecting in mullet. The development stages of *Myxobolus* species followed common pattern. Plasmodium has pinocytotic channels, marked surfaces contact with host cell. *M. supamattaya*i showed large pinocytotic channels; however, the only one could be found in each plasmodium. This incident is not typical in this genus since *M. exiguus* and other species showed numerous pinocytotic channels and pinocytotic vesicles in plasmodium membrane (Pulsford and Matthews, 1982, Ali *et al.*, 2003). All stages of parasite including asynchronous developing stage, the generative cells, early stages of sporogony and mature spore could be observed in the endoplasm zone of plasmodium. These findings are slightly different to many other myxosporeans. It

might be due to the large dimension of pinocytitic channel, which necessitate an intense uptake of nutrients. Capsulogenesis of the present species followed the usual pattern observed in most myxosporeans. Capsulogenic cells were recognized by the presence of large amount of external tubes and capsular primordial. After the polar capsule was fully developed, it was plugged with a stopper, which was covered by a cap-like structure at its apical end. These were similar to the structure of those recorded in the genus *Myxobolus* (Ali *et al.*, 2007) and in other myxosporeans genera such as *Sphaerospora* (Supamattaya *et al.*, 1990) and *Zschokkella* (Lom and Dyková, 1996). The sposoplasm cell of genus *Myxobolus* is commonly characterized by a single binucleated sporoplasm (Pulsford and Matthews, 1982 and Bahri and Marques, 1996). In contrast, this presented species showed only one nucleus in the development stage and mature spore of sporoplasm cell. However, there are some reported *Myxobolus* species with uninucleated sporoplasm such as *M. stomun* (Ali *et al.*, 2003). Dense spherical inclusions and sporoplasmosomes were identified in the sporoplasm of the present species which seem to be common feature of *Myxobolus* species and other myxosporidia (Abdel-Ghaffar *et al.*, 2008). Valvogenic cell of mostly *Myxobolus* species appeared by the time the polar capsule primordium and sporoplasm achieved differentiation (Ali *et al.*, 2007). In contrast, valvogenic cell and distinct sutural line of presented species were observed before the appearance of other spores' structures. The typical flat valve cell with its flat nucleus was observed during the valvogenesis. The microtubules generally founding the shell valves were unclearly observed in the present materials which similar with some studies including *M. stomum* (Ali *et al.*, 2003).

This study has provided the important biological data of the prevalence, occurrence locations, molecular diagnosis and spore developmental state

of *M. supamattayai* in bluespot mullet. These data are important for understanding of the myxobolus diseases in wild fish which is scarce in Southeast Asia.

References

Abdel-Ghaffar, F., El-Toukhy, A., Al-Quraishy, S., Al-Rasheid, K., Abdel-Baki, A. S., Hegazy, A. and Bashter, A. R. 2008. Five new myxosporean species (Myxozoa: Myxosporea) infecting the Nile tilapia *Oreochromis niloticus* in Bahr Shebin, Nile Tributary, Nile Delta, Egypt. Parasitol. Res. 103 : 1197–1205.

Ali, M. A., Abdel-Baki, A. S., Sakran, T., Entzeroth, R. and Abdel-Ghaffar, F. 2003. Light and electron microscopic studies of *Myxobolus stomum* n. sp. (Myxosporea: Myxobolidae) infecting the blackspotted grunt *Plectorhynicus gaterinus* (Forsskal, 1775) in the Red Sea, Egypt. Parasitol. Res. 91 : 390–397.

Ali, M. A., Abdel-Baki, A. S., Sakran, Th., Entzeroth, R. and Abdel-Ghaffar, F. 2007. Myxobolus lubati n. sp. (Myxosporea: Myxobolidae), a new parasite of haffara seabream Rhabdosargus haffara (Forsskal, 1775), Red Sea, Egypt: a light and transmission electron microscopy. Parasitol. Res. 100 : 819–827.

Andree, K. B., MacConnell E. and Hedrick, R. P. 1998. A nested polymerase chain reaction for the detection of genomic DNA of Myxobolus cerebralis in rainbow trout *Oncorhynchus mykiss*. Dis. Aquat. Org. 34 : 145–154.

Bomfim, M. R., Barbosa-Stancioli, E.F. and Koury, M. C. 2008. Detection of pathogenic leptospires in urine from naturally infected cattle by nested PCR. Vet J. 178 : 251–256.

Bahri, S., Andree, K. B. and Hedrick, R. P. 2003. Morphological and phylogenetic studies of marine Myxobolus spp. from mullet in Ichkeul Lake, Tunisia. J. Eukaryot. Microbiol. 50 : 463–470.

Bahri, S. and Marques, A. 1996. Myxosporean parasites of the genus Myxobolus from

Mugil cephalus in Ichkeul lagoon, Tunisia: description of two new species. Dis. Aquat. Org. 27 : 115–122.

Diamanka, A., Fall, M., Diebakate, C., Faye, N. and Toguebaye, B. S. 2008. Identification of Myxobolus episquamalis (Myxozoa, Myxobolidae) in flathead mullet *Mugill cephalus* (Pisces, Teleostei, Mugilidae) from the coast of Senegal (eastern tropical Atlantic Ocean). Acta Adriat 49 : 19–23.

Holzer, A. S., Sommerville, C. and Wooten, R. 2004. Molecular relationships and phylogeny in a community of myxosporeans and actinosporeans based on their 18S rDNA sequences. Int. J. Parasitol. 34 : 1099–1111.

Holzer, A. S., Sommerville, C. and Wootten, R. 2006. Molecular studies on the seasonal occurrence and development of five myxozoans in farmed *Salmo trutta* L. Parasitology 132 : 193–205.

Lom, J. and Dyková, I. 1996. Notes on the ultrastructure of two myxosporean (Myxozoa) species, *Zschokkella pleomorpha* and *Ortholinea fluviatitis*. Folia Paraitol. 43 : 189–202.

Lom, J. and Dyková, I. 2006. Myxozoan genera: definition and notes on taxonomy, life-cycle terminology and pathogenic species. Folia Parasitol. 53 : 1–36.

Longshaw, M., Frear, P. A. and Feist, S. W. 2005. Descriptions, development and pathogenicity of myxozoan (Myxozoa: Myxosporea) parasite of juvenile cyprinids (Pisces: Cyprinidae). J. Fish Dis. 28 : 489–508.

Maeno, Y., Sorimach, M., Ogawa, K. and Egusa, S. 1990. *Myxobolus spinacurvatura* sp. n. (Myxosporea: Bivalvulida) parasitic in deformed mullet, *Mugil cephalus*. Fish Pathol. 25 : 37–41.

Molnár, K., Székely, C., Hallett, S. L. and Atkinson, S. D. 2009. Some remarks on the occurrence, host-specificity and validity of *Myxobolus rotundus* Nemeczek, 1911 (Myxozoa: Myxosporea). Syst. Parasitol. 72 : 71–79.

Moncada, L. I., López, M. C., Murcia, M. I., Nicholls, S., León, F., Guío, O. L. Corredor, A. 2001. *Myxobolus* sp., Another opportunistic parasite in immunosuppressed patients? J. Clin. Microbiol. 39 : 1938–1940.

Pulsford, A. and Matthews, R. A. 1982. An ultrastructure study of *Myxobolus exiguus* Thelohan, 1895 (Myxosporea) from grey mullet, *Crenimguil labrosus* (Risso). J. Fish Dis. 5 : 509–526.

Redondo, M. J., Quiroga, M. I., Palenzuela, O., Nieto, J. M. and Alvarez-Pellitero, P. 2003. Ultrastructural studies on the development of *Enteromyxum scophthalmi* (Myxozoa), an enteric parasite of turbot (*Scophthalmus maximus* L.). Parasitol. Res. 90 : 192–202.

Rothwell, J. T., Virgona, J. L., Callinan, R. B., Nicholls, P. J. and Langdon, J. S. 1997. Occurrence of cutaneous infections of *Myxobolus episquamalis* (Myxozoa: Myxobolidae) in sea mullet, *Mugill cephalus* L, in Australia. Aust. Vet. J. 75 : 349–352.

Supamattaya, K., Fischer-Scherl, T., Hoffmann, R. W. and Boonyaratpalin, S. 1990. Renal sphaerosporosis in cultured grouper *Epinephelus malabaricus*. Dis. Aquat. Org. 8 : 35–38.

Umur, Ş., Pekmezci, G. Z., Beyhan, Y. E., Gürler, A. T. and Açici, M. 2010. First record of *Myxobolus muelleri* (Myxosporea: Myxobolidae) in flathead grey mullet *Mugil cephalus* (Teleostei, Mugilidae) from Turkey. Ankara Üniv Vet Fak Derg 57 : 205–207.

Urawa, S., Iida, Y., Freeman, M. A., Yanagida, T., Karlsbakk, E. and Yokoyama, H. 2009. Morphological and molecular comparisons of Myxobolus spp. in the nerve tissues of salmonid fishes with the description of Myxobolus murakamii n. sp., the causative agent of myxosporean sleeping disease. Fish Pathol. 44 : 72–80.

U-taynapun, K., Penprapai, N., Bangrak, P., Mekata, T., Itami, T. and Tantikitti, C. 2010. Myxobolus supamattayai n. sp. (Myxosporea: Myxobolidae) from Thailand parasitizing the scale pellicle of wild mullet (Valamugil seheli). Parasitol. Res. in press. 10.1007/s00436-010-2223-1.

Yokoyama, H., Yanagida, T., Freeman, M. A., Katagiri, T., Hosokawa, A., Endo, M., Hirai, M. and Takagi, S. 2010. Molecular diagnosis of Myxobolus spirosulcatus associated with encephalomyelitis of cultured yellowtail, *Seriola quinqueradiata* Temminck & Schlegel. J. Fish Dis. 33 : 939–946.

Zakeri, S., Najafabadi, S. T., Zare, A. and Djadid, N. D. 2002. Detection of malaria parasites by nested PCR in south-eastern Iran: Evidence of highly mixed infections in Chahbahar district, Malar. J. 1 : 2–7.

8. SUMMARY

In the last thirty years, there are two factors that help advancing our understanding of the *Myxozoa*. First, the phenomenal increase in fin fish aquaculture in the 1990s has led to the increased importance of these parasites, as a result, leading to intensified research efforts which have increased knowledge of the development, diagnosis and pathogenesis of myxozoans. Second, after the hallmark discovery in the 1980s which the life cycle of *Myxobolus cerebralis* requires development of an actinosporean stage in the oligochaete, *Tubifex tubifex*, the life cycles of several other myxozoans has been elucidated. Although myxosporean have been known over 180 years ago, a large number of new knowledge regarding new taxonomic classification procedure and applied technology have been reported in wild and cultured fish.

In Southeast (SE) Asia, Székely *et al.* (2009a and 2009b) have shown the present of myxosporean occurrence in Malaysia and described 9 new species. Baska *et al.* (2009) described 2 myxosporean species detected in ornamental fish fry, *Pangasianodon hypophthalmus*, exported from Thailand to Europe. The knowledge of the myxosporean in economic fish of Asia including Thailand is restrictive and non-comprehensive. Total new myxosporean species found in SE Asia was more than 10 species after starting novel strategies.

The important discovery of this study is as follows; 1. The occurrence of many myxosporean species including one known species, *Sphaerospora epinepheli*, nevertheless, most of them are unidentified. *S. epinepheli* was first described by Supamattaya *et al.* (1991) in malabar grouper, *Epinephelus malabaricus*. Most myxosporean are highly host specific, our results indicated the new host recorded of this parasite, *E. coioides*. This finding therefore led us to focus on the

159

biological character, histopathology and molecular phylogeny detail of *S. epinepheli* in the new host record. 2. We also found that the occurrence of *S. epinepheli* is highly spread in net cage cultured and wild fish, especially in Phang-Nga Bay, the main grouper production of Thailand. *S. epinepheli* could cause the violent histopathological damage in fish kidney. To monitor and apply in the epidemiological study of this species, the rapid assays were developed. The highest reliable diagnostic method is real time loop mediated isothermal amplification (real time LAMP). 4. The new species *Myxobolus supamattayai* n. sp. parasitizing the scale pellicle of wild mullet, *Valamugil seheli* was discovered and described following the novel taxonomic criteria based on microscopic characters, ultra-structure morphology and molecular phylogeny classification. Seasonal occurrence, ultra-structure of developmental stage of spore and PCR based diagnosis to deliberate in the part of biology and epidemiology of *M. supamattayai* n. sp. are also studied.

Recommendations and further studies

For myxosporean biodiversity in the present study, there are five un-described myxosprean species which is not yet completely described, the continuing studies should be conducted. Though, they are little knowledge in over all of its diversity. The early stages of Myxozoa biodiversity have been progressed in SE Asia with high degree of variation in tropical zone as similar as those data from Amazon. First, we recommend the basic research in the field of taxonomy and epidemiology in both economic freshwater and marine fish, such as Nile tilapia, barb and Asian sea bass for developed knowledge. Afterward, complete life cycle of important myxosporean species causing economic loss might be concentrated. Since, it is very complicated to design the experiment to monitor life cycle, especially within natural

field. We have proposed idea of using applied molecular diagnosis to monitor and limit the target for parasitic infected second host (actinosporean in annelid) of high distribution areas. Although we developed and compared between frontier diagnoses, real time LAMP and qPCR, both assays have already used in conventional based technique.

References

Székely, C.S., Shaharom-Harrison, F., Cech, G., Ostoros, G. and Molnár, K. 2009a. Myxozoan infections in fishes of the Tasik Kenyir Water Reservoir, Terengganu, Malaysia. Dis. Aquat. Org. 83 : 37–48.

Székely, C.S., Shaharom-Harrison, F., Cech, G., Mohamed, K. and Molnár, K. 2009b. Myxozoan pathogens of Malaysian fishes cultured in ponds and net-cages. Dis. Aqua. Organ. 83 : 49–47.

APPENDIX

Myxobolus supamattayai n. sp. (Myxosporea: Myxobolidae) from Thailand parasitizing the scale pellicle of wild mullet (Valamugil seheli)

Kittichon U-taynapun · Norasing Penprapai ·
Phuwadol Bangrak · Tohru Mekata · Toshiaki Itami ·
Chutima Tantikitti

Abstract A new myxosporean species, *Myxobolus supamattayai* n. sp., was isolated from wild mullet (*Valamugil seheli*) from the Andaman Sea, Thailand and described based on its morphology and molecular data. The myxosporean produced black plasmodia-like unique clinical sign on the skin with sporogonic stages and mature spores. Polysporous plasmodia, up to 2.5 mm in diameter, were found in epithelium tissue in the scale pocket. The spores measured 6.6 (6.2–7.0) μm in length, 6.5 (6.2–6.7) μm in width, smooth, and round board to ellipsoidal in valvular view. Spores were enclosed with intracapsular process which represents 5–7 and 11–12 in amount revealed in light microscopy and ultrastructure, respectively. The polar capsules were pyriform and of equal size, measuring 3.5 (3.4–3.6) μm in length and 2.0 (1.9–2.2) μm in width, with four to five turns of polar filament arranged perpendicularly to longitudinal axis of the polar capsule. In conclusion, this new species is entirely different from those previously described; however, this finding was assured by the partial sequence of SSU rRNA gene (1,666 bp) analysis that differed from all known species of *Myxobolus* Bütschli, 1882. The phylogenetic tree of the sequence data sets including those of freshwater and marine of *Myxobolus* spp. and the sister group (*Henneguya* spp.) was constructed to establish the relationship of this new species in *Myxobolus* clade and to explore its relations between their sister groups. Phylogenetic analysis indicated that a monophyletic group with *Myxobolus* spp. which infected mullet represents the newly formed species. These results suggested the presumably nearby evolution prospecting of *Myxobolus* species that were found in the same host.

K. U-taynapun · C. Tantikitti (✉)
Aquatic Animal Health Research Center,
Department of Aquatic Science, Faculty of Natural Resources,
Prince of Songkla University,
Songkhla, Thailand
e-mail: chutima.t@psu.ac.th

K. U-taynapun
Center of Excellence on Agricultural Biotechnology
(AG-BIO/PERDO-CHE),
Bangkok, Thailand

N. Penprapai
Faculty of Science and Fisheries Technology,
Rajamangala University of Technology Srivijaya,
Trang campus,
Trang, Thailand

P. Bangrak
School of Science, Walailak University,
Nakhon Si Thammarat, Thailand

T. Mekata
National Research Institute of Aquaculture,
Oita, Japan

T. Itami
Department of Marine Biology and Environmental Sciences,
Faculty of Agriculture, University of Miyazaki,
Miyazaki, Japan

Introduction

The genus *Myxobolus* of the phylum *Myxozoa* contains more than 792 species; some are the most important parasitic pathogens of economic fish such as *Myxobolus cerebrasis*, causative of the whirling diseases in salmon. Most members of *Myxobolus* are histozoic parasite of freshwater fish; however, about 30 species live in marine or estuarine water. Some of them have coelozoic plasmodia of far less compact structure than histozoic trophozite (Lom

and Dyková 2006). Although there are numerous detailed descriptions of species of the genus *Myxobolus* from teleost of nearly all geographical areas, information about this genus in Southeast Asia, mainly *Myxobolus* as a parasite in economic marine fish such as Asian seabass, grouper, and mullet, remains scarce. Mullet species is one of the most important economic fish of Southeast Asia, particularly in southern Thailand. Culture of mullet has been increased in Thailand in recent years, which is performed in cage-polyculture systems along with Asian seabass, grouper, and red snapper. In addition, wild-caught mullet has been decreasing while the demand is very high. Coinciding with the growing economic value of this fish, its increasing parasite loads are likely to affect the aquaculture industry.

The taxonomic methodology for identification of myxosporean species have been principally based on spore morphology for the primary classification of the species character until the acceptance of molecular data with reference to phylogenetic tree in taxonomic myxosporea (Liu et al. 2010). When determining the validity of the identification of similar morphological myxosporea, especially from identical tissue of the taxonomically closely related host species (Székely et al. 2009), these classical morphological methods are very difficult to use. Although host and tissue specificity are of great help in differentiating morphologically similar spores, there are some myxosporea, such as *Myxobolus rotundus*, that are classified from 27 cyprinid fish species and from different sites in the fish body (Eiras et al. 2005; Molnár et al. 2009; Zhang et al. 2010). However, recent reports have described a specific parasite of common bream using molecular data and the actinosporean stage development in oligochaete, *Tubifex tubifex* (Molnár et al. 2009; Székely et al. 2009). The wide host range and multiple infection sites are still yet to be explored. Unfortunately, spores of many species of the genus *Myxobolus* vary from each other; many species descriptions of this genus that have long been discovered are not definite and many are inconsistent with their documentation (Dyková et al. 2002). The combination of morphology and molecular-based classification, with the consideration of host range and tissue specificity, provides a precise approach to distinguish valid species from identified taxa (Molnár et al. 2009). A list of parasites of the wild mullet species has been introduced including 15 species of the genus *Myxobolus* (Bahri and Marques 1996; Kent et al. 2001; Buhri et al. 2003), which can be found in various organs of their host fish. Only *Myxobolus episquamalis* and *Myxobolus exiguus* were observed in the scales of mullet (Pulsford and Matthews 1982; Egusa et al. 1990). However, most of the mullet parasite, *Myxobolus* spp., were described based on their morphology while six species have been studied for both morphology and phylogeny (Buhri et al. 2003). The recent classification model, designed for gaining more sufficient and reliable resolution, requires morphological information along with molecular analysis. The morphological data have been obtained from the fine structures of the genus *Myxobolus* appearances followed from typical myxozoa pattern including shape of spore, polar capsule, polar filament turns, and ultrastructural studies. The SSU rRNA gene sequences, typically 18S rDNA, have indicated a proof of molecular classification (Fiala 2006).

In the present study, *Myxobolus supamattayai* n. sp., a new species belonging to the genus *Myxobolus*, found in wild mullet (*Valamugil seheli*) from the Andaman Sea, Thailand was described. Light microscopic, ultrastructure study and phylogenetic analysis using SSU rDNA were performed to determine the evolutionary relationships of this particular species among genus *Myxobolus* to assess the reliability of spore morphology-based classification.

Materials and methods

Fish samples and sampling

The samples collected in 2007 and 2008 were 143 specimens of *V. seheli* ranging in weight from 30 to 120 g from two different areas on the coast of the Andaman Sea in Satun province (station 1—6°50′33″ N, 99°46′19″ E; station 2—6°47′03″ N, 99°49′44″ E), Thailand. These fish samples were caught using floating seine and beach seine, which are fishing tools of an artisanal fishery. According to the previous work from our group, the black cyst scale is the hallmark of host infected with interesting *Myxobolus* species; thus, the mullets exhibiting this symptom were separated to the restrictive tank. The infected and uninfected fish with or without symptoms were transported alive in aerated seawater to the Aquatic Animal Health Research Center, Prince of Songkla University, Thailand immediately after collection. Moribund fish were killed by overdose of clove oil, packed in a plastic bag, and kept in temperature-controlled freezer boxes during the transportation. Standard procedures of myxosporean examination, internal organs, body surface, and body fluid, were used to diagnose myxosporean infection in the collected fishes.

Morphology analysis

Morphological measurement of species description was obtained among 50 spores according to Lom and Arthur (1989) and Lom and Dyková (2006). Fresh spores and Giemsa-stained spores were analyzed to identify their morphology and photographed. Species descriptions were based on several *Myxobolus* populations from more than one host specimen. Spores were observed under an Olympus AX 70 microscope and photographed using

Olympus DP 71 cool CCD camera with differential interference contrast (DIC) optics.

For ultrastructure studies by electron microscopy, fresh plasmodia were dissected from infected fish skin and fixed in 3% glutaraldehyde in cacodylate buffer (pH 7.4) at 4°C for 6 h. Samples were post-fixed in 1% (w/v) osmium tetroxide using the same buffer. Transmission electron microscopy samples were dehydrated through graded acetone series before embedding in Epon-812, ultrathin sectioned, and stained with uranyl acetate and lead citrate. They were examined under a JEOL transmission electron microscopy (JEM-123) at 80 kV. The images were digitally recorded for further analysis.

Genomic DNA extraction

The DNA extraction method was modified from Salim and Desser (2000). Briefly, spores were centrifuged and pelleted at 8,000×g for 10 min, washed twice with PBS, and resuspended in 200 μl of 2% (v/v) proteinase K in STE buffer (pH 8.0) containing 1% SDS. Spores were incubated overnight at 30°C. The spore suspension was boiled for 10 min and then plunged into liquid nitrogen; the same process was repeated three times. The suspension was examined using light microscopy to verify whether most spores released their sporoplasms. The DNA was subsequently extracted with phenol/chloroform/IAA (25:24:1, v/v/v) method, incubated overnight, and precipitated with 70% ethanol. The DNA pellet was obtained after centrifugation at 12,000×g for 15 min at 4°C, followed by washing with 70% ethanol, and was air dried and resuspended with 20–30 μl of double distilled water. The DNA samples were kept at −20°C until use.

PCR amplification and purification of the 18S rDNA

The 18S rDNA of the *Myxobolus* parasite was amplified with MX 5 (5′ CTGCGGAC GGCTCAGTAAATCAGT 3′) and MX 3 (5′ CCAGGACATCTTAGGGCATCACAGA 3′), which bind to the conserved regions in the 5′ and 3′ end, respectively (Andree et al. 1998). The PCR was performed in a 50-μl reaction containing 2 μl of template DNA (100–150 ng of genomic DNA), 100 pmol of each of forward and reverse primer, 250 mM dNTP, 5 μl of 10× PCR buffer, and 1 μl of 5 U/μl Taq DNA polymerase (Invitrogen). Amplifications were conducted with an MJ Research DNA Engine 100 (MJ Research) using the following cycling protocol: an initial denaturation step of 95°C for 5 min, 40 cycles of 95°C/1 min–60°C/1 min–72°C/1 min, and a final extension of 10 min at 72°C. The PCR products were electrophoresed on 1.5% agarose gel (Vivantis) in TAE buffer for approximately 30 min at 100 V. The expected band of the 18S rDNA fragments of *Myxobolus* were directly cut from the

gel and further purified with QIAquick Gel Extraction kit (Qiagen). The purified DNA was immediately used as inserted DNA in cloning system.

DNA cloning of PCR products and sequencing

The 18S rDNA gene of *Myxobolus* species was cloned into pGEM®-T Easy Vector using the pGEM®-T Easy Vector Systems cloning kit (Promega) and transformed into *Escherichia coli* TOP10 cells according to the manufacturer's instructions. The plasmids were purified from positive clones and selected upon the blue/white color screening method using the QIAprep Spin Miniprep Kit (Qiagen). Inserted parasitic genes in the plasmid was confirmed before sequencing by PCR using either the same primers as those used in the original amplification (MX 5 and MX 3) or the primers that flanked the insertion site (T7 and SP6). The purified plasmids containing insert were sequenced on a CEQ™ 8000 automatic sequencer (Beckman Coulter) using CEQ DTCS Dye Kit (Beckman Coulter) according to the manufacturer's protocol. In addition, the internal part of 18S rDNA was sequenced using the internal forward (5′ CCAGTAGCGTATCTCAAAGTTGC 3′) and reverse (5′ CCCGTGTTGAGTCAAAT TAAGC 3′) primers which were designed based on conserved sequences within the SSU rDNA gene of this species.

Phylogenetic analysis

The 18S rDNA sequence of *M. supamattayai* n. sp. was compared to those of other species available in the GenBank using nucleotide BLAST protocol (Altschul et al. 1990). Taxa included in the alignments were based on similarities from BLAST results including congeners of the novel species and representatives from each of the major clades reported in previous studies (Fiala 2006). The malacasporean *Tetracapsuloides bryosalmonae* was used as an out-group species in phylogenetic analyses. In addition, 35 selected taxa of platysporinid rDNA sequence from the genus *Myxobolus* and related species, mostly *Henneguya* spp., used in the analysis were restricted to the same length of the sequence of those isolated from hosts living in all habitats: freshwater, brackish, and marine. CLUSTAL X algorithm (Thompson et al. 1994) was used for initial sequence alignment with default setting for gap opening/extension penalties, and regions of ambiguous sequence alignments were manually edited using the BioEdit sequence alignment editor (Hall 1999). We used neighbor-joining (NJ), maximum parsimony (MP), and maximum likelihood (ML) methods to infer phylogenetic relationships among the *Myxobolus* spp. and its sister group. There were a total of 2,220 positions in the final dataset. Phylogenetic analyses of the NJ method and MP

method were conducted using the MEGA V. 4.0 program (Kumar et al. 1993). For the NJ method, evolutionary distances were analyzed using the Kimura two-parameter (K2P) evolution sequence model (Kimura 1983). The evolutionary history was concluded using the NJ method. Statistical consensus trees inferred from 1,000 replications bootstrapping were taken to present the evolutionary history of the taxa analyzed. The MP tree was obtained using the Close-Neighbor-Interchange algorithm (Nei and Gojobori 2000) with search level 3 in which the initial trees were obtained with the random addition of sequence (100 replications). Parsimonious trees were shown with the percentage of replicate trees in which the associated taxa clustered together in the bootstrap test (1,000 replicates). All alignment gaps/missing data were set as the complete deletion in both analysis methods. We used MEGA 4 for these analyses including the primary tree-based drawing of NJ tree.

The SeaView V 4 program (Gouy et al. 2010) was executed using the GTR model for ML analysis. The selecting models were evaluated by using jModelTest (Posada 2008). The BioNJ (Gascuel 1997) algorithm was selected for starting trees. Nearest-neighbor interchange and subtree pruning and regrafting were used for tree searching operation. The data sets were built with 500 bootstrap replications for the ML reconstruction.

Results

Morphology and clinical signs

Several cyst-like plasmodia, with diameter up to 2.5 mm, containing numerous sporogonic stages and mature spores were observed in the epithelium tissue above the scale. Twenty five of 143 specimens (17.48%) were infected with parasites classified, based on the spore morphology, as a myxosporean belonging to the genus *Myxobolus* Bütschli, 1882 (Lom and Dyková 2006). All characteristics of the genus *Myxobolus* were observed in the spores' stage of these parasites found in macroscopical lesions localized in the epithelium scales pocket. Black cystic formations as parasite plasmodia were detected only in the target organ while no other tissues or organs contained visible parasites revealed by light microscopy. The majority of the parasitized fish showed more than 100 cyst-like structures in different locations, mostly in the pectoral to anal fin below the lateral line body area (Fig. 1a).

Myxobolus supamattayai n. sp.

Vegetative stages More developed plasmodia contained late sporogonic stages and mostly mature spores. Black, polysporous spot to ellipsoidal-shaped histozotic cyst-like plasmodia measuring up to 2.5 mm in diameter were found in the epithelial tissue above the scales. The scales were destroyed as a plasmodium hole pocket (Fig. 1b). Missing scale and small ulcerated patches on the skin were occasionally found particularly in severely infected fish. Numerous plasmodia could be found in each infected fish; however, only one plasmodium per scale could be observed. In addition, this was not found in other organs.

Morphology of spores (based on 50 mature spores) Spores with typical character of the genus *Myxobolus* were observed. The mature spores were round board to ellipsoidal in frontal view. Most of them are round with several edge markings (normally 5–7), whereas a few are variable in shape. Spore size was 6.6 (6.2–7.0) μm in length and 6.5 (6.2–6.7) μm in width. The two spherical polar capsules were equal in size and close together in the plane of sutural line at the apical end which measured 3.5 (3.4–3.6) μm in length and 2.0 (1.9–2.2) μm in width. Polar filaments formed four to five coils opening at the spores anterior nearby the sutural line. The coil arrangement was almost perpendicular to the sutural line. Polar filaments extruding from mature spores of fresh material were evaluated as 10.5 (10–11) μm in length (Fig. 1d). A small intercapsular appendix was located between the polar capsules at the anterior end of the spore and discernible vacuole-like body in the sporoplasm of the spore. Spore morphology observations under light microscopy and Giemsa staining are shown in Fig. 1c and e, respectively..

Type host Blue spot mullet (*Valamugil seheli*)

Type locality The coast of the Andaman Sea, Satun province, Thailand (6°47'03.68" N, 99°49'44.60" E)

Site of infection Epithelial tissue located in the center of the scale

Prevalence Up to 17.48% (25/143)

Type material Slides with stained spore (syntype) and formalin-preserved infected host fish (*V. seheli*) have been deposited in the collection of the Princess Maha Chakri Sirindhorn Natural History Museum, Prince of Songkla University, Songkhla, Thailand (accession number PSUZC-20090216.01).

Etymology The species name (*M. supamattayai*) is in homage to Assoc. Prof. Dr. Kidchakan Supamattaya, one of the pioneers in the study of aquatic animal disease in Thailand and the first director of this project (myxosporidia disease and biodiversity of parasite in economic marine fish of Thailand), who passed away in 2008.

Fig. 1 *Myxobolus supamattayai* n. sp. in mullet (*Valamugil seheli*) from the coast of the Andaman Sea. **a** Cysts of *M. supamattayai* n. sp. on the infecting mullet scales (*arrows*). **b** Pathology of *M. supamattayai* n. sp. on the scales (*arrow*). **c** Fresh mature spore (DIC photography). **d** Spore in Giemsa staining. **e** Fresh spore with ejected polar filament. All *scale bars* are 10 micrometers
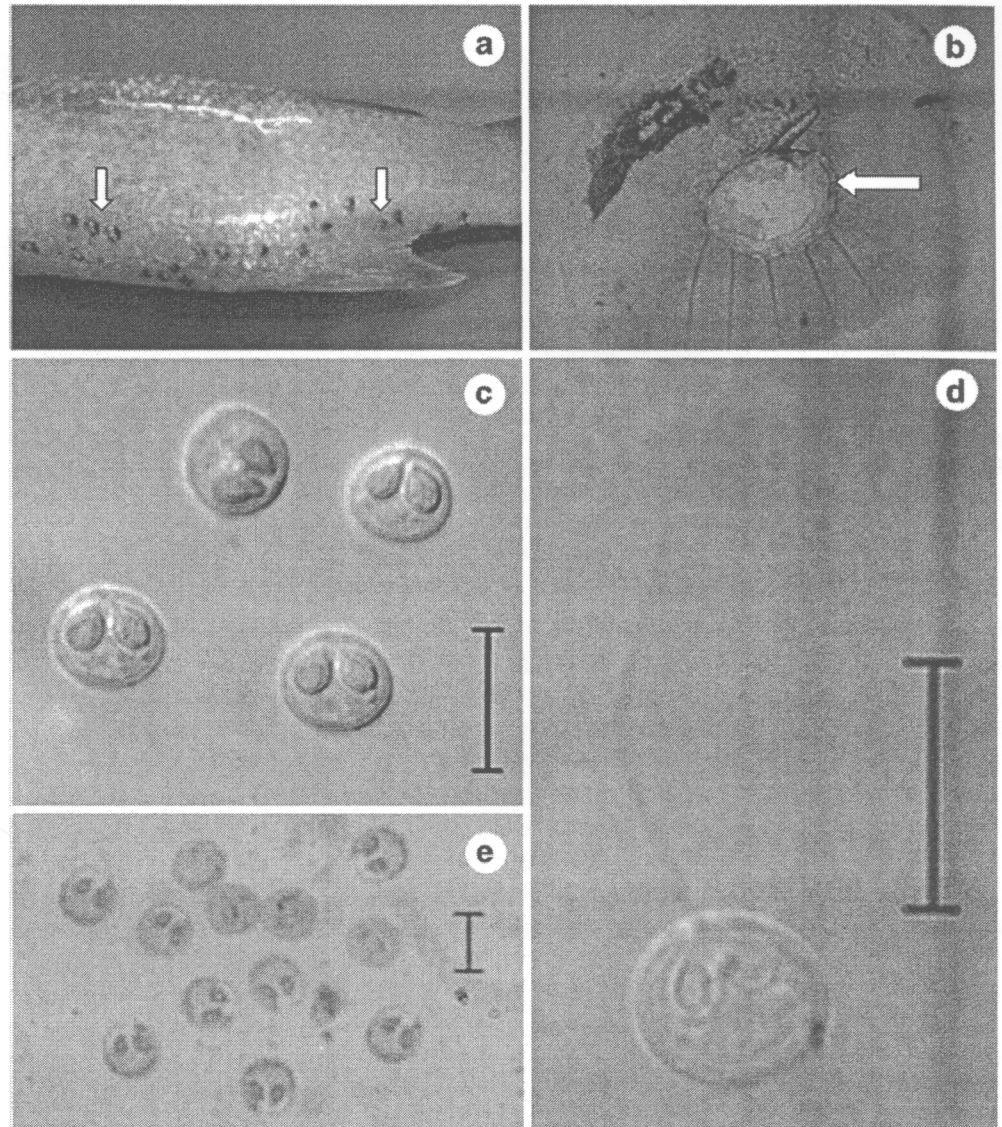
Electron microscopy

Fine structure of mature spores presented the complete developing cells comprising two shell valves, mononucleated sporoplasm, and two polar capsules (Fig. 2a, b). The spore body was formed by two smooth shell valves, each one with two caudal projections for releasing the polar filament. The internal sutural line, the overlap of two spore valves, contained 11–12 intracapsular processes. The two equal polar capsules were pyriform, elongated, and a little converged at the apex of the spore. The polar capsules with a polar filament, basal straight central shaft, and coils of four to five turns were visible. Polar capsules were composed of thin electron-dense external wall along with thick and lighter inner wall. The apical channel for the polar filament discharge showed close contact with caudal projection in valves. The sporoplasmic cell was located in the posterior pole of the spore and the cytoplasm contained three distinct organelles; mononuclei were close to each other, low density electron-dense body, like a cell vacuole and sporoplasmosomes. These spherical-shaped vesicles were membrane bounded and contained an electron-dense and homogenous matrix. The nucleus was found in the sporoplasm cell, whereas other cells in mature spore could not show the basis of complete cell structure. A semi-schematic illustration of the spore, based on TEM observations, is shown in Fig. 3.

Molecular characterization and phylogenetic tree

Overall SSU rDNA sequences were determined for 12 samples (six samples from each sampling site). All the sequence samples showed 99.9% homology to the rDNA nucleotide sequences. The amplified and sequenced 18S rDNA gene of *M. supamattayai* n. sp. was 1,617 nucleotides in length excluding the region corresponding to MX
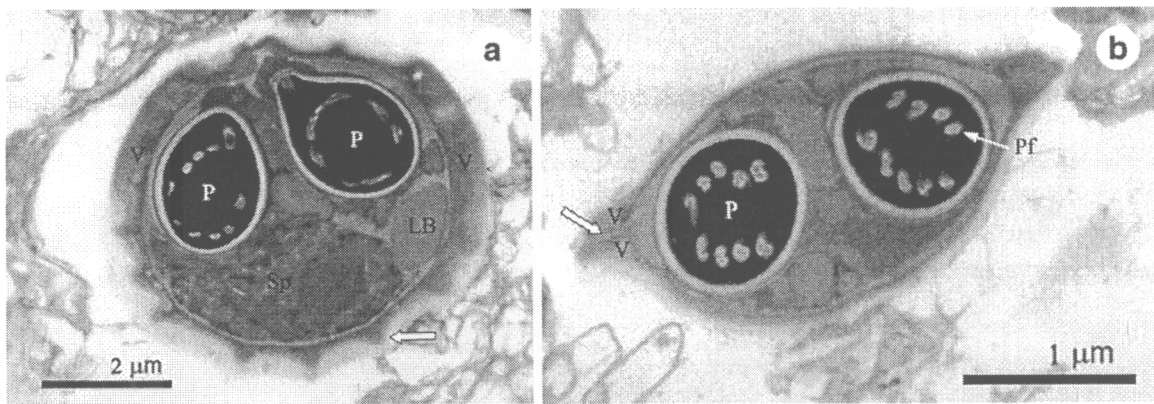
Fig. 2 Transmission electron micrographs of the mature spore of *Myxobolus supamattayai* n. sp. **a** The detail of spore longitudinal ultrathin section showing the valves (*V*) with internal capsular process (*arrow*), the two polar capsules (*P*) and sporoplasm (*Sp*) with one nucleus and low density electron dense body (*LB*), like a vacuole. **b** The detail of spore sectioned transversally showing the valves (*V*) and sutural line (*arrow*), two polar capsules (*P*) with four to five polar filament turns

5–MX 3 primers while the G+C content was 43.0%. The sequence was deposited at the National Center for Biotechnology GenBank (accession number HQ166720). The 18S rDNA gene of this *Myxobolus* species isolated from mullets revealed the sequence identity with other parasite species in the same host: 88% with *Myxobolus muelleri*, 90% with *M. episquamalis*, 91% with *Myxobolus bizerti*, 88% with *M. exiguus*, 87% with *Myxobolus ichkeulensis*, and 88% with *Myxobolus spinacurvatura*. The nucleotide sequences of *M. supamattayai* n. sp. obviously differed, more than 25% of 1,666 base pairs, from those of all other *Myxobolus* species available in the GenBank.

Phylogenetic analysis was conducted using the NJ algorithm resulting in a single most parsimonious tree (Fig. 4), while the member species in each clade of the MP tree and ML tree remained the same. Some branches were swapped within clades, but this did not significantly change the apparent evolutionary relationship. The clades of *Myxobolus* species were divided into three main clades that were strongly supported by bootstrap values. However, the demise of *Myxobolus* clades distinctly interferes with the clade of *Henneguya* species. All the phylogenetic topology analysis trees demonstrated that the mullet parasite *Myxobolus* species containing seven species (*M. supamattayai* n. sp., *M. muelleri*, *M. episquamalis*, *M. bizerti*, *M. exiguus*, *M. ichkeulensis*, and *M. spinacurvatura*) correspond to a monophyletic group (clade A). This is separated into a distinct clade strongly supported by high bootstrap values. The representation of marine *Myxobolus* clade, infected mullet fish host, partitioned within the clade formed by the *Henneguya* species which was separated from other *Myxobolus* clades (B and C) was composed of 18 species which are involved in freshwater fish parasites.
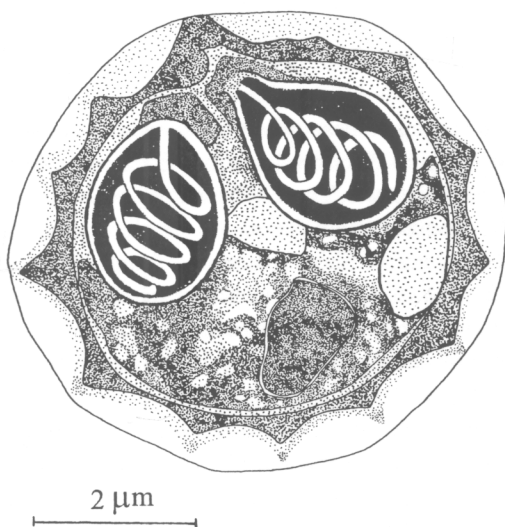

Fig. 3 Semi-schematic illustration of a longitudinal view of a mature spore of the *Myxobolus supamattayai* n. sp., a parasite of blue spot mullet *Valamugil seheli* showing species-specific characters including spore size and shape, two equal polar capsules with four to five polar filament turns, uninucleated sporoplasm, vacuole with sporoplasmosome, and 11–12 intercapsular processes in sutural line

Discussion

Morphological and ultrastructural taxonomic classification

The light morphology of the spores described in the present work corresponds to those of the genus *Myxobolus*, myxozoa parasite. Myxozoa species are very common parasites of fish. Many researchers demonstrated that more than one species of myxosporea parasite infect the same

Fig. 4 Phylogenetic tree
generated by neighbor-joining
(NJ), maximum likelihood
(ML), and maximum parsimony
(MP) analyses of the 18S rDNA
sequence of myxosporeans, root
at *Tetracapsuloides bryosalmo-
nae*. *Numbers* at nodes indicate
bootstrap confidence levels pre-
sented as percentage for NJ,
ML, and MP, respectively (NJ
and MP=1,000 repetitions and
ML=500 repetitions). GenBank
accession numbers of each spe-
cies are given in *parentheses*.
The distance scale is shown
beside the tree. Myxosporean
identified in the present study is
given in *gray background*. The
dashed lines indicate the differ-
ences between the three trees,
taking NJ as basic topology
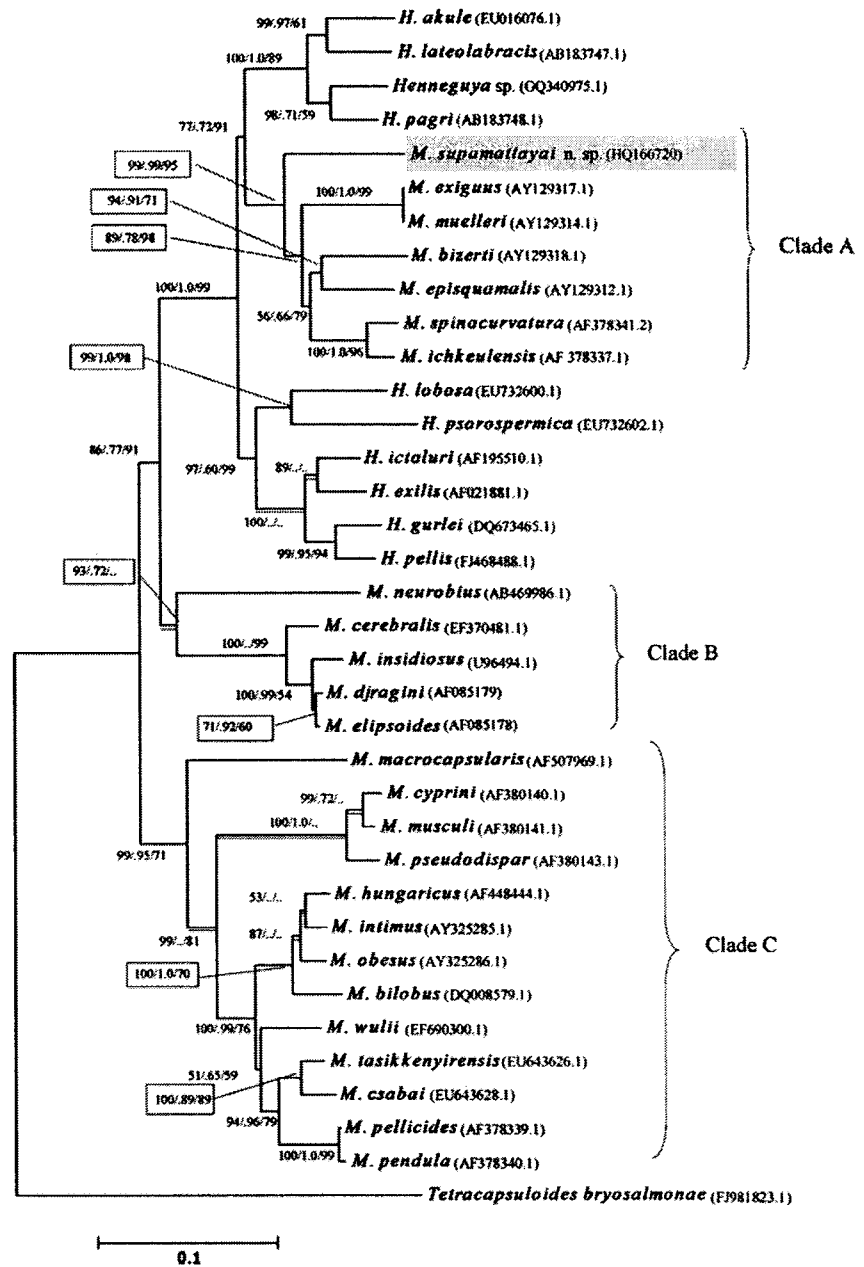
host fish. Although few studies on host specificity are reported, recent data indicated that most species are strictly host specific or only capable of developing in closely related fish host (Tajdari et al. 2005). According to previously described species, 15 species belonging to the *Myxobolus* genus have been demonstrated to infect mullet (Bahri and Marques 1996). *Myxobolus* species infecting mullet have been reported on various geological regions including the west coast of Tunisia, Mediterranean coast, in the Atlantic at Ria de Aveiro in northern Portugal, South Florida coast, Australia, and the Japanese coast (Maeno et al. 1990; Rothwell et al. 1997; Diamanka et al. 2008; Umur et al. 2010). All characteristics of this new species were also compared to confirm morphological similarities to the spores of different species of the genus *Myxobolus* described previously (see Table 1). Two species, *M. episquamalis* and *M. exiguus*, occurring on the host scales, which are the parasites infecting the epithelial tissue over the scales of species, are similar to that of *M. supamattayai* n. sp. However, *M. episquamalis* differ from our newfound species because of the less elongated shape of the spore and polar capsule, smaller overall dimensions, and the type and

Table 1 Comparison of spore characteristics between *Myxobolus* species infecting mullet (the mean and standard deviation or range of spore is provided, ND = no data)

Species	Host	Localization	Spore		Polar capsule		Polar filament	
			Length (μm)	Width (μm)	Length (μm)	Width (μm)	Length (μm)	Number of coils
M. bizerti (Bahri and Marques 1996)	*M. cephalus*	Gill filaments	14.25±0.22	14.25±0.22	6.5±0.54	5.75±0.27	45–50	6–7
M. episquamalis (Egusa et al. 1990)	*M. cephalus*	Scales	7.5–9.5 8.5±0.51	6–7.5 6.5±0.51	3.8–5 4±0.42	2–3 2±0.15	25–44	5–6
M. exiguus (Pulsford and Matthews 1982; Buhri et al. 2003)	*L. ramada*	Intestine	9.5±0.51	7.5±0.51	3.5±0.13	2.25±0.26	22–30	ND
		Scales	9.0	7.5	ND	ND	35	4–5
M. ichkeulensis (Bahri and Marques 1996)	*M. cephalus*	Gill arches	13.5±0.54	12.5±0.54	5.5±0.54	4.25±0.27	45–63	7–8
M. muelleri (Buhri et al. 2003)	*L. ramada*	Mesenteric vessels	10.5±0.51	8.5±0.51	4.5±0.31	2.5±0.21	22–40	6–7
M. spinacurvatura (Maeno et al. 1990)	*M. cephalus*	Mesentery Brain	10.5–12.5	9–11	3.5–5	2.5–3.5	22–43	4–5
		Gill filaments	12±0.63	10±0.57	4.75±0.67	2.75±0.59		
M. parvus (Buhri et al. 2003)	*M. cephalus*	Gill lamellae	6.6–7	5.5–6	4–4.2	3.8–4.2	ND	ND
M. cheni (Buhri et al. 2003)	*M. cephalus*	Muscles Fins	8–8.5	6–6.5	4.5–5	2	ND	ND
M. mugcephalus (Lansberg and Lom 1991)	*M. cephalus*	Gill filaments	4.8	5.2	ND	ND	ND	ND
M. rohdei (Lom and Dyková 1994)	*M. cephalus*	Kidney	9.8–11.6	8.4–9.1	3.7–5	2.5–3.1	ND	ND
M. platanus (Eiras et al. 2007)	*M. platanus*	Spleen	10.7 (10–11)	10.8 (10–11)	7.7 (7–8)	3.8 (3.5–4)	ND	5–6
M. goensis (Eiras and D'Souza 2004)	*M. cephalus*	Gill	9.7 (9.5–10.5)	6.6 (6–7.5)	5.3 (4.5–6) 2.4 (2–3)	2.4 (2–3) 1.8 (1.5–2)	ND	5 3
M. branchialis (Bahri and Marques 1996)	*M. cephalus*	Gill filaments	7.6–8	6.8–8.5	4.4–4.8	2.5–4.1	ND	ND
M. achmerovi (Bahri and Marques 1996)	*M. cephalus*	Mesentery	12–14	9–10	ND	2.3–3.5	ND	ND
M. cephalus (Bahri and Marques 1996)	*M. cephalus*	Gill arches	14–15	10–11	4–5	3–4	ND	ND
M. supamattayai n. sp. Present work	*V. seheli*	Scales	6.2–7.0 6.6±0.32	6.2–6.7 6.5±0.21	3.4–3.6 3.5±0.13	1.9–2.2 2.0±0.09	12–15	4–5

color of the plasmodia. Conversely, *M. exiguus* has a bigger spore size and longer polar filament length than those of *M. supamattayai* n. sp. Although spore shape of *Myxobolus parvus* (Bahri and Marques 1996) showed higher similarity to the spore of *M. supamattayai* n. sp., the first one has a bigger polar capsule. *M. bizerti* and *M. ichkeulensis* have the larger spore and polar capsule, more polar filament coils in the polar capsule, and longer polar filament length indeed than those observed from *M. supamattayai* n. sp. The shape of spore and polar capsule of *M. spinacurvatura* is larger than that found in *M. supamattayai* n. sp. even if it also occurs in the epithelial tissue over the scale (Lom and Dyková 1994). The ellipsoidal spores of *Myxobolus branchialis* have a longer space and in overall dimensions besides the polar capsule are bigger. *Myxobolus cheni* occurs in muscles and fins; in addition, the shape of the

spores is larger and more ellipsoid. *Myxobolus achmarovi*, *Myxobolus cephalus*, and *Myxobolus rohdei* occur in the mesentery, gill filament, and kidney, respectively, and all these species have a larger spore and polar capsule than those of *M. supamattayai* n. sp. The morphological data of spores of *Myxobolus mugcephalus* parasitizing in gill arches was insufficient for comparison; however, it can be discriminated from *M. supamattayai* n. sp. by its smaller and more round board spore shape. *M. muelleri*, a high variable morphology detailed parasite, can be separated from *M. supamattayai* n. sp. by a number of considerable features. Spores seem much more oval than those of *M. supamattayai* n. sp., and a bigger polar capsule and six to eight coil turns to the polar filament in *M. muelleri* distinguish it from our species, which contains only four to five coils.

Moreover, the ultrastructural morphology of the spores described in the present study also confirms that this parasite belongs to the genus *Myxobolus* Bütschli, 1882 according to previous studies and is the key for the determination of myxosporean genera (Lom and Dyková 2006). The ultrastructural data of mature spore of *Myxobolus* species infecting mullet remains scarce. However, fine structure of *M. exiguus* and *M. episquamalis* infecting the scales of grey mullet and flathead mullet has been described (Pulsford and Matthews 1982; Bahri and Marques 1996). *M. supamattayai* n. sp. is fundamentally similar to both *Myxobolus* species mentioned above which infected mullet and is similar throughout other myxosporeans, although there is a minor difference observed in size and structure. The presented mature spores and polar capsule were plugged with a stopper, which was covered by a cap-like structure at its apical end. These characters were similar to those recorded for the genus *Myxobolus* (Ali et al. 2007) and also from other myxosporean genera such as *Sphaerospora* (Supamattaya et al. 1991) and *Zschokkella* (Lom and Dyková 1996). The sporoplasm cell of genus *Myxobolus* is commonly characterized by a single binucleated sporoplasm (Pulsford and Matthews 1982; Bahri and Marques 1996). In contrast, this presented species showed only one nucleus in the mature spore of sporoplasm cell. However, uninucleated sporoplasm has been reported in some *Myxobolus* species such as *Myxobolus stomum* (Ali et al. 2003). Dense spherical inclusions and sporoplasmosomes were identified in the sporoplasm of the present species, which seem to be the common features of *Myxobolus* species and other myxosporeans (Abdel-Ghaffar et al. 2008).

Phylogenetic tree analysis by SSU rDNA approach

Species of the genus *Myxobolus* have been found in several clades over a broad analysis of the Myxozoa (Kent et al. 2001). Modern phylogenetic analysis classifications of myxosporeans have been described into two major clades: freshwater and marine species (Fiala 2006). SSU rDNA is widely used for studying phylogenetic relationships among taxa (Avise 2004). Moreover, it is the only molecular marker available for the broad range of *Myxobolus* species at present. Therefore, SSU rDNA sequences have been used as the main information source for reconstruction of *Myxobolus* evolutionary history. Obtained discrepancies between SSU rDNA gene phylogeny and taxonomy, based on the morphological data, may suggest that the molecular phylogeny is not congruent with the true phylogeny or may indicate that the characters of spore morphology are homoplasious. Consequently, molecular data of other genes, for instance, large subunit ribosomal DNA (LSU rDNA) or intergenic transcribed spacer (ITS), is required to

confirm the myxosporean rDNA phylogeny (Fiala 2006). However, phylogenetic analyses of SSU rDNA suggest that pore morphology is of minor importance in phylogenetic relationships of myxosporean clades (Andree et al. 1999; Canning and Okamura 2004; Eszterbauer 2004; Holzer et al. 2004). Since different spore morphologies occur in the same clade even when there is another similar species in the other clade due to convergence, it seems that *Myxobolus* evolution may not depend on the change of spore shape. Moreover, separation of the minor clade of marine *Myxobolus* spp., infecting mullet, from other *Myxobolus* species in the *Myxobolus* clade was established in the present study.

Our comparative molecular genetic analysis included sequences from 36 species of expanded myxosporeans to the extent of SSU rDNA sequence availability. The intention of this analysis was to verify the differentiation of *M. supamattayai* n. sp., first from infected blue spot mullet *Myxobolus* species followed by the possibility in its closest relatives. Phylogenetic analyses formed one large clade that includes one of the out-group species, *Tetracapsuloides bryosalmonae*. This large clade was further divided into more sub-clades, one of which represented all of the mullet-infecting *Myxobolus* species, as marine myxozoa, including *M. episquamalis*, *M. muelleri*, *M. spinacurvatura*, *M. ichkeulensis*, *M. bizerti*, *M. exiguus*, and *M. supamattayai* n. sp.

In summary, *M. supamattayai* n. sp. does not correlate with any other *Myxobolus* spp. previously reported to infect mullet or another species among the genus *Myxobolus*. It tends to be differentiated from all known species of *Myxobolus* spp. by the presence of morphology, ultrastructure, and phylogenetic analysis.

References

Abdel-Ghaffar F, El-Toukhy A, Al-Quraishy S, Al-Rasheid K, Abdel-Baki AS, Hegazy A, Bashter AR (2008) Five new myxosporean species (Myxozoa: Myxosporea) infecting the Nile tilapia *Oreochromis niloticus* in Bahr Shebin, Nile Tributary, Nile Delta, Egypt. Parasitol Res 103:1197–1205

Ali MA, Abdel-Baki AS, Sakran T, Entzeroth Abdel-Ghaffae F (2003) Light and electron microscopic studies of *Myxobolus stomum* n. sp. (Myxosporea: Myxosporea) infecting freshwater fishes of the River Nile, Egypt. Parasitol Res 88:9–15

Ali MA, Abdel-Baki AS, Sahran TH, Entzeroth R, Abdel-Ghaffae F (2007) *Myxobolus lubati* n. sp. (Myxosporea: Myxobolodae), a new parasite of Haffara seabream *Rhabdosargus haffara* (Forsskal, 1775), Red Sea, Egypt: a light and transmission electron microscopy. Parasitol Res 100:819–827

Altschul SF, Gish W, Miller W, Myers EW, Lipman DJ (1990) Basic local alignment search tools. J Mol Biol 215:403–410

Andree KB, MacConnell E, Hedrick RP (1998) A nested polymerase chain reaction for the detection of genomic DNA of *Myxobolus cerebralis* in rainbow trout *Oncorhynchus mykiss*. Dis Aquat Organ 34:145–154

Andree KB, Szekely C, Molnár K, Gresoviac SJ, Hedrick RP (1999) Relationships among members of the genus *Myxobolus* (Myxozoa: Bilvalvulidae) based on small subunit ribosomal DNA sequences. J Parasitol 85:68–74

Avise JC (2004) Molecular marker, natural history, and evolution. Sinauer, Sunderland

Bahri S, Marques A (1996) Myxosporean parasites of the genus *Myxobolus* from *Mugil cephalus* in Ichkeul lagoon, Tunisia: description of two new species. Dis Aquat Organ 27:115–122

Buhri S, Andree KB, Hedrick RP (2003) Morphological and phylogenetic studies of marine *Myxobolus* spp. from mullet in Ichkeul Lake, Tunisia. J Eukaryot Microbiol 50:463–470

Canning EU, Okamura B (2004) Biodiversity and evolution of the Myxozoa. Adv Parasitol 56:44–131

Diamanka A, Fall M, Diebakate C, Faye N, Toguebaye BS (2008) Identification of *Myxobolus episquamalis* (Myxozoa, Myxobolidae) in flathead mullet *Mugill cephalus* (Pisces, Teleostei, Mugilidae) from the coast of Senegal (eastern tropical Atlantic Ocean). Acta Adriat 49:19–23

Dyková I, Fiala I, Nie P (2002) *Myxobolus lentisuturalis* sp. n. (Myxozoa: Myxobolidae), a new muscle-infecting species of the Prussian carp, *Carassius gibelio* from China. Folia Parasitol 49:253–258

Egusa S, Maeno Y, Sorimach M (1990) A new species of Myxozoa, *Myxobolus episquamalis* sp. n. infecting the scales of the mullet, *Mugil cephalus* L. Fish Pathol 25:87–91

Eiras JC, D'Souza J (2004) *Myxobolus goensis* n. sp. (Myxozoa, Myxosporea, Myxobolidae), a parasite of the gills of *Mugil cephalus* (Osteichthyes, Mugilidae) from Goa. India Parasite 11:243–248

Eiras JC, Molnár K, Lu YS (2005) Synopsis of the species of *Myxobolus* Butschli, 1882 (Myxozoa: Myxosporea: Myxobolidae). Syst Parasitol 61:1–46

Eiras JC, Abreu PC, Robaldo R, Júnior J (2007) *Myxobolus platanus* n. sp. (Myxosporea, Myxobolidae), a parasites of *Mugil planus* Günther, 1880 (Osteichthyes, Mugilidae) form Lagoa dos Patos, RS, Brazil. Arq Bras Med Vet Zootec 59:895–898

Eszterbauer E (2004) Genetic relationships among gill-infecting *Myxobolus* species (Myxosporea) of cyprinids: molecular evidence of importance of tissue specificity. Dis Aquat Org 58:35–40

Fiala I (2006) The phylogeny of Myxosporea (Myxozoa) based on small subunit ribosomal RNA gene analysis. Int J Parasitol 36:1521–1534

Gascuel O (1997) BIONJ: an improved version of the NJ algorithm based on a simple model of sequence data. Mol Biol Evol 14:685–695

Gouy M, Guindon S, Gascuel O (2010) SeaView version 4: a multiplatform graphical user interface for sequence alignment and phylogenetic tree building. Mol Biol Evol 27:221–224

Hall TA (1999) BioEdit: a user-friendly biological sequence alignment editor and analysis program for Windows 95/98/NT. Nucleic Acids Symp Ser 41:95–98

Holzer AS, Sommerville C, Wootten R (2004) Molecular relationships and phylogeny in a community of myxosporeans based on their 18S rDNA sequence. Int J Parasitol 34:1099–1111

Kent ML, Andree KB, Bartholomew JB, El-Matbouli M, Desser SS, Devlin RH, Feist SW, Hedrick RP, Hoffman RW, Khattra J, Hallett SL, Lester JG, Longshaw M, Palenzuela O, Siddall ME, Xiao C (2001) Recent advances in our knowledge of the Myxozoa. J Eukaryot Microbiol 48:395–413

Kimura M (1983) The neutral theory of molecular evolution. Cambridge University Press, Cambridge

Kumar S, Tamura K, Nei M (1993) MEGA: molecular evolutionary genetics analysis. Pennsylvania State University Press, University Park

Lansberg JH, Lom J (1991) Taxonomy of the genera of the *Myxobolus/Myxosoma* group (Myxobolidae: Myxosporea), current listing of species and revision of synonyms. Syst Parasitol 18:165–186

Liu Y, Gu ZM, Luo LY (2010) Some additional data to the occurrence, morphology and validity of *Myxobolus turpisrotundus* Zhang, 2009 (Myxozoa: Myxosporea). Parasitol Res 107:67–73

Lom J, Arthur JR (1989) A guideline for the preparation of species descriptions in Myxosporea. J Fish Dis 12:151–156

Lom J, Dyková I (1994) Studies on protozoan parasites of Australian fishes III. Species of genus *Myxobolus* Bütschli, 1882. Eur J Protistol 30:431–439

Lom J, Dyková I (1996) Notes on the ultrastructure of two myxosporean (Myxozoa) species, *Zschokkella pleomorpha* and *Ortholinea fluviatilis*. Folia Parasitol 43:189–202

Lom J, Dyková I (2006) Myxozoan genera: definition and notes on taxonomy, life-cycle terminology and pathologenic species. Folia Parasitol 53:1–36

Maeno Y, Sorimach M, Ogawa K, Egusa S (1990) *Myxobolus spinacarvatura* n. sp. (Myxosporea: Bivalvulida) parasitic in deformed mullet, *Mugil cephalus*. Fish Pathol 25:37–41

Molnár K, Székely C, Hallett SL, Atkinson SD (2009) Some remarks on the occurrence, host-specificity and validity of *Myxobolus rotundus* Nemeczek, 1911 (Myxozoa: Myxosporea). Syst Parasitol 72:71–79

Nei M, Gojobori T (2000) Molecular evolution and phylogenetics. Oxford University Press, New York

Posada D (2008) jModelTest: phylogenetic model averaging. Mol Biol Evol 25:1253–1256

Pulsford A, Matthews RA (1982) An ultrastructure study of *Myxobolus exiguous* Thelohan, 1895 (Myxosporea) from grey mullet, *Creninguil labrosus* (Risso). J Fish Dis 5:509–526

Rothwell JT, Virgonia JL, Callinan RB, Nicholls PJ, Langdon JS (1997) Occurrence of cutaneous infections of *Myxobolus episquamalis* (Myxozoa: Myxobolidae) in sea mullet, *Mugill cephalus* L, in Australia. Aust Vet J 75:349–352

Salim KY, Desser SS (2000) Description and phylogenetic systematics of *Myxobolus* spp. from cyprinids in Algonquin Park, Ontario. J Eukaryot Microbiol 47:309–318

Supamattaya K, Fischer-Scherl T, Hoffmann RW, Boonyaratpalin S (1991) *Sphaerospora epinepheli* n. sp. (Myxosporea: Sphaerosporidae) observed in grouper (*Epinephelus malabaricus*). J Eukaryot Microbiol 5:448–454

Székely C, Hallett SL, Atkinson SD, Molnár K (2009) Complete life cycle of *Myxobolus rotundus* (Myxosporea: Myxobolidae), a gill myxozoan of common bream *Abramis brama*. Dis Aquat Organ 85:147–155

Tajdari J, Matos E, Mendonça I, Azevedo C (2005) Ultrastructural morphology of *Myxobolus testicularis* sp. n., parasite of the testis of *Hemiodopsis microlepis* (Teleostei: Hemiodontidae) from the NE of Brazil. Acta Protozool 44:377–384

Thompson JD, Higgins DG, Gibson TJ (1994) ClustalW: improving the sensitivity of progressive multiple sequence alignment through sequence weighting, position-specific gap penalties and weight matrix choice. Nucleic Acids Res 22:4673–4680

Umur Ş, Pekmezci GZ, Beyhan YE, Gürler AT, Açici M (2010) First record of *Myxobolus muelleri* (Myxosporea: Myxobolidae) in flathead grey mullet *Mugil cephalus* (Teleistei, Mugilidae) from Turkey. Ankara Üniv Vet Fak Derg 57:205–207

Zhang JY, Wang JG, Li AH, Gong XN (2010) Infection of *Myxobolus turpisrotundus* sp. n. in allogynogenetic gibel carp, *Carassius auratus gibelio* (Bloch), with revision of *Myxobolus rotundus* (s. l.) Nemeczek reported *from C. auratus auratus* (L.). J Fish Dis 33:625–638
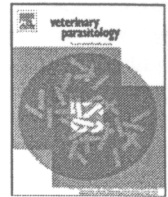
A new host record of *Sphaerospora epinepheli* (Myxosporea: Bivalvulida) occurring on orange-spotted grouper *Epinephelus coioides* from Thailand: Epidemiology, histopathology and phylogenetic position

Kittichon U-taynapun [a], Nion Chirapongsatonkul [b], Phudit Maneesaay [c], Toshiaki Itami [d], Chutima Tantikitti [a,*]

[a] *Aquatic Animal Health Research Center, Department of Aquatic Science, Faculty of Natural Resources, Prince of Songkla University, Thailand*
[b] *Department of Biochemistry, Faculty of Science, Prince of Songkla University, Thailand*
[c] *Department of Pathology, Faculty of Veterinary Medicine, Kasetsart University, Thailand*
[d] *Department of Marine Biology and Environmental Sciences, Faculty of Agriculture, University of Miyazaki, Japan*

ARTICLE INFO

ABSTRACT

In 1991, the first record of *Sphaerospora epinepheli* was described as a kidney parasite of wild and cultured malabar grouper, *Epinephelus malabaricus*, along coastlines of Thailand, the Gulf of Thailand and the Andaman Sea. However, the present study detected high infection of this parasite in kidney renal tubes of orange spotted grouper, *Epinephelus coioides*, collected from Andaman Sea. The highest infection rate of 36.82% was observed during the rainy season in 2009 in Phang-Nga Bay, in the north of Andaman Sea, which is an important grouper production site in Thailand. The biological and histopathological data of the parasite in this new host record are presented. Species classification is described based on morphological data of mature spore and molecular analysis of myxosporean 18S rDNA phylogeny including that of *S. epinepheli* which infected *E. malabaricus*. The genetic position of this parasite found in two host species was also studied. The phylogenetic tree analysis of small-subunit rDNA sequences of *S. epinepheli* from both infected hosts was constructed using two algorithms, maximum likelihood (ML) and Bayesian inference (BI). They were placed in the clustered basal sphaerosporid clade that contain four long SSU rDNA sphaerosporid species including *Sphaerospora truttae*, *Sphaerospora elegans*, *Sphaerospora ranae*, *Sphaerospora fugu* and *Bipteria formosa* with strong bootstrap supports. Histopathologically, renal intratubular myxosporean spores were associated with tubulonephosis, tubular necrosis, chronic interstitial nephritis and mimic membranoproliferative glomerulonephritis. This myxosporean parasite appears to be a significant pathogen on the basis of pathological changes in the renal tubules and is highly distributed in orange-spotted grouper.

© 2012 Elsevier B.V. All rights reserved.

1. Introduction

Myxosporean species play a significant pathogenic role as parasites of wild and cultured teleost fish in both marine and freshwater habitats with over 2180 described species (Liu et al., 2010). Additionally, there have been numerous reports of myxosporeans in elasmobranchs, amphibians, reptiles and mammals including humans with immunodeficiency (Moncada et al., 2001; Longshaw et al., 2005). Among them, the genus *Sphearospora* Thélohan, 1892 with 78 described species is found to distribute in different freshwater and marine clades (Lom and Dyková, 2006).

* Corresponding author. Tel.: +66 74465102; fax: +66 74465102.
  E-mail address: chutima.t@psu.ac.th (C. Tantikitti).

2   K. U-taynapun et al. / Veterinary Parasitology xxx (2012) xxx–xxx

Many species belonging to this genus are pathogenic as coelozoic parasites in the urinary system and are usually highly specific to certain hosts. Some species are serious disease agents in cultured economic fish; for example, *S. dicentrarchi* and *S. testicularis* represent important parasites of wild and cultured European seabass, *Dicentrarchus labrax* in the western Mediterranean basin (Fioravanti et al., 2004). However, only one species, *Sphaerospora epinepheli* has been reported to infect brackish and marine fish in South East Asia. It is a renal parasite of wild and cultured malabar grouper, *Epinephelus malabaricus*, in Thailand (Supamattaya et al., 1990).

Grouper species, which inhabit subtropical and tropical areas, have become an economically important marine teleost and are currently been cultured in ASEAN countries (Harikrishnan et al., 2010). In Thailand, grouper productions have been from an artisanal fishery (wild capture) and semi-intensive net-cage culture. Among more than 150 species of grouper, orange-spotted grouper *Epinephelus coioides*, malabar grouper *E. malabaricus*, brown marbled grouper *Epinephelus fuscoguttatus*, duskytail grouper *Epinephelus bleekeri* and six-banded grouper *Epinephelus stictus* are the main production of Thailand. *E. coioides* is the main species in net-cage aquaculture. In the last few years, the phenomenon of spherosporosis has increased significantly in grouper net-cages culture.

Although advanced techniques have been applied in the last few decades to study phylogeny and taxonomy, the complete life cycle of many *Sphearospora* species remains unclear (Bermúdez et al., 2010), particularly those in marine or brackish water habitat. Therefore, efficacious treatments, prevention and control of myxosporean infection is particularly difficult and lacking (Yokoyama et al., 1990). The geographic distribution, host specificity and parasitic indication of *S. epinepheli* in economic grouper species in Thailand is one of the cases that are rarely reported.

The aims of this present work were to conduct a parasitological survey and elucidate the classification of *S. epinepheli* in a new host record, *E. coioides* inferring from both morphological and phylogenetic analysis. Furthermore, the histopathological damages of infected kidney were also demonstrated. The rediscovery of a renal sphaerosporesis in orange-spotted grouper as a new host record from Thailand was provided by the description of its sporogonic morphology and phylogenetic analysis inferred from the small subunit ribosomal DNA evidently *S. epinepheli*.

2. Materials and methods

2.1. Fish sample

Between 2007 and 2009, orange-spotted grouper, *E. coioides*, and other four species of economic grouper including *E. malabaricus*, *E. fuscoguttatus*, *E. stictus*, and *E. bleekeri* from Thailand were investigated for parasitic *S. epinepheli* infection. In Thailand, only orange-spotted and malabar grouper are the only cultured species in which farmers collect juvenile fish (50–200 g) from the wild and transfer

them to net-cage culture for 1–2 years to obtain marketable size of 1–3 kg.

Fish samples ranging in weight from 200 to 1200 g were obtained from wild and cultured farms covering the main production areas. The sampling locations included northern Andaman Sea (Phang-Nga Bay; 5 sampling sites) and southern Andaman Sea (Satun province; 4 sampling sites) as shown in Fig. 1. Fish samples were collected separately in dry season (February–May) and rainy season (August–November). Live fish were collected from marine cage culture or purchased from fishermen while moribund fish were first killed, then transported alive and on dry ice, respectively, to the Aquatic Animal Health Research Center (AAHRC), Prince of Songkla University. Standard procedures were used for the examination of myxosporean in internal and external organs, especially the kidney, since it has been reported as a specific organ of this parasite (Supamattaya et al., 1990). Fresh samples were subsequently used for the morphological and histopathological examination and some infected kidney tissues were collected in cryotube™ (Nunc, Denmark) and stored in liquid nitrogen for the molecular study.

2.2. Parasite identification and histopathology

Morphology of fresh myxosporean spore was studied under Olympus AX 70 microscope and photographed using Olympus DP 71 cool CCD camera with differential interference contrast (DIC) optics. The vitality of the mature spore was checked by mixing spores with 0.4% (v/v) urea (Molnár et al., 2009). Descriptions and measurements of spores were performed following the guideline of Lom and Dyková (2006). Spore measurements were done based on the total of spores which obtained from 5 fish (30 spores/fish). For histology study, the infected tissues were fixed in 10% (v/v) formalin for 3 days, dehydrated in graded alcohol and embedded using routine procedures. Three-five μm sections were stained with hematoxylin and eosin (H&E), toluidine blue (TB) and periodic acid-Schiff (PAS).

2.3. Molecular analysis procedures

Frozen infected kidneys of 3–5 g were thawed and then homogenized in Hank's balanced salt solution (HBSS; Gibco, US) using a sterile plastic Eppendorf pestle. The resultant slurry was collected and centrifuged at $2000 \times g$ for 15 min at 4 °C. The pellets were resuspended in 1 ml of HBSS and the suspension transferred into 15 ml polypropylene centrifuge tubes containing discontinuous gradients of Percoll™ (2.5 ml layers of 20% and 40% (v/v) Percoll™ in phosphate buffered saline, PBS pH 7.4; Sigma, US). The tubes were centrifuged at $2000 \times g$ for 30 min at 4 °C. The resulting pellets of *S. epinepheli* were washed to remove the trace Percoll™ by two repetition of resuspending in 2 ml HBSS followed by centrifugation at $5000 \times g$ for 10 min at 4 °C.

Pretreatment of proteinase K was applied (U-taynapun et al., 2011) and DNA was then extracted using DNeasy Tissue Kit (Qiagen, CA) according to the manufacturer's instructions. The primer pairs 18e (5′-CTGGTTGATTCTGCCAGT-3′) and 18g
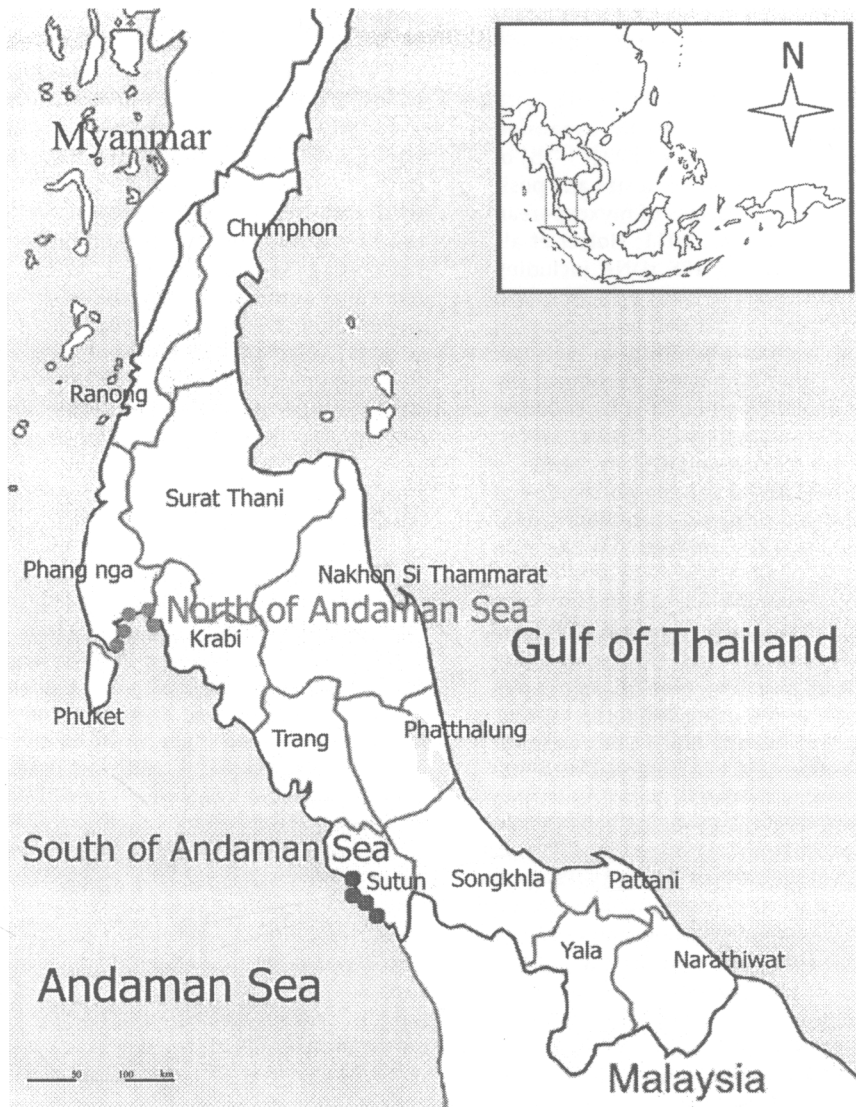
Fig. 1. Sampling locations of *S. epinepheli* infected grouper in the Andaman Sea, Thailand.

(5′-CGGTACTAGCGACGGGCGGTGTG-3′) (Hillis and Dixon, 1991) were used to amplify the 18S rDNA gene of the parasite. The PCR product was isolated from the gel using QIAquick Gel Extraction kit (Qiagen, CA) and cloned into pGEM®-T Easy Vector (Promega, US) following the manufacturer's instructions. The plasmids containing insert, purified from single clones of the 6 individual samples by spin columns (QIAGEN® Plasmid Purification, Qiagen, CA) were sequenced on automatic sequencer CEQ™ 8000 (Beckman Coulter) using CEQ DTCS Dye kit (Beckman Coulter). Primers for sequencing included the specific promoter primers of pGEM®-T Easy (T7 and Sp6) and the internal primer intF1 5′-GCCCCATCAATT AGTTGGTT-3′, intF2 5′-TACCTCGGTATGGGGTTCAC-3′, intR1 5′-CAGTTAT CAAGACGACCAAA-3′ and intR2 5′-GATCTTTAGCCGGTCTTAGA-3′. Cloning sequence traces were checked for quality and assembled manually using BioEdit 7.0.5.3 (Hall, 1999) and Genetyx (Genetyx, JP). The

obtained sequence was submitted to the National Center for Biotechnology Information (NCBI) GenBank database (http://www.ncbi.nlm.nih.gov/).

2.4. Phylogenetic analysis

In order to demonstrate the position of *S. epinepheli* with specific common structure in the phylogram and to obtain homologous sequences, a partial part of 18S rDNA of *S. epinepheli* from both hosts, *E. coioides* and *E. malabaricus*, was compared to those sequences of other myxosporean species available in the GenBank using nucleotide BLAST protocol. Malacosporeana species *Tetracapsuloides bryosalmonae* and *Buddenbrockia plumatellae*, representing a lineage phylogenetically close to myxosporean, were set as outgroups in our analysis. The basal sphaerosporid species sequences were aligned using the ClustalW algorithm in BioEdit (Hall, 1999). The result of

primary alignment was edited following the secondary structure criterion of long myxosporean 18S rDNA and V4 insertion region of *Sphaerospora truttae* (Holzer et al., 2007). The structures which could be homologized with certainty were analyzed. The group specific expansion segment in V4 region (V4 E23_1–7 and V4 E23_13–15) of basal sphaerosporid species which varied in size and position (Holzer et al., 2007) from all species of myxosporean taxa were excluded (Bartošová et al., 2011; Holzer et al., 2010). The resulting alignments of 18S rDNA including modified V4 sequences of species in basal sphaerosporid clade and related available myxosporean sequences were aligned with the Muscle algorithm in Seaview 4.2.5 (Gouy et al., 2010). Other ambiguous regions of the alignment output were classified and edited by choosing the guideline from default parameters of Gblocks server, http://molevol.cmima.csic.es/castresana/Gblocks.html (Castresana, 2000). We performed genetic positioning of *S. epinepheli* in the phylogram using two confidence algorithms, maximum likelihood (ML) analysis and Bayesian inference (BI).

ML phylogram was examined via PhyML v 3.0.1 (Guindon and Gascuel, 2003) which combines the nearest neighbor interchanges (NNI) and subtree pruning and regrafting (SPR) algorithms. The best-fit parameters model (GTR+I+Γ) were selected using jModelTest v.0.1.1 (Posada, 2008). Ten random starting BioNJ trees were set for the analysis. Nodes robustness was assessed with 500 bootstrap replicates. BI analyses were constructed using MrBayes v. 3.0b4 (Ronquist and Huelsenbeck, 2003). Clade support was estimated utilizing a Markov chain Monte Carlo (MCMC) algorithm. Parameters in MrBayes were set to 1,000,000 generations and 10,000 trees sampled (sampled every 100th generation), corresponding to the model estimated (GTR+I+Γ) DNA substitution (nst=6; rates=invgamma; ncat=4) and the default random tree option to begin the analysis. Log-likelihood scores were plotted and only the final 25% of generations were discarded as burn-in. The 50% majority rule consensus tree was computed from trees showing likelihoods of stations. The differences among individual bootstraps or posterior probabilities from BI computation affecting the influential phylogram were presented in tree-based drawing of ML analysis.

2.5. Statistical analysis

Statistical analyses of parasite distribution were performed using SPSS 17 for Windows (SPSS Inc., Chicago). All data were calculated into percentages before further analysis. Differences between the presence of the *S. epinepheli* in host fish from the same location were determined by an independent sample *t*-test statistical analysis. The occurrences of infected new recorded host in the same location according to season were analyzed with one-way ANOVA followed by Tukey's HSD multiple comparison test. Statistical significance was taken at $P < 0.05$. All results are expressed as mean ± S.D.

3. Results

The seasonal survey of *S. epinepheli*, a fish kidney myxosporean parasite, was demonstrated in five important economic grouper species of Thailand from the main grouper production areas of Andaman Sea during 2007–2009. We found that *E. coioides* is the new host record of this parasite. Moreover, the prevalence of infection in the new host was higher than that of the first recorded host *E. malabaricus* (Supamattaya et al., 1990). However, no evidence was authenticated for the infection of *S. epinepheli* in the other 3 grouper species, *E. stictus, E. fuscoguttatus* and *E. bleekeri*. The morphological analysis, seasonal distribution, histopathological changes and molecular phylogenetic analysis are circumspectly summarized for the new host record of this myxosporean species.

3.1. Morphological description and specific organ infection

Microscopically, mature spores and developmental stages of parasite were detected specifically in the kidney of infected fish hosts, *E. malabaricus* and *E. coioides*, whereas they could not be observed in other organs. The parasite was identified as a myxosporean belonging to the genus *Sphaerospora* (Lom and Dyková, 2006). The spore type found in the present study corresponded with *S. epinepheli* described by Supamattaya et al. (1991) as regards to the asymmetric morphology of the polar capsules with the polar filaments and details of spore characters. The detailed morphology of *S. epinepheli* from kidney of the new recorded host, *E. coioides* is presented for the first time. This finding was confirmed with data describing the spore from malabar grouper (Table 1). In addition, the sutural line was prominent and straight forming a notch at the apex and posterior end of the spore (Fig. 2). Spore characterizing parameters from the new host record matched with those of the parasite isolated from *E. malabaricus*, the first reported host (Supamattaya et al., 1991).

3.2. Seasonal distribution

The repeat occurrence of *S. epinepheli* species was found in malabar grouper from Andaman Sea as well as in the new *E. coioides* fish host. The overall parasite infection was higher in *E. coioides* (25.07%) than *E. malabaricus* (8.68%) during our research period (30 months). The parasite occurrence in the new host collected from wild and cultured fish of northern Andaman Sea was 34.60% and 32.12%, respectively, while the incidence decreased to 16.97% and 15.54% for the wild and cultured fish from the southern Andaman Sea (Table 2). Comparison of infection in *E. malabaricus* and *E. coioides* (Fig. 3) revealed that the north of the Andaman Sea is the only location exhibiting statistically significant differences in different seasons ($P < 0.05$). In the south of the Andaman Sea, the occurrence of this parasite was slightly higher in *E. coioides* than that detected in *E. malabaricus* in every sampling period and was significantly different in the rainy season 2008 ($P < 0.05$). The incidence of infection in *E. coioides* in the Andaman Sea was not related to the seasonal changes. However,

Table 1
Morphological comparison of S. epinepheli in two host record with original description.

Fresh spores characteristics	Host species		
	E. coioides (present work)	E. malabaricus (present work)	Reference data (Supamattaya et al., 1991)
Spores	Subspherical to spherical	Subspherical to spherical	Subspherical to spherical
Length[a]	8.8 ± 0.5	8.7 ± 0.5	8.7 ± 0.4
Width[a]	8.3 ± 0.5	8.3 ± 0.6	8.2 ± 0.5
Thickness[a]	13.4 ± 0.6	13.5 ± 0.4	13.4 ± 0.5
Polar capsules (Pc.)	Spherical	Spherical	Spherical
LPc[a]	3.6 ± 0.4	3.6 ± 0.4	3.7 ± 0.3
CPf[a]	6–7	6–7	6–7
LPf[a]	57.23 ± 5.2	56.71 ± 5.5	55.57 ± 4.6
Infected organ	Kidney tubules	Kidney tubules, glomerulus	Kidney tubules, glomerulus
Host	E. coioides	E. malabaricus	E. malabaricus

LPc, length of polar capsule; CPf, coils of the polar filament; Lpf, length of the polar filament.

[a] Number in μm.

Table 2
Occurrence of S. epinepheli in economic grouper species from two locations of the Andaman Sea.

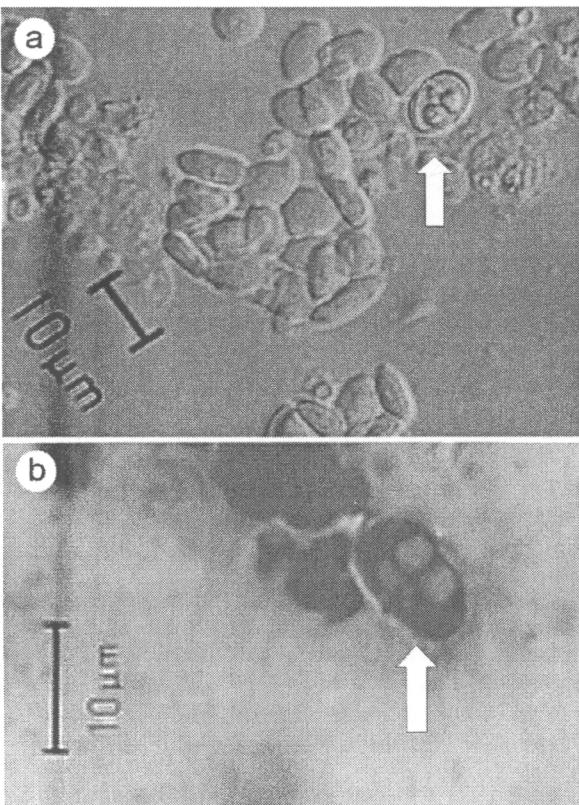|	E. malabaricus		E. coioides		E. fmcoguttatm		E. stictus		E. bleekeri	
	Wild	Cultured	Wild	Cultured	Wild	Cultured	Wild	Cultured	Wild	Cultured
North Andaman Sea	16/205 (7.81%)	15/155 (9.67%)	73/211 (34.60%)	53/165 (32.12%)	0/292	ND	0/288	ND	0/276	ND
South Andaman Sea	21/339 (8.79%)	9/104 (8.65%)	28/165 (16.97%)	30/193 (15.54%)	0/148	ND	0/225	ND	0/47	ND
Total	61/703 (8.68%)		184/734 (25.07%)		0/440		0/513		0/423	

ND: not determine.

Fig. 2. Morphological micrograph of S. epinepheli in new host record, E. coioides. (a) Fresh mature spore (DIC photograph). (b) Spore in Giemsa staining.

the infection in rainy season of all observed locations was slightly higher than that in dry season although not statistically significant. By means of comparison across locations, the north and the south of the Andaman Sea revealed a significant difference of the percentage of hosts infected with S. epinepheli. The north of the Andaman Sea had a higher infection rate than other locations at all sampling times.
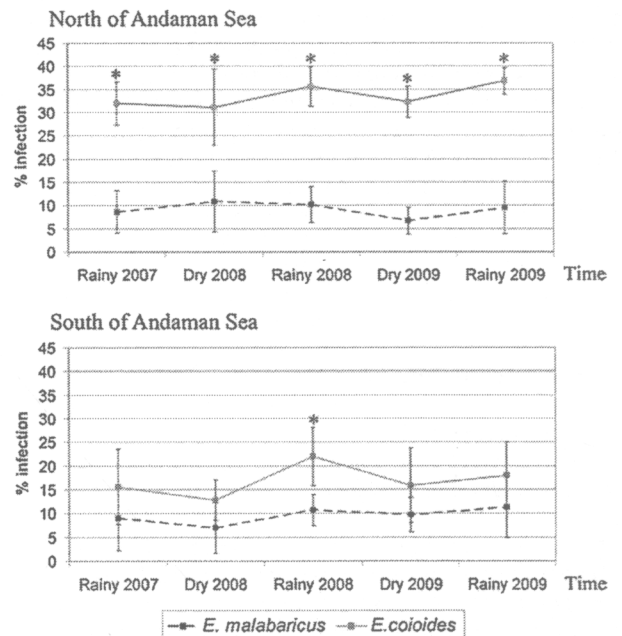
Fig. 3. Seasonal occurrence of S. epinepheli infected in two host record from the Andaman Sea. *Significantly different of infection in same period time.

The prevalence of isolated parasite was 31.81% (dry season, 2008) to 36.82% (rainy, 2009) in the northern Andaman Sea while the infection in the south of Andaman sea was between 12.78% and 22.01%.

3.3. Histopathology and host immune response

Orange-spotted groupers infected by *S. epinepheli* showed heavy infection and severe pathological damage of the kidney. Various stages of the parasite were observed in the renal tubules. Large amounts of pseudoplasmodia attached to the brush border of renal tubular epithelial cells while mature spores were predominantly found in the center of the tubular lumens. Many tubules filled with a large number of spores and pseudoplasmodia where the tubular epithelium became necrotic or underwent necrosis (Fig. 4a). The infected proximal tubules showed significant dilation (Fig. 4b). Moreover, they exhibited severe cytoplasmic vacuolation and pyknotic nuclei of low columnar epithelial cells. A high degree of cellular degeneration and necrosis were observed (Fig. 4c and d). In early stages, proximal tubule architecture could still be recognized and some small pseudoplasmodia appeared in the brush border. After parasitic accretions, the distal tubules were obstructed and vacuolation attaching to parasitic pseudoplasmodia was observed in epithelial cells. Finally, epithelial cell membrane, brush border and whole renal tubules were totally destroyed and disappeared. Only intact spores, cellular debris and surrounded mononuclear phagocytic cells were observed. Occasionally in heavy necrotic tissue, a few melanomacrophages were present especially in the interstitium. Therefore, degenerated appearances of renal tubules as a result of this parasite infection were variable from gradual tissue destruction to atrophy renal parenchyma in chronic stage (Fig. 4f). In the PAS staining, all infected proximal tubules with remaining parasites were commonly associated with mucus hypersecretion characterized by distinctively higher positive PAS staining on the brush border than in normal cells (Fig. 4e). Histopathologically, inflammatory responses of the fish host were only immunological cell infiltration and a few melanomacrophage centers. The common immunological host response to the myxosporean group such as melanization and eosinophilic granular cell (EGC1) were not evident in this study. The main inflammatory response was mononuclear phagocytic cells infiltrating throughout renal parenchyma which involved renal corpuscle and tubules. However, evidence of invasion or damage of tubular epithelium and the histopathological changes in the brush border were clearly observed as well as dilatation of infected tubules.

3.4. Molecular data and phylogenetic analysis

The nucleotide sequences of 18S rDNA of six *S. epinepheli* collected from each host, *E. malabaricus* and *E. coioides*, from two sampling locations were obtained and determined. The sequences revealed two distinct sequences of *S. epinepheli* type SEM (GenBank Accession Number: HQ871152) from *E. malabaricus* and type SEC (GenBank Accession Number: HQ871153) from *E. coioides*. Both

sequence types were submitted to GenBank and displayed a 99.9% homology of nucleotide sequence. The BLAST analysis of *S. epinepheli* with SSU rDNA myxosporean sequences available in GenBank revealed the highest homology to *Bipteria formasa* (GenBank Accession Number: FJ790309) which also showed 97% sequence identity with 70% of SSU rDNA of *S. epinepheli*. The preprimary alignment of SSU rDNA *S. epinepheli* sequence from both hosts with other member sequences of *Sphaerospora* sensu stricto showed two long independent inserts in the V4 region that represents numerous bases in V4 E23_1–7 and V4 E23_13–15 areas of the SSU rDNA differed from those of most myxosporeans.

The phylogenetic trees constructed using ML and BI revealed the same gross topology and showed that *S. epinepheli* is deeply embedded in the basal sphaerosporid clade (Fig. 5). Parametric bootstrapping (ML) and posterior probabilities (BI) of clusters of interest within these lineages and at the base of the tree are generally high. Some branches were swapped within clades; however, this did not significantly change the apparent evolutionary relationship. Both topology analyses demonstrated *S. epinepheli* in the monophyletic group which was composed of four *Sphaerospora* species and one *Bipteria* species (*Spherospora* sensu stricto). In the phylogram, the ML constructed tree was used as the base tree with the three major clusters including (1) the cluster of basal *Sphaerospora*, (2) predominantly freshwater taxa and (3) the predominantly marine species cluster, with high bootstrap value support. Our *S. epinepheli* of interest presented in the basal sphaerosporid subclade in which all contributing members inhabit the marine fish host. However this group was manifestly separated from marine myxosporean cluster by exhibiting common large expansion segment in variable region. To date, 13 species of *Sphaerospora* Thélohan, 1892 have been sequenced and their positions are in varied clades of the phylogram. In addition, phylogenetic analysis from both algorithms showed the predominance of *Sphearospora* spp., including *S. epinepheli* in the basal sphaerosporid clade, as a primitive cluster of myxosporea clade supported by high bootstrap values.

4. Discussion

The combination of morphology and molecular analysis, with an investigation of host range and tissue tropism, play important roles in the classification of complicated myxosporean species (U-taynapun et al., 2011). This study describes *E. coioides* as the new host record of *S. epinepheli* deduced from both morphological and molecular characters.

Morphological characters of our reported *S. epinepheli* from both fish hosts closely resemble those in the original description. The resemblance of fresh spores isolated from both hosts was corroborated. Moreover, the mature spores presented as a drawing line by Supamattaya et al. (1991) were definitely the same as our observations. The similar spore morphology and organ infection of the different hosts were found in *S. epinepheli* as well as presented in previous reports of *Sphaerospora ranae* in *Rana dalmatina* and *Rana temporaria* (Jirku et al., 2007). Eszterbauer
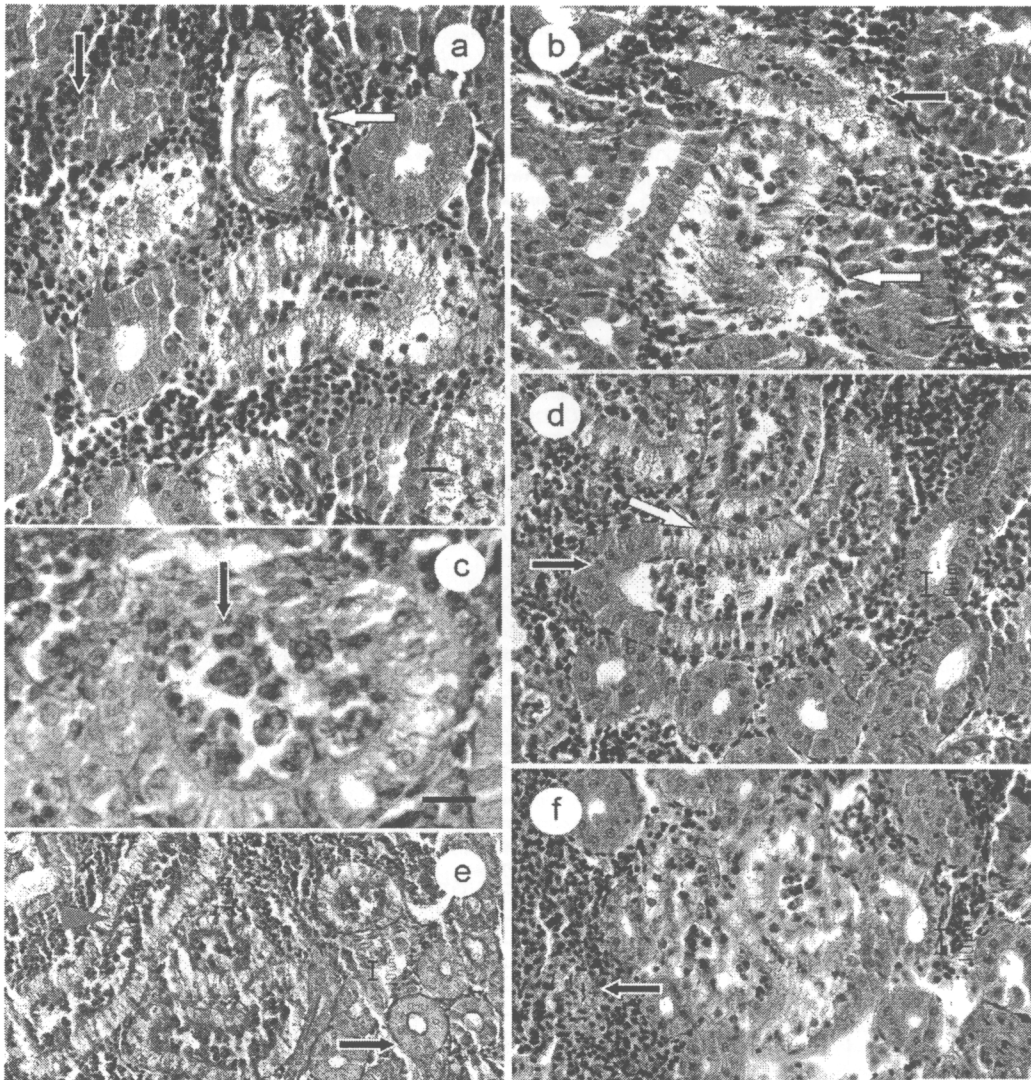
Fig. 4. Histopathological damage of *E. coioides* kiney infected by *S. epinepheli* (a–f). (a) The heavy infection shows the decay of the brush border (red arrow head) and renal tubule (white arrow) with mononuclear phagocytic cells infiltrated (black arrow). (b) Renal tubule occluded by various sporogonic stages (red arrow head) and degenerated (white arrow) and pyknotic nuclei (black arrow) of low columnar epithelial cell. (c) Evidence of tubule epithelium destroyed by parasite. (d) Low columnar epithelial cells showed vacuolation particularly to which attached parasitic pseudoplasmodia (white arrow), while other cells are normal (black arrow). (e) Infected tubule (red arrow head) showing the thick mucosubtract layer and the normal tubule (black arrow). (f) Renal parenchyma became atrophied later in chronic stages and inflammatory response from the host, melanomacrophage centre (black arrow). Sections are H&E (a, b, d and f) PAS (e) and toluidine blue (c). Scale bars (a–c): 10 μm. (For interpretation of the references to color in this figure legend, the reader is referred to the web version of this article.)

and Székely (2004) suggested that in most cases of variable host infected by myxosporean, the locations (organ and/or tissue tropism) within the new fish host remained unchanged. Liu et al. (2010) also reported that the majority of *Sphearospora* prefers developing in a single organ or specific host tissue. Our results suggest that the high degree of host specificity of *S. epinepheli* is recently restricted to specific to two species of the economic *Epinephelus* spp. A relatively narrow host spectrum was also reported in other species of the basal sphearosporid group, *S. elegans* and *S. truttae*, parasitizing only related fish species of the family Dasterosteidae and Salmonidae, respectively (Lom and Dyková, 2006).

The incidence of *S. epinepheli* infection in *E. coioides* of 25.07% is higher than that of 8.68% in *E. malabaricus* indicating that *S. epinepheli* prefers infecting the orange-spotted grouper. This may be due to some parameters which promote parasite susceptibility in host–parasite interaction (Nuismer and Otto, 2005); however, those parameters have yet to be elucidated. The seasonal patterns of *S. epinepheli* occurrence from both fish hosts were not related to the incidence of infection. The population dynamics of *S. epinepheli* in *E. malabaricus* was similar to the previous report 20 years ago (Supamattaya et al., 1991).

The severity of kidney damage in *E. coioides* infected by *S. epinepheli* was similar to that reported in *E.*
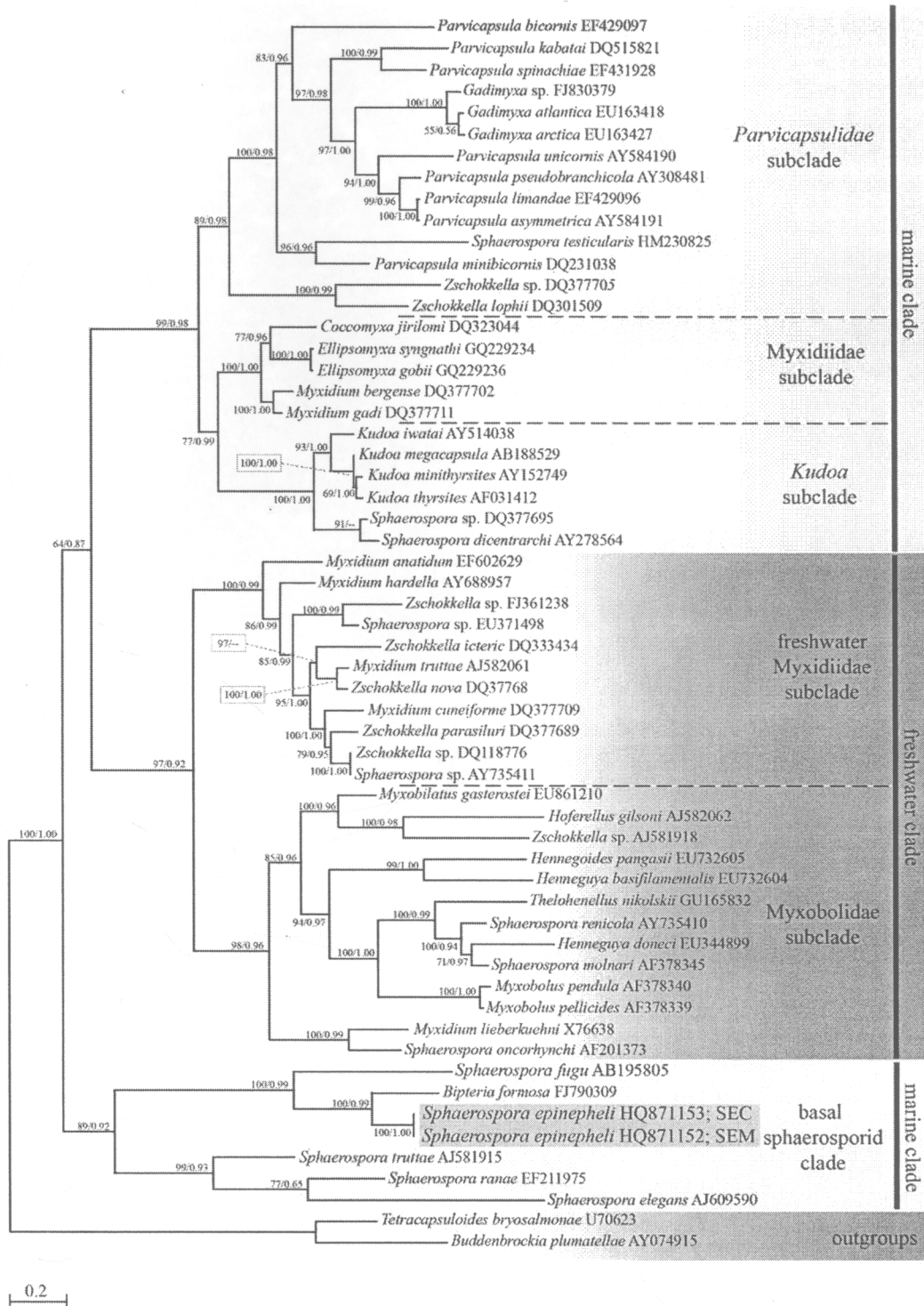
Fig. 5. Maximum likelihood tree (−*In* = 41,635·62,655) of the SSU rDNA sequence of selected myxozoans species was shown the genetic position of *S. epinepheli*. Malacosporeans; *Tetracapsuloides bryosalmonae* and *Buddenbrockia plumatellae* were set as outgroups. Nodal supports are indicated for ML (bootstrap, *n* = 500) and BI (posterior probabilities, 1,000,000 generations) with less than 50% support are not shown. GenBank Accession Numbers for each taxon are listed. The distance scale is shown under the tree.

malabaricus. Histopathological changes demonstrated the harmful effect of this parasite infection. Spores and developmental stages of *S. epinepheli* were often found in large numbers which partially obstructed the renal tube. However, the mature spores that were found in the Bowman's space could not be observed in *E. coioides*. In contrast, the infected renal tubules of both fish hosts revealed that intraluminal stages of parasite induced many vacuoles and pyknotic nuclei in the tubular epithelial cells. Chen et al. (2001) have reported that spores of *Sphaerospora* spp. a coelozoic parasite of kidney in cobia, *Rachycentron canadum* could be detected causing mass mortality with dilation, hypertrophy and hyperplasia of renal tubules. Some other myxosporean species which affect their hosts in a similar pattern are *Myxidium hardella*, the parasite infecting turtle, *Hardella thurjii* kidney resulting in tubular necrosis and chronic interstitial nephritis (Garner et al., 2005). Trivial host immune responses have been detected in *S. epinepheli* infection. The infected renal tubules were besieged by mononuclear phagocytic cell from surrounding renal parenchyma and a few melanomacrophage centers were found. In some cases of infection, spores were found in destroyed renal tubules, suggesting host immune responses. Inability of tissue reactions or host responses to myxosporean infections have been mentioned by many other authors (Alvarez-Pellitero et al., 2007; Sitja-Bobadilla, 2008).

As pointed out by many researchers (Molnár et al., 2009; Adriano et al., 2009; Bartošová et al., 2009; Liu et al., 2010), molecular phylogenetic analyses have become a novel standard of taxonomic tools for the classification of complicated myxosporean. In this study, 18S rDNA analysis of *S. epinepheli* from both fish hosts exhibited the inserted long variable regions causing longer than expected sequences. This finding is close to the previous reports in sphaerorid species (Holzer et al., 2004; Bartošová et al., 2011). The investigation of the main variable region length showed the presence of 2 areas, V4 E23_1–7 and V4 E23_13–15 with extensive inserts in the V4 region (Holzer et al., 2007). The phylogenetic position of *S. epinepheli* isolated from *E. malabaricus* and *E. cioiodes* were placed together with other long SSU rDNA *Sphaerospora* spp. in the clade of basal sphaerosporid which was separated from the freshwater and marine myxosporean clade with high bootstrap value support. This is consistent with previous reports (Holzer et al., 2007, 2010; Bartošová et al., 2011). On the other hand, *S. epinepheli* was placed in a close relationship with *Bipteria formosa*, a gallbladder parasite of marine fish. To date, only 18S rDNA of *Bipteria* genus is available in GenBank. However, the previous report discussing *B. formosa* suggested that the molecular data are related to *S. fugu* and the members belonging to sphaerosporid clade (Karlsbakk and Køir, 2009). Modern phylogenetic clustering, conducted based on ML and BI algorithms, revealed the related evolution of myxosporean species in the sphaerosporid clade. Nevertheless, the hosts of this parasite clade are variable including teleost fish and frog.

Our results indicate that *S. epinepheli* is a member of *Sphaerospora* sensu stricto (basal sphaerosporid clade). However, the phylogenetic analysis showed some species of *Sphaerospora* spp. placed in variable clades. This leads

us to conclude that the genetic position of *Sphaerospora* might be polyphyletic. The clade variation of this genus may be due to inconsistency of the methods and tools used in phylogenetic analysis. The data provided on *S. epinepheli* could be useful for the future revision of the classification of *Sphaerospora* genus.

In conclusion, spore morphology, genetic analysis and histological validity in the present study have demonstrated that coelozoic *Shaerospora* spp. in the kidney tubules of *E. coioides* is that of *S. epinepheli* which was reported to infect in *E. malabaricus*. The new host record of *S. epinepheli* was firmly asserted and acceptable via the individual conceptions of *Sphaerospora* genus. Further studies of *S. epinepheli* will be focused on the rapid diagnosis and a survey of infection in different fish culture conditions and habitat, which are important for clarification of pathological characters of this parasite in grouper aquaculture.

References

Adriano, E.A., Arana, S., Alves, A.L., Silva, M.R.M., Ceccarelli, P.S., Henrique-Silva, F., Maia, A.A.M., 2009. *Myxobolus cordeiroi* n. sp., a parasite of *Zungaro jahu* (Siluriformes Pimelodiade) from Brazilian Pantanal: morphology, phylogeny and histology. Vet. Parasitol. 162, 221–229.

Alvarez-Pellitero, P., Palenzuela, O., Sitjà-Bobadilla, A., 2007. Histopathology and cellular response in *Enteromyxum leei* (Myxozoa) infections of *Diplodus puntazzo* (Teleostei). Parasitol. Int. 57, 110–120.

Bartošová, P., Fiala, I., Hypša, V., 2009. Concatenated SSU and LUS rDNA data confirm the main evolutionary trends within myxosporeans (Myxozoa Myxosporea) and provide an effective tool for their molecular phylogentics. Mol. Phylogenet. Evol. 53, 81–93.

Bartošová, P., Freeman, M.A., Yokoyama, H., Caffara, M., Fiala, I., 2011. Phylogenetic position of *Sphaerospora testicularis* and *Latyspora scomberomori* n gen. n. sp. (Myxozoa) within the marine urinary clade. Parasitology 138, 381–393.

Bermúdez, R., Losada, A.P., Vázquez, S., Redondo, M.J., Álvarez-Pellitero, P., Quiroga, M., 2010. Light and electron microscopic studies on turbot *Psetta maxima* infected with *Entermyxum scophthalmi*: histopathology of enteromyxosis. Dis. Aquat. Org. 89, 209–221.

Castresana, J., 2000. Selection of conserved blocks from multiple alignments for their use in phylogenetic analysis. Mol. Biol. Evol. 17, 540–552.

Chen, S.C., Kou, R.J., Wu, C.T., Wang, P.C., Su, F.Z., 2001. Mass mortality associated with a sphaerospora-like myxosporidean infection in juvenile cobia, *Rachycentron canadum* (L.), marine cage cultured in Taiwan. J. Fish Dis. 24, 189–195.

Eszterbauer, E., Székely, C., 2004. Molecular phylogeny of the kidney-parasite *Sphaerospora renicola* from common carp (*Cyprinus carpio*) and *Sphaerospora* sp. from goldfish (*Carassius auratus auratus*). Acta Vet. Hung. 52, 469–478.

Fioravanti, M.L., Caffara, M., Florio, D., Gustinelli, A., Marcer, F., 2004. *Sphaerospora dicentrarchi* and *S. testicularis* (Myxozoa

Sphaerosporidae) in farmed European seabass (*Dicentrarchus labrax*) from Italy. Folia Parasitol. 51, 208–210.

Garner, M.M., Bartholomew, J.L., Whipps, C.M., Nordhausen, R.W., Raiti, P., 2005. Renal myxozoanosis in crowned river tutles *Hardella thurjii*: description of the putative agent *Myxidium hardella* n. sp. by histopathology, electron microscopy, and DNS sequencing. Vet. Pathol. 42, 589–595.

Gouy, M., Guindon, S., Gascuel, O., 2010. SeaView Version 4. A multiplatform Graphical user interface for sequence alignment and phylogenetic tree building. Mol. Biol. Evol. 27, 221–224.

Guindon, S., Gascuel, O., 2003. A simple, fast, and accurate algorithm to estimate large phylogenies by maximum likelihood. Syst. Biol. 52, 696–704.

Hall, T.A., 1999. BioEdit: a user-friendly biological sequence alignment editor and analysis program for windows 95/98/NT. Nucl. Acids Symp. Ser. 41, 95–98.

Harikrishnan, R., Balasundaram, C., Heo, M., 2010. Molecular studies, disease status and prophylactic measures in grouper aquaculture: economic importance, disease and immunology. Aquaculture 309, 1–14.

Hillis, D.M., Dixon, M.T., 1991. Ribosomal DNA-molecular evolution and phylogenetic inference. Q. Rev. Biol. 66, 410–453.

Holzer, A.S., Sommerville, C., Wooten, R., 2004. Molecular relationships and phylogeny in a community of myxosporeans and actinisporeans based on their 18S rDNA sequences. Int. J. Parasitol. 34, 1099–1111.

Holzer, A.S., Wooten, R., Sommerville, C., 2007. The secondary structure of the unusually long 18S ribosomal RNA of the myxozoan *Sphaerospora truttae* and structural evolutionary trends in the Myxozoa. Int. J. Parasitol. 37, 1281–1295.

Holzer, A.S., Wooten, R., Sommerville, C., 2010. *Zschokkella hildae* Auerbach, 1910: phylogenetic position, morphology, and location in cultured Atlantic cod. Parasitol. Int. 59, 133–140.

Jirku, M., Fiala, I., Modry, D., 2007. Tracing the genus *Sphaerospora*: rediscovery, redescription and phylogeny of the *Sphaerospora ranae* (Morelle, 1929) n. comb. (Myxosporea, Sphaerosporidae), with emendation of the genus *Sphaerospra*. Parasitology 134, 1727–1739.

Karlsbakk, E., Køir, M., 2009. *Bipteria formosa* (Kovaleva et Gaevskaya, 1979) comb. N. (Myxozoa, Myxosporea) in whiting *Merlangius merlangus* (Teleostei: Gadidae) from Denmark. Folia Parasitol. 56, 86–90.

Liu, Y., Gu, Z.M., Luo, L.Y., 2010. Some additional data to the occurrence, morphology and validity of *Myxobolus turpisrotundus* Zhang, 2009 (Myxozoa, Myxosporea). Parasitol. Res. 107, 67–73.

Lom, J., Dyková, I., 2006. Myxozoan genera: definition and notes on taxonomy, life-cycle terminology and pathogenic species. Folia Parasitol. 53, 1–36.

Longshaw, M., Frear, P.A., Feist, S.W., 2005. Descriptions, development and pathogenicity of myxozoan (Myxozoa: Myxosporea) parasite of juvenile cyprinids (Pisces: Cyprinidae). J. Fish Dis. 28, 489–508.

Molnár, K., SzéKely, C., Hallett, S.L., Atkinson, S., 2009. Some remarks on the occurrence, host-specificity and validity of *Myxobolus rotundus* Nemeczek, 1911 (Myxozoa: Myxosporea). Syst. Parasitol. 72, 71–79.

Moncada, L.I., López, M.C., Murcia, M.I., Nicholls, S., León, F., Guío, O., Corredor, A., 2001. *Myxobolus* sp., another opportunistic parasite in immunosuppressed patients? J. Clin. Microbiol. 39, 1938–1940.

Nuismer, S.L., Otto, S.P., 2005. Host–parasite interaction and the evolution of gene expression. PLoS Biol. 3, 1283–1288.

Posada, D., 2008. jModelTest: phylogenetic model averaging. Mol. Biol. Evol. 25, 1253–1256.

Ronquist, F., Huelsenbeck, J.P., 2003. MrBayes 3: Bayesian phylogenetic inference under mixed models. Bioinformatics 19, 1572–1574.

Sitja-Bobadilla, A., 2008. Fish immune response to myxozoan parasites. Parasite 15, 420–425.

Supamattaya, K., Fischer-Scherl, T., Hoffmann, R.W., Boonyaratpalin, S., 1990. Renal sphaerosporosis in cultured grouper *Epinephelus malabaricus*. Dis. Aquat. Org. 8, 35–38.

Supamattaya, K., Fischer-Scherl, T., Hoffmann, R.W., Boonyaratpalin, S., 1991. *Sphaerospora epinepheli* n. sp. (Myxosporea: Sphaerosporidae) observed in grouper (*Epinephelus malabaricus*). J. Eukaryot. Microbiol. 38, 448–454.

U-taynapun, K., Penprapai, N., Bangrak, P., Metaka, T., Itami, T., Tantikitti, C., 2011. *Myxobolus supamattayai* n. sp. (Myxosporea: Myxobolidae) from Thailand parasitizing the scale pellicle of wild mullet (*Valamugil seheli*). Parasitol. Res. 109, 81–91.

Yokoyama, H., Ogawa, K., Wakabayashi, H., 1990. Chemotherapy with fumagilin and toltazuril aginst kidney enlargement disease of goldfish caused by the myxosporean *Hoferells carassii*. Fish Pathol. 25, 157–163.